CHALMERS
UNIVERSITY OF TECHNOLOGY

Risk analysis of collision-damaged ship structures

Master's thesis in the International Master's Programme in Naval Architecture and Ocean Engineering

ANIRUDH MALLYA ULLAL

PAVAN JANARDHANA BANGERA

DEPARTMENT OF MECHANICS AND MARITIME SCIENCES

CHALMERS UNIVERSITY OF TECHNOLOGY
Gothenburg, Sweden 2021
www.chalmers.se

MASTER'S THESIS IN THE INTERNATIONAL MASTER'S PROGRAMME
NAVAL ARCHITECTURE AND OCEAN ENGINEERING

RISK ANALYSIS OF COLLISION-DAMAGED SHIP STRUCTURES

ANIRUDH MALLYA ULLAL and PAVAN JANARDHANA BANGERA

Department of Mechanics and Maritime Sciences
Division of Marine Technology
CHALMERS UNIVERSITY OF TECHNOLOGY
Göteborg, Sweden 2021

RISK ANALYSIS OF COLLISION-DAMAGED SHIP STRUCTURES

ANIRUDH MALLYA ULLAL and PAVAN JANARDHANA BANGERA

Master's Thesis 2021:49
Department of Mechanics and Maritime Sciences
Division of Marine Technology
Chalmers University of Technology
SE-412 96 Göteborg
Sweden
Telephone: + 46 (0)31-772 1000

Cover:
A collision of Tunisian Ro-Ro ship, the Ulysses with the Cypriot container ship CLS Virginia, © FRENCH NATIONAL MARINE / AFP (*Collision de Navires En Corse : Quels Risques Pour l'environnement ?*, 2018).

Chalmers Reproservice
Göteborg, Sweden 2021-06-04

RISK ANALYSIS OF COLLISION-DAMAGED SHIP STRUCTURES

Master's thesis in Naval Architecture and Ocean Engineering

ANIRUDH MALLYA ULLAL and PAVAN JANARDHANA BANGERA

Department of Mechanics and Maritime Sciences
Division of Marine Technology
Chalmers University of Technology

Abstract

Shipping is the biggest mode of transport for bulk goods both by volume and value. But there were many cases where the shipping owners had to face huge losses due to ship-ship collisions, indirectly affecting the revenue flow in the shipping market. To quantify the consequences and reduce the loss behind these setbacks, an engineering solution of risk analysis has been done for a collision-damaged vessel.

Three major post-collision hazards are considered in the scope of this thesis. Risk analysis on these three major hazards is done to quantify the severity of the consequences faced after a collision. The whole objective of this thesis is to build a general methodology that accounts for the stability risks of any vessel after damage, assesses the structural safety and ultimate strength risk, and develops an oil pollution response model that presents an economic valuation of the environmental impacts caused by the collision.

Three methodologies are built addressing two different locations to showcase the accident based on the marine traffic density and history of ship collision on the west coast of Sweden. The analysis is made reliable by directly mapping the wave characteristics of the accident location on the seakeeping, survival probability, ultimate strength exceedance probability, and oil drift assessments. Considering the vulnerability, two ship types (RoPax & tanker) were used to showcase the versatility of the developed methodologies.

A graphical user interface of the risk analysis tool is developed for all three major risk modules. The influence of the wave characteristics of the location on the risks are shown. The damage stability risk tool presents the motion responses and the survival risks; the ultimate strength risk tool delivers the ultimate strength exceedance probability, consequence, risks, and proposes mitigation actions; finally, the oil pollution response tool quantifies the consequences concerning the environmental impacts in the Swedish waters.

It was shown that the wave characteristics vary for different locations in the same region and have a significant influence on the results of the risks on both RoPax and tanker vessels. It was concluded that the damage stability risk is sensitive towards the maximum time for evacuation. It was also shown that the simple act of manoeuvring the vessel can be an efficient way of ultimate strength risk mitigation. Analysing the oil drift simulation results it was concluded that viscosity and density play a very major role during the oil pollution response cost assessment.

Keywords: Consequence analysis, metocean statistics, oil discharge, oil pollution response, probability of capsizing, risk analysis tool, rose plots, survival probability, ULS risk.

Contents

Abstract V
Contents VII
Preface IX
Nomenclature XI
1 Introduction 1
1.1 Background and motivation 1
1.2 Objectives 4
1.3 Assumptions and limitations 5
1.4 Outline of the thesis 7
2 Methodology 9
2.1 Location 10
2.2 Collision scenario 11
2.3 Metocean condition and statistics 14
2.3.1 Data extraction and processing 14
2.3.2 Visualization 15
2.4 Seakeeping and stability analyses 16
2.4.1 Main dimensions of the model 17
2.4.2 SIMCAP analysis 18
2.4.3 Survival probability 21
2.4.4 Damage stability risk 21
2.5 Structural integrity simulation and ULS risk 22
2.5.1 ULS simulation 22
2.5.2 Structural loading history 23
2.5.3 Safety assessment 24
2.5.4 Parametric sensitivity analysis 24
2.5.5 Relative wave encountering angle 25
2.5.6 Probability of exceedance of ULS 26
2.5.7 ULS consequence and risk 27
2.5.8 ULS risk mitigation action 27
2.6 Environmental impacts and risk 28
2.6.1 Simulation for oil drift 28
2.6.2 Parameters for oil drift simulation 29
2.6.3 Oil pollution response cost assessment 31
3 Results and discussion 33

3.1 Metocean condition and statistics 33
3.1.1 Rose plots 33
3.1.2 Maximum likely occurring wave direction 34
3.1.3 Probability of significant wave height 35
3.2 Seakeeping and stability analyses 36
3.2.1 Probability of capsizing 36
3.2.2 Time to capsize 36
3.2.3 Damage stability GUI 37
3.2.4 Sensitivity analyses 38
3.2.5 Motion responses of the tanker vessel 39
3.3 Structural integrity simulation and ULS risk 40
3.3.1 Structural adequacy plot 40
3.3.2 Parametric sensitivity analysis 41
3.3.3 ULS risk GUI 42
3.3.4 Showcasing ULS risk and mitigation measures 43
3.3.5 Sensitivity analyses 46
3.4 Environmental impacts and risk 47
3.4.1 Parametric sensitivity analyses 47
3.4.2 Environmental impact consequence GUI 56
3.4.3 Oil pollution response cost assessment 56
3.4.4 Natural resource damage assessment 57
4 Summary and conclusions 61
5 Future work 63
6 References 65
7 Appendices 69
7.1 Appendix 1: Seakeeping and stability analyses 69
7.2 Appendix 2: Structural integrity and ULS risk 71
7.3 Appendix 3: Environmental impacts and risk 72

Preface

This thesis is a part of the Naval Architecture and Ocean Engineering programme's requirements for the master's degree at Chalmers University of Technology and has been carried out in the Division of Marine Technology, Department of Mechanics and Maritime Sciences, Chalmers University of Technology from January through June of 2021.

We would like to thank the supervisor and examiner for this thesis, Professor Jonas W. Ringsberg, for accepting us to this momentous long-term research project. We would also like to thank him for his constant motivation, inspiration, and feedback that has steered us throughout this thesis project.

We would also like to thank the co-supervisor for this thesis project, Artjoms Kuznecovs, for his guidance throughout these months. His kind advice, short tips, and quick response have helped us along the way. This also gave us insights into how dedicated one can be in his work.

We are much obliged to Erland Johnson from RISE Research Institute of Sweden for giving us expert opinions and kind advise throughout the project. Special thanks to Swedish coast guard officials, Oskar Feltenstedt and Johan Genestig. Their expertise and the discussions with them were helpful. A heartfelt thanks to Ida-Maja Hassellöv for sparring some time and sharing her thoughts despite the busy schedule. Not to forget Adam Nord from SMHI for his generosity in providing us with the commercial license of Seatrack Web for this research.

Finally, we would like to thank our family and friends from the bottom of our hearts for their endless love and support. Finally, we would like to thank each other for having great teamwork, cooperation, and trust throughout this thesis project.

Göteborg 2021-06-04

ANIRUDH MALLYA ULLAL and PAVAN JANARDHANA BANGERA

Nomenclature

η	Structural adequacy	[-]
θ	Vessel heading direction	[deg]
θ_{init}	Initial heading direction	[deg]
θ_{safe}	Safe heading direction	[deg]
ρ	Density of the oil	[kg/m^3]
ρ_w	Density of sea water	[kg/m^3]
$\varphi_{Least\ Prob\ ULS}$	Wave encountering angle with least P_{ULS}	[deg]
φ_r	Relative wave encountering angle	[deg]
A	Area of the damage	[m^2]
C_d	Coefficient of discharge	[-]
g	Acceleration due to gravity	[m/s^2]
H_s	Significant wave height	[m]
LW	Maximum likely occurring wave direction	[deg]
M	Mass flow rate of the discharged oil	[kg/s]
P_{H_s}	Probability of significant wave heights	[-]
$P_{survival}$	Survival probability of crew and passengers	[-]
P_{ULS}	Probability of exceedance of ULS	[-]
$R_{Damage\ Stability}$	Damage stability risk	[-]
R_{ULS}	ULS Exceedance risk	[-]
T_{actual}	Actual time available for evacuation	[s]
$T_{capsize}$	Time to capsize	[s]
T_{max}	Maximum time for evacuation suggested by IMO	[s]
$T_{max,\,modified}$	Modified maximum time for evacuation	[s]
T_p	Wave encounter period	[s]
V	Velocity of discharge	[m/s]

1 Introduction

Shipping has become the biggest mode of goods transport in the world, through its invaluable ability to ship bulk cargo in most of the tough times (Shipping fact, 2021). Shipping could also be regarded as the backbone of international trade and the global economy accounting for an average of 75% global trade both by volume and value (Asariotis et al., 2018). Looking at the above-stated figures it can be argued that shipping is and will be a huge market. To understand the efficacy of any huge market it is necessary to understand the critical issues faced by its primary resources that can disturb the consistency of the market. Ship-ship collision is one of the critical issues as it is a challenge to the shipping companies to prevent their losses because of the damage to the crew and cargo (Love, 2020).

Hence, this Chapter presents the historical background on the demand for shipping to understand the reasons behind the consequences faced due to this demand. This Chapter also describes the strong motivation to discover an engineering solution for tackling the problems associated with the ship-ship collisions to prevent a significant loss for the shipping companies. Finally, a clear definition of the objectives and goals behind the work along with reasonable assumptions for achieving a solution is exhibited.

1.1 Background and motivation

Shipping is the cheapest mode of transportation available for bulk goods. The recent report on the review of maritime transport by Asariotis et al. (2020) describes the growth in the maritime trade of 0.5% in 2019 and also estimates a growth of 4.8% in 2021, which is a shred of clear evidence on the shipping demand rise. The statistics on future prediction by GTA Forecasting (2020) about maritime trade both by volume and value as shown in Figure 1.1. This information gives a general idea of the demand for bulk carriers in the future. By 2030 the global trade volume is expected to increase by 50% compared to its present value (GTA Forecasting, 2020).

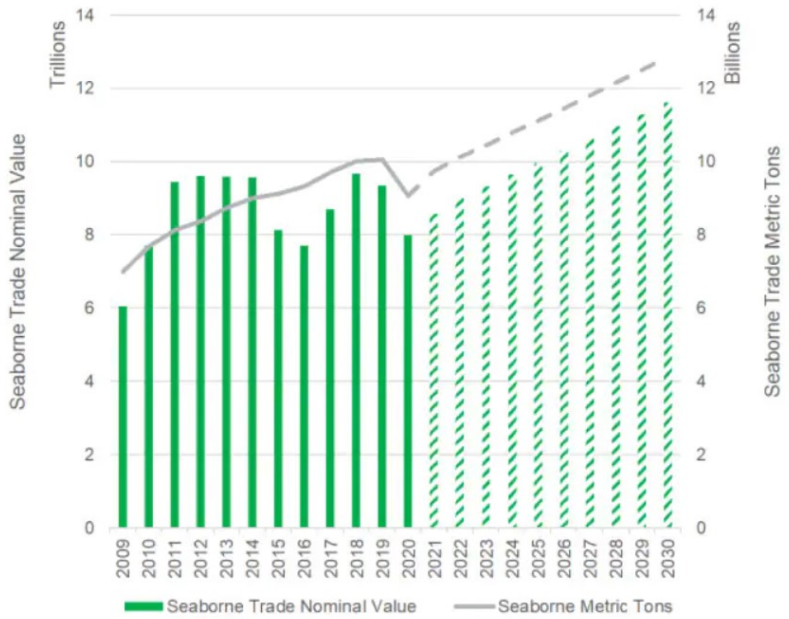

Figure 1.1 Global seaborne trade forecast taken from (GTA Forecasting, 2020).

Currently, over 90% of the world trade is done through shipping (OECD, 2021). This would reflect on the marine traffic that could be visualised in Figure 1.2, which is a real-time image on the west coast of Europe (captured at 14:30 on 02-02-2021). Based on the predictions on future shipping demand can be argued that the density of the ships in oceans will increase year by year. Thus, more and more ships channelize themselves in the same route every year which can lead to disorder in shipping routes. Due to the intersections in the route corridors and despite the advanced maritime traffic control systems, there is still a high chance of ships getting uncontrollable and collide with each other in the future, resulting in a terrible loss.

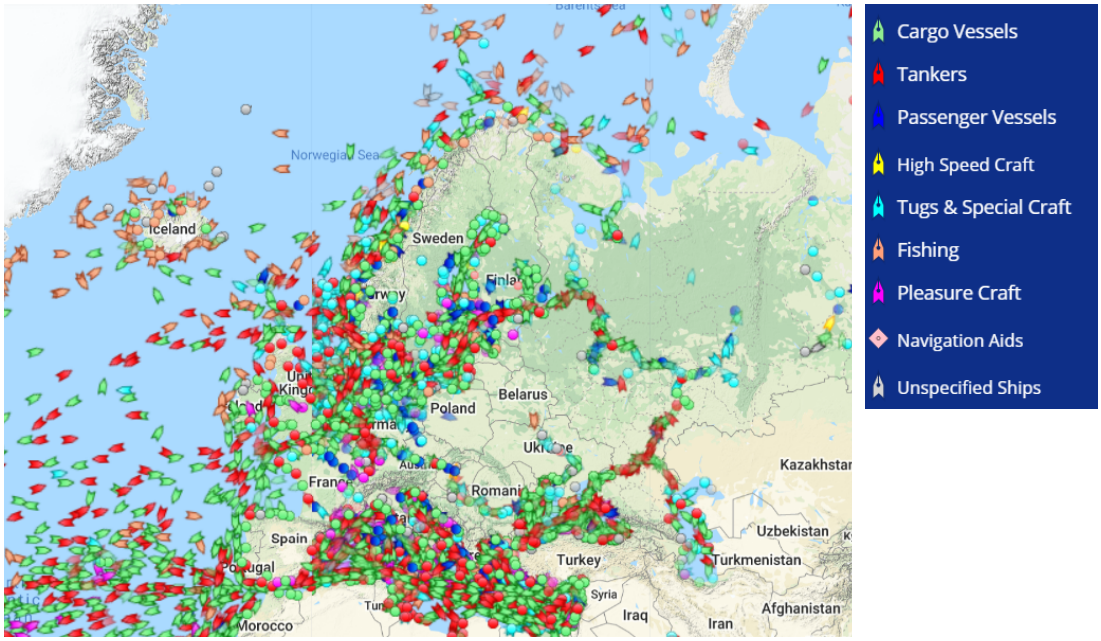

Figure 1.2 Marine traffic on the west coast of Europe (MarineTraffic, 2021).

Looking at the history of maritime accidents on a broader perspective, a total of 19500 casualties has occurred between 2014-2019 which averages to be 3236 casualties per year (EMSA, 2020). These numbers convey the amount of risk that marine transport still has despite having well-developed collision avoidance tools and maritime traffic control systems.

A study carried out by European Maritime Safety Agency (EMSA, 2020) on marine casualties and incidents that happened between 2014-2019 categorizes major types of ships involved in the accidents. It says the major contribution to the event is from cargo vessels and passenger ferries accounting for 69% of accidents. A pictorial representation of the data can be seen in Figure 1.3.

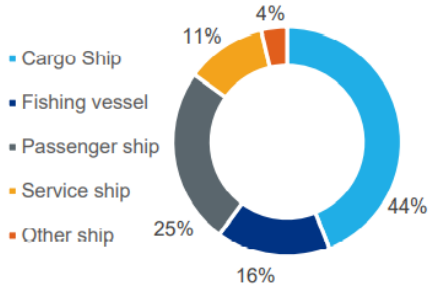

Figure 1.3 Distribution of major ships involved in casualties (EMSA, 2020).

Based on the severities, ships will experience different types of consequences after the collision, the consequences can be direct or indirect. The major consequences to the ships can be found from the accident investigation reports (Transportstyrelsen, 2011) documented after the accident gets reported to the shoreline authority. Between 2014-2019 there has been a lot of cases reported for damage among which the largest contribution is from the cargo ships (~ 48%) (EMSA, 2020). The consequences due to the damages could be classified as economic, social, and environmental consequences based on its target of loss.

The number of ships getting damaged is increasing year by year and has a positive slope trend as shown in Figure 1.4. A collision between LNG carrier 'Aseem' and a VLCC 'Shinyo Ocean' in March 2019, resulted in the breaching of hulls below the waterline (Safety4sea, 2020-a) is an example of economical loss to the ship owners. It was recorded that both the shipowners had to bear the fines (22,000 US $) from the local authorities despite the hull damage repair (Splash247, 2019). An extensive image of the hull after the investigation can be seen in Figure 1.5.

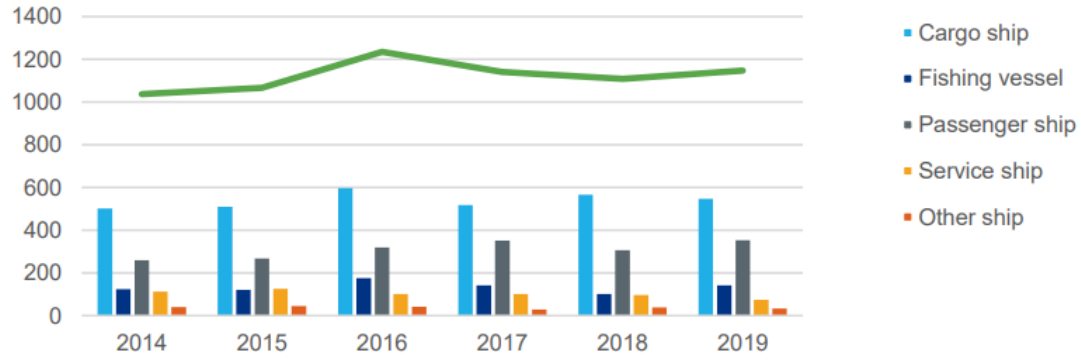

Figure 1.4 Ship damage trend from 2014 to 2019 (EMSA, 2020).

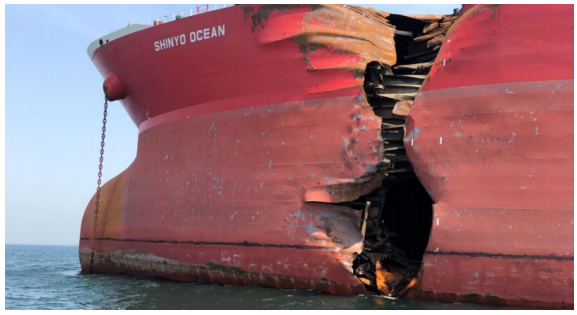

Figure 1.5 Damage after the collision between LNG carrier and VLCC in March 2019 Safety4sea, 2020-b).

Along with the damages and contaminations of marine waters due to the cargo leakage, there is also a threat to the human lives onboard the vessel. For many years there are a lot of cases being reported on crew injuries and fatalities due to the ships' damages, which could be regarded as the social consequences of the damage. Among them, 88% of the lost lives are the crew members onboard the vessel (EMSA, 2020). The trend of these fatalities started decreasing from 2014 to 2017 due to a drop in the shipping demand as seen in Figure 1.1 and then started increasing again with a positive slope. The statistical fatality trend is displayed in Figure 1.6.

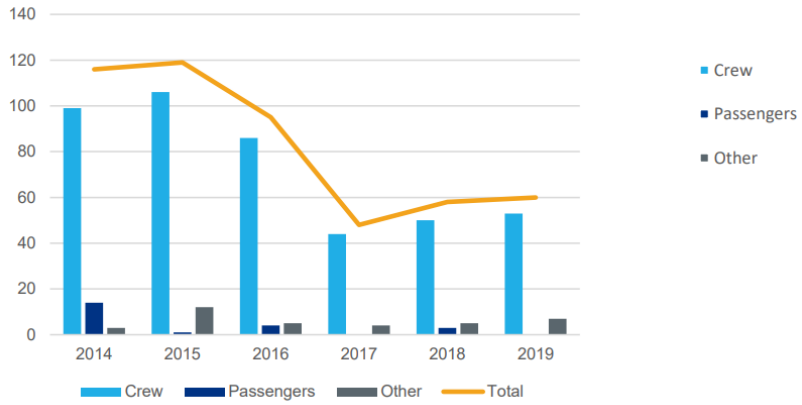

Figure 1.6 Distribution of fatalities between 2014-2019 (EMSA, 2020).

The impacts of the collision on the environment could be due to the fire/explosion, hull grounding, capsizing due to flooding, and instability but the threat is due to the pollution caused by these incidents. It is recorded that pollution due to bunkers contributes the maximum to the environmental impacts (EMSA, 2020).

The EU/EEA flag state vessels have a very large contribution with 18180 reported ships compared to 3085 non-EU/EEA flagged ships in the EU/EEA waters (EMSA, 2020). As per the statistics, the cargo vessels which are considered as the backbone for shipping have the largest contribution to the accidents and incidents. On a long range, these accidents could be a threat to the future of the marine transport systems.

Therefore, to secure the bulk transport systems, human as well as marine lives and to reduce the inconsistency in the revenue flow inside the shipping market after the collisions, it is important to possess solid knowledge to mitigate the consequences even after the vessels collided. Thus, the behaviour of the vessels after a collision and the severity of the consequence it faces based on the damage state should be studied thoroughly and processed. Hence a risk analysis on the collision-damaged ship structures is a much-needed assignment in the present time and considered as worth the effort.

1.2 Objectives

Passive safety measures are getting significant importance in recent times (IMO, 2008, 2018). Based on the statistics provided in Section 1.1, it is more evident that though IMO has various regulations regarding the pro-active safety measures for different vessels (IMO, 2018), still the accident rates are not decreasing. This could be due to the density of vessel traffic in the same economic sea routes as shown in Figure 1.2.

The increasing shipping demand as presented in Section 1.1 and Figure 1.2 indirectly gives rise to an increased risk of collision. The risk here is a product of a probability of occurrence and the corresponding consequence (IMO, 2018) that could be regarded as a decision-making variable. Thus, depending upon the measure of the risk, one could understand the chance of survivability after the collision. The surviving chance always depends on the safety level at which the vessel lies after the collision impact.

The main objective of this thesis is to develop a methodology for risk assessment that accounts for the time integrity of wave loads, crew & passenger fatalities due to ship instability, an exploration of the post-collision structural safety level, and the

environmental impacts from the cargo leakage. With this methodology, it should be possible to:

1. Map the metocean condition and statistics of the accident location on the risk analysis of the collision damaged vessel.
2. Assess the probability of capsizing and the risk behind the crew survivability after the collision for any desired ship type.
3. Exhibit the ultimate strength exceedance risk by simulating the post-collision structural safety for any vessel and suggest risk mitigation actions to combat the situation.
4. Uncover the consequences of oil discharge from the damaged vessel due to a collision and develop an oil pollution response model that exhibits the economical valuation of the assessment.
5. Explore a user-friendly graphical interface for the risk analysis tool onboard the vessel.

1.3 Assumptions and limitations

This thesis is a part of the project SHARC (2021) thus, the history of ship-ship collision and marine traffic density is carefully observed only on the west coast of Sweden. Analysing the intersections in the shipping route corridors and marine traffic density in this region, the two best suitable locations were chosen. The methodology developed is not limited to the location rather to the availability of metocean conditions and statistics of the location. If the necessary data is available, any location could be incorporated into the tool.

Extracting the annual metocean statistics consisting of four different seasons limits the proper usage of the resource since it is well known that sea wave characteristics change with seasons. Hence a valid assumption of using the metocean statistics of each season separately for different years is made. From the weather rose plot created using the described assumptions, the data extracted using the maximum likelihood (ML) method with one standard deviation is assumed to include all the possible occurring significant wave heights.

For showcasing the extent and the outcomes of the developed methodologies, two different ship models (RoPax and Tanker) are used. The analyses done on the RoPax model is developed by Schreuder (2014). Hence, the assumptions for the damage stability are therefore similar to the method of simulation described by Schreuder (2014). The RoPax model uses the damage opening created by the collision of two ships as the input which is simulated through explicit finite element analysis (FEA) in a study of the development of a method for simulation of damaged and intact ships in waves by Schreuder (2014). The damage opening of the Tanker model used in this thesis was developed by Kuznecovs et al. (2021b). Responses such as manoeuvring the ship to a better angle against the waves, counters to the incoming water in the damaged compartment, or any other way of preventing or containing the flooding or damages are not considered (Schreuder, 2014).

In this thesis, only RoPax ships are considered for an extensive analysis on the stability. The RoPax ship in this study has a displacement hull and a low beam to length ratio (Schreuder, 2014). As manoeuvring of the RoPax ship is not considered, it is not studied and thus the ship is assumed to have no forward speed.

Due to time constraints, computational limitations on the purpose of showcasing the developed methodology, a RoPax model from the study done by Schreuder (2014) is only considered for the damage stability risk analysis. While assessing the passenger survival probability after a collision, the maximum time for evacuation is adopted from the range (10-15 min) suggested in the works of Vanem & Skjong (2004). The actual time for evacuation is replaced by the time for capsizing while estimating the survival probability of a collided vessel.

To showcase the extent of developed methodology on structural integrity simulation and ULS risk, a Tanker ship model is assumed for the analysis. The damaged Tanker model and the interaction curve data are not explicitly built in this thesis rather it is obtained as an input from the former research carried out by Kuznecovs (2020). Thus, the tool URSA built by Kuznecovs (2020) to analyse the ultimate biaxial bending moment of the ship structure is not directly used but will be regarded as the backbone of the ULS risk analysis. The following are the technical assumptions and limitations for the ULS risk analysis:

- Structural strength risk evaluations are only limited to the exceedance of the ship hull's ultimate strength in biaxial bending.
- It is considered that the maximum likely occurring wave direction relative to the ship heading direction yields the most likely ULS exceedance probability.
- For computing the structural adequacy values corresponding to directions other than the multiples of 45°, a linear interpolation technique is used. This could limit the accuracy of obtained results due to the absence of data on intermediate encounter directions.
- While quantifying the consequences, the human fatalities and injuries are treated equally but with a relation defined by IMO (2018), and it is also assumed that crew members will be rescued by the coast guards if the vessel is allowed to sink.
- It is assumed that total cargo is lost if the vessel is allowed to sink (Williams, 2013). This assumption is made mainly to encounter the legal issues related to the insurance claims, and it remains valid until there are no changes in the insurance claim terms and conditions.
- All the market risk factors in the ULS consequence quantification are assumed to be covered in the miscellaneous factor given at the end.

The chosen ship type for the analysis in both the damage stability risks and ULS exceedance risks does not limit the versatility of the developed methodology. The ship types chosen are only to showcase the extent and results of the developed methodology.

This thesis considers the oil discharge from a damaged compartment of a Tanker as an accident scenario for the oil pollution response assessment. To understand the oil drift after the spillage, a well-established tool Seatrack Web (2021) is used. This tool allows one to simulate the drift pattern of oils based on metocean data available on the tool at the time. For this thesis, the oil outlet depth is assumed to be 0 m i.e., on the surface of the water.

However, the commercial license to this web application, which was used for this thesis, allows access to data within a week's difference from the day of simulation i.e., one week before and one week after the day of simulation. The limitation is that one day from each season could not be chosen. This hampers the study of the oil drift

patterns as only the metocean data from April to May 2021 is available on the web application.

In response to the oil spills that are assumed to occur in this thesis, the following assumptions are also made about the response of the Swedish coast guard:

- Swedish coast guard oil clean-up operation is assumed to start from the nearest station available to the location of discharge.
- It is assumed that all the recovery vessels and equipment needed for the clean-up operation are available in the nearest station at the time of the accident report.
- The Swedish coast guard response is assumed to be quick and starts immediately as soon as the accident gets reported to reduce the area of oil drift.
- It is assumed that vessels from Swedish coast guards exhibit 100% efficiency on the oil recovery and clean-up irrespective of the sea states of the location.

1.4 Outline of the thesis

This thesis is consisting of 6 Chapters. The introduction chapter presents the problem statement along with brief background on the subject and a strong motivation towards achieving the solution. The literature behind the methods available and the methods used and developed to achieve the goals of this thesis are presented in Chapter 2. Chapter 3 presents the results obtained for the methodologies proposed and some qualitative discussion on the non-quantified results. The entire work of this thesis is summarized and concluded from the results and findings in Chapter 4. Based on the work done so far in this thesis, the scope for future developments is defined and presented in Chapter 5. All the references used for developing the risk analysis tool are listed in the final Chapter 6. The additional details available within the methodology and results are displayed in the respective Appendix.

2 Methodology

The focus of this thesis is to understand the metocean condition and statistics on the most likely occurring collision location and thereby formulate a methodology that could map the influence of metocean data on the collided ships and evaluate the risk associated with the collision-damaged ship structures. As described in the formal safety assessment guidelines by IMO (2018), the hazards of concern must be defined before the risk assessment. Thus, three hazards were defined:

1. Ship instability due to flooding
2. Reduction of the ULS after collision damage
3. Impacts on the marine environment due to cargo leakage.

The risks associated with the above-defined major hazards were analysed using a deterministic approach to have a quantified result for the consequence and risk. Thus, the methodology is divided into modules and integrated along with the subsequent steps as shown in Figure 2.1.

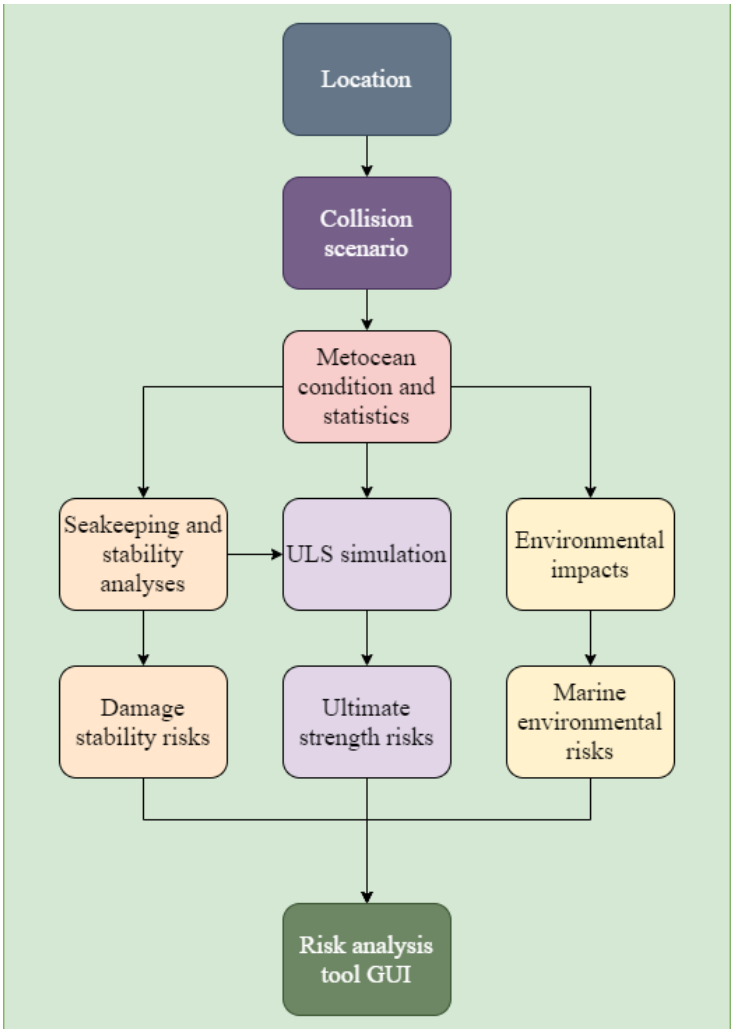

Figure 2.1 Overview of the risk analysis model.

Each module illustrated in Figure 2.1 is explained in detail along with the previous research on the topic, its scope, features, and desired results in the following Sections.

2.1 Location

The Swedish coastal water region is primarily the region of concern in the project SHARC (2021). This thesis aims to develop a methodology that works for any location, thus the methodology described will be general and holds good for all the locations based on the availability of metocean statistics. Since this thesis is a part of the project SHARC (2021), the location to showcase for the analysis will also be chosen in the region specified in the project. The selection of the location is made based on ship traffic density, and route intersection and collision frequency. The detailed workflow of the module is illustrated in Figure 2.2.

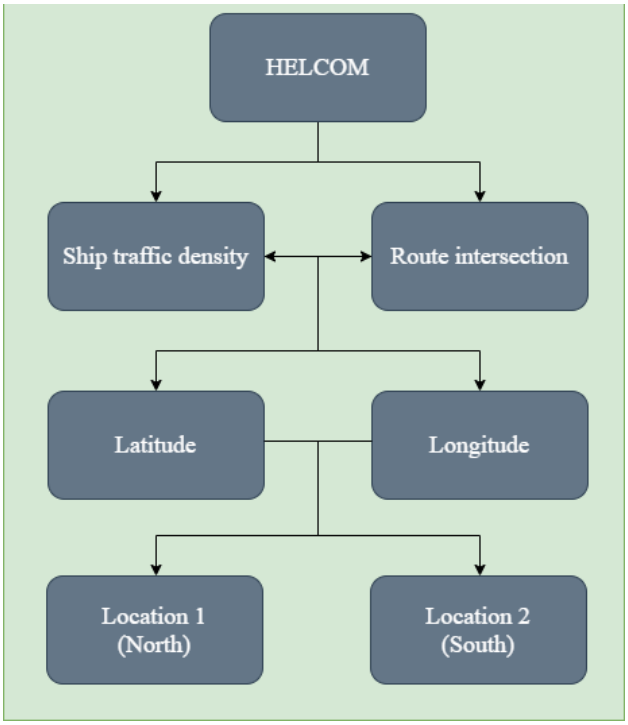

Figure 2.2 Flowchart for specifying the location.

Based on shipping route corridors' intersection and the available data on collision frequency, two locations were selected i.e., approx. 54 NM apart. The ship traffic density and the most frequent collision locations are obtained using the open-source database from "The Baltic Marine Environment Protection Commission" – also known as the Helsinki Commission (HELCOM, 2021).

The Kattegat region of the North Sea was considered as the major sea route in this region, because of its intersections at multiple locations and the highest anticipated risk of collisions between ships. Two locations in this region are considered, both of which have had collisions taken place within the last four years. A map view of the chosen locations is displayed in Figure 2.3. The region marked with a blue box is the selected location, the red lines refer to the shipping route corridors and its thickness represents the marine traffic density relatively. The details of the locations are presented in Table 2.1.

Table 2.1 Selected location details for the risk analysis.

Location	Latitude	Longitude
North	57.6081	11.5138
South	56.7248	11.8749

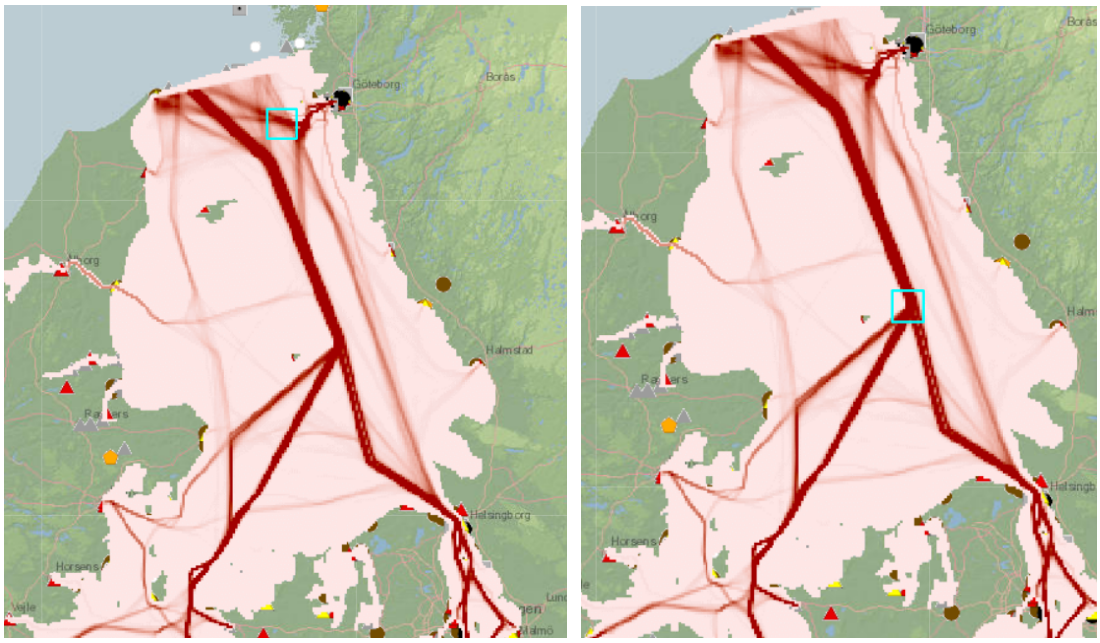

(a) (b)

Figure 2.3 Chosen location for the risk analysis map view taken from HELCOM (2021) (a): Location 1 (North), (b): Location 2 (South).

2.2 Collision scenario

For the RoPax ship considered in the seakeeping and stability analyses, the defined damage opening is a V-cut opening in the hull projected onto the compartment (Schreuder, 2014). The damage opening on the hull opens the car deck, the main engine room, and two spaces aft of the main engine room (Schreuder, 2014). The two spaces aft of the main engine room are one above the other and are asymmetric. The main engine room and the car deck have starboard/port symmetry. The damage opening on the RoPax ship obtained from FE analysis by Schreuder et al. (2011) is shown in Figure 2.5. The damage opening has a total damage area of 79.4 m^2. Figure 2.5 (a) shows the structural damage caused by the collision and Figure 2.5 (b) shows an illustration of the damaged ship in a seaway (Schreuder et al., 2011).

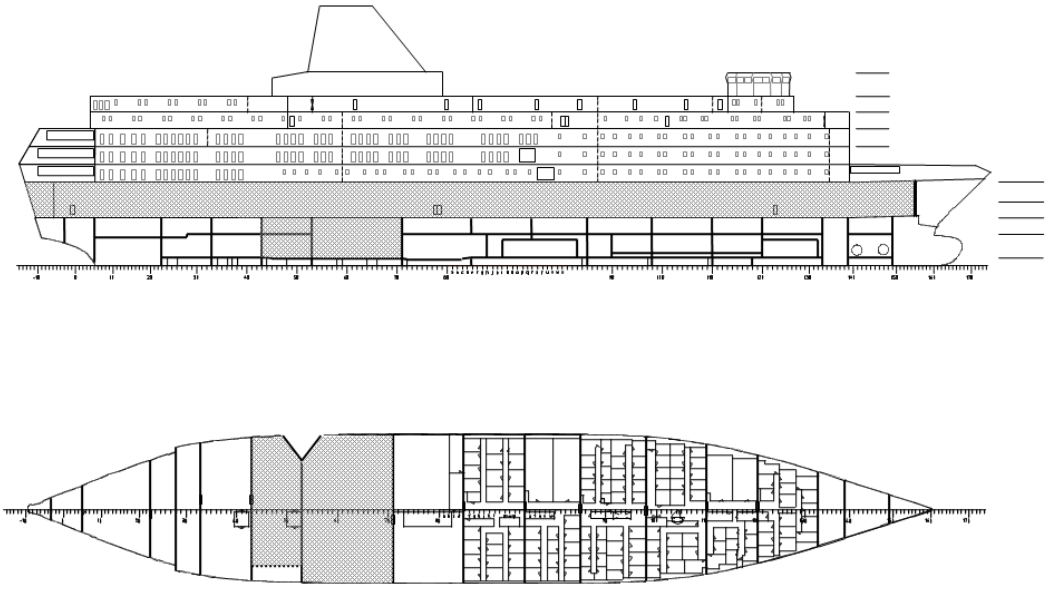

Figure 2.4 Damaged compartments of the RoPax ship (Schreuder, 2014).

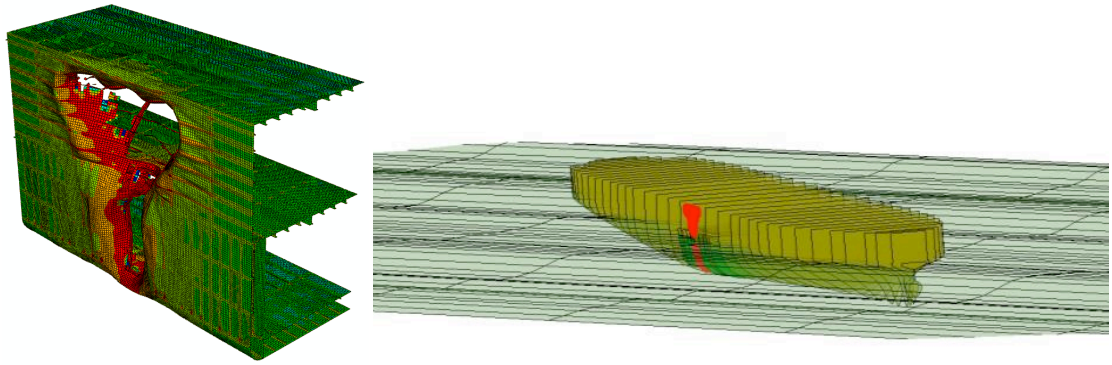

(a) (b)

Figure 2.5 Structural damage and damage opening from FE analysis; (b) Illustration of damaged ship in a seaway (Schreuder et al., 2011).

The car deck is assumed to be empty and the permeability of this deck is assumed to be 1. The permeability of the main engine and the other two spaces is assumed to be 0.85 (Schreuder, 2014), where permeability is a coefficient that indicates the total percentage volume that a liquid can occupy if that space is flooded. As the damage opening of the RoPax ship is very rough, i.e. does not have smooth edges, the coefficient of discharge for this study is kept at a constant value of 0.6 (Schreuder, 2014; Spanos & Papanikolaou, 2011). The coefficient of discharge is the ratio of the actual discharge to the theoretical discharge and is set to be a constant as all the edges of the damage opening are assumed to have the same exit pressure.

For the Tanker, the damage opening on the ship was caused by another ship of similar size. The collision is assumed to be at a 90° angle to the struck ship with the striking ship having a speed of 5 knots and is at amidships. From a study done by Brown (2002), it was seen that the speed of striking Tanker ships was reduced due to some measures taken to prevent collision right before the actual collision which was around 5 knots in most cases. It was also seen that the most likely collision angle between Tankers is 90°

(Brown, 2002). The volume of the compartment that is then opened in the collision is 1340 tonnes(Schreuder, 2014). The terminology used in this thesis is a more specific derivative of the terminology employed by Kuznecovs et al. (2021b) and is shown in Table 2.2.

Table 2.2 Terminology used to describe different case studies of the Tanker.

Parameter	Value	Notation
Vessel type	Tanker	T
Structural degradation	As-built	1
	Corroded	5
Structural damage	Intact	I
	Damaged	D

From the simulation methodology proposed by Kuznecovs et al. (2021b), the projected damage opening area for the tanker is shown in Table 2.3. The damage opening models for the tanker ship were developed in a study conducted by Kuznecovs et al. (2021b). In Table 2.3, T-1-D denotes a tanker that is as-built but is damaged and T-5-D denotes a tanker that is corroded and damaged (Ringsberg et al., 2018). To model the corrosion of the T-5 cases, Ringsberg et al. (2018) reduced the thickness of the structural members by removing the full corrosion margin from the initial plate thickness. Along with the corrosion margins, Ringsberg et al. (2018) also reduced the stiffness, yield limit, ultimate strength, and fracture strain were reduced and the coefficient of friction was increased for corroded surfaces to 0.5 from 0.3, which was the coefficient of friction used for non-corroded surfaces. Both cases have individual damage openings considering the state of the outer shell of the tanker. The mapping of these damage cases can be seen in Figure 2.6. The red colour is a mapping of the damage opening in the T-1-D case on the left and the T-5-D case on the right and the orange panel indicates the design water line of the tanker.

Table 2.3 Damage openings on the outer shell of the tanker for the cases considered.

Parameter	T-1-D	T-5-D
Projected damage opening area [m^2]	4.2	8.8

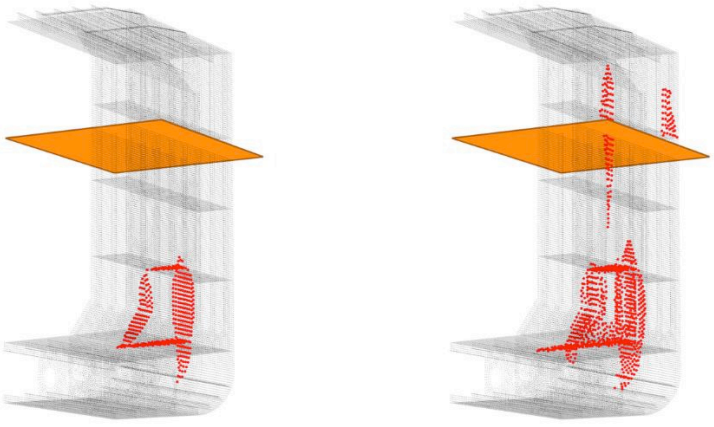

(a) (b)

Figure 2.6 Mapping of damage openings (in red) in the SIMCAP damage stability simulations for the (a) T-1-D and (b) T-5-D cases. The orange panels mark the design water level.

2.3 Metocean condition and statistics

The metocean statistics include time-variant wave parameters such as wave direction, significant wave height, mean peak wave period, etc (CMEMS, 2021). The data also varies concerning the location (Lavidas & Polinder, 2019); thus, the location for the analysis must be clearly defined. Based on the location, the metocean statistics must be imported and processed for the analysis and displayed as a user-understood pictorial data format. Hence this module again is divided into two sub-modules:

1. Data extraction and processing
2. Visualization

2.3.1 Data extraction and processing

The time-variant wave data is extracted from a weather database Copernicus marine services (CMEMS, 2021) based on the requirements. The extracted data were sea surface wave from the direction, significant wave height, and mean peak wave period. To ease the process of data extraction, the location was chosen to be a point instead of an area as shown in Table 2.1 (refer to Section 2.1) The database follows the Baltic sea wave model hindcast product, which is based on wave model WAM cycle 4.6.2, and surface forcing from ECMWF's ERA5 reanalysis products (CMEMS, 2021).

The wave direction from the extracted metocean statistics is divided into equal intervals to ease the processing because of its continuous variability. Based on the intervals the histogram counting algorithm is applied to obtain the occurrences at each interval. This would result in the marginal probability distribution of significant wave heights with the direction groups. The obtained marginal probability distribution of significant wave heights along with direction groups is used to produce the results of data extraction for demonstration.

The data on wave direction across all the heading directions is not necessary for the risk analyses as the worst-case scenario is concerned. Therefore, the maximum likely occurring wave direction with one standard deviation data is chosen for the simulation and it is believed that this interval consists of all the encountered wave heights. Hence the corresponding significant wave heights that belong to the interval are extracted separately and given as an input for the seakeeping and stability analyses in the later stage. The detailed flow of the above-described sub-module is illustrated in Figure 2.7.

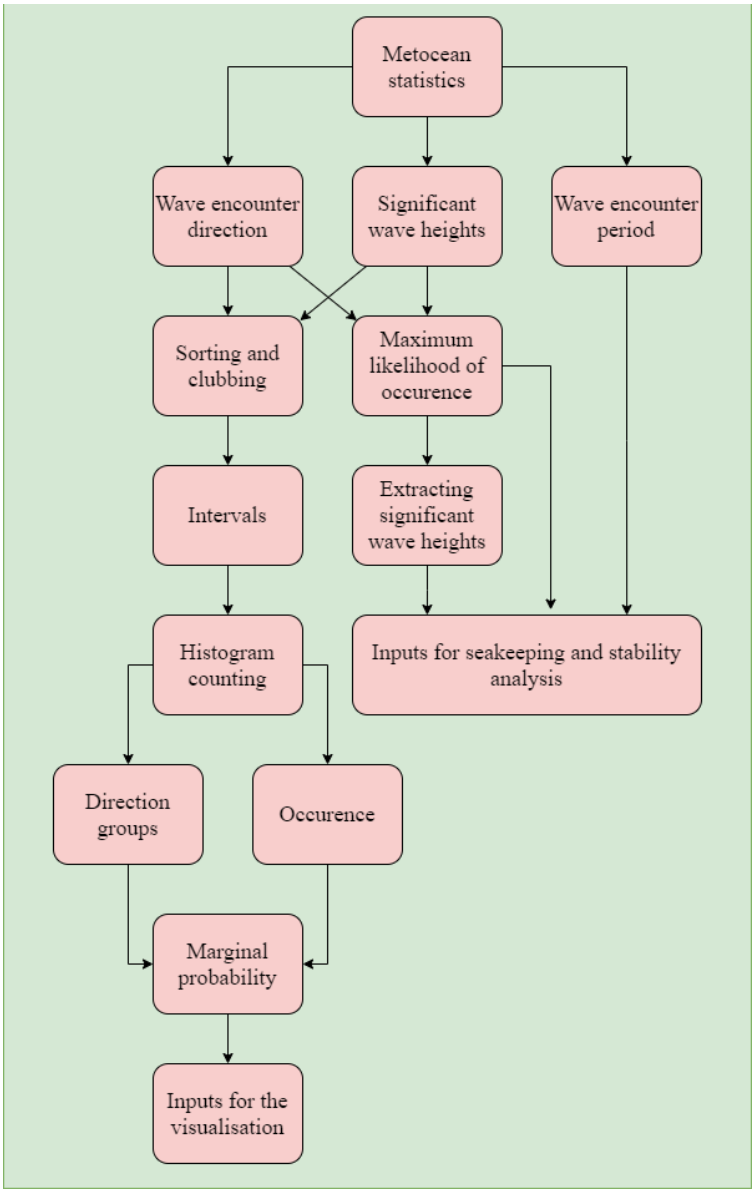

Figure 2.7 Flowchart for data extraction and processing.

2.3.2 Visualization

Marginal probability and direction groups obtained as an input from the data extraction and processing sub-module should be displayed as a user-understandable result. Thus, a rose plot is used similar to the concept used by Lavidas & Polinder (2019) for the illustration of the probability of occurrence of encountered significant wave heights against different wave directions at the specified location. As seen in the example displayed in Figure 2.8, there are a set of bars representing the probability of occurrence of significant wave height with an increasing radius representing their magnitudes, and the colours representing different wave heights. Here, the wave direction is defined as the wave travelling towards the centre of the rose plot.

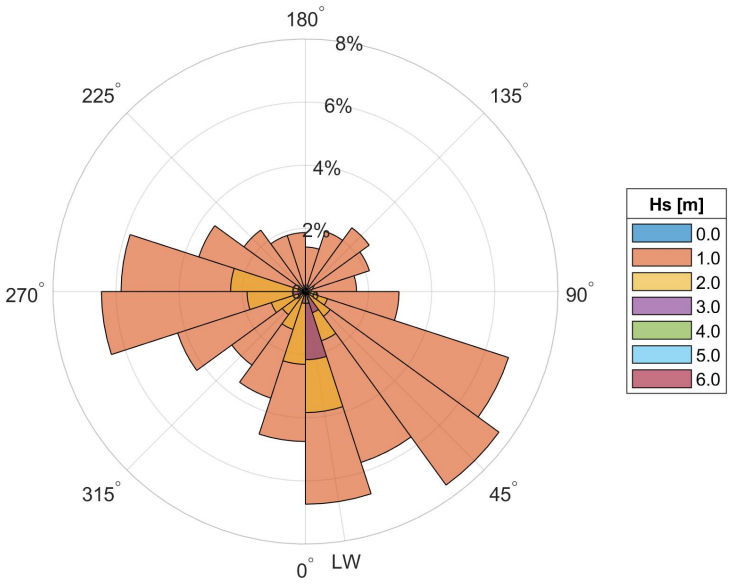

Figure 2.8 Example of a weather rose plot.

2.4 Seakeeping and stability analyses

The seakeeping and stability analyses mainly consist of seven stages as shown in Figure 2.9. The gathered data is then sorted into different seasons every year and then combined to form the rose plot as shown in Figure 2.8. These rose plots serve as the basis for the inputs that an analysis tool takes to determine the motion responses of the ship and the compartment flooding. Here the seakeeping and stability analyses will be carried out using the SIMCAP code developed by Schreuder (2014).

The results of the simulations conducted with the SIMCAP code give the motion responses of the RoPax ship. Along with the motion responses, the time to capsize is also obtained in the simulations done. The time to capsize is the time that a RoPax ship takes to exceed the 20° roll angle. A roll angle of 20° is chosen from the methodology developed by Schreuder (2014) as choosing any other definition for time to capsize would not result in a change in the time. Along with this, from the motion responses produced by the SIMCAP simulations, the roll angle of the RoPax ship never goes below 20° if it goes beyond it. The time that the ship takes to capsize completely is one of the main criteria to determine the consequences that may occur at this time. For the tanker vessel, the rate of discharge of water or oil from the damaged compartment is also calculated from the compartment flooding results obtained from the analysis, which is the other main criteria to determine the consequences. These consequences are then used to calculate the risk involved. The working of the SIMCAP code is given in Section 2.4.2.

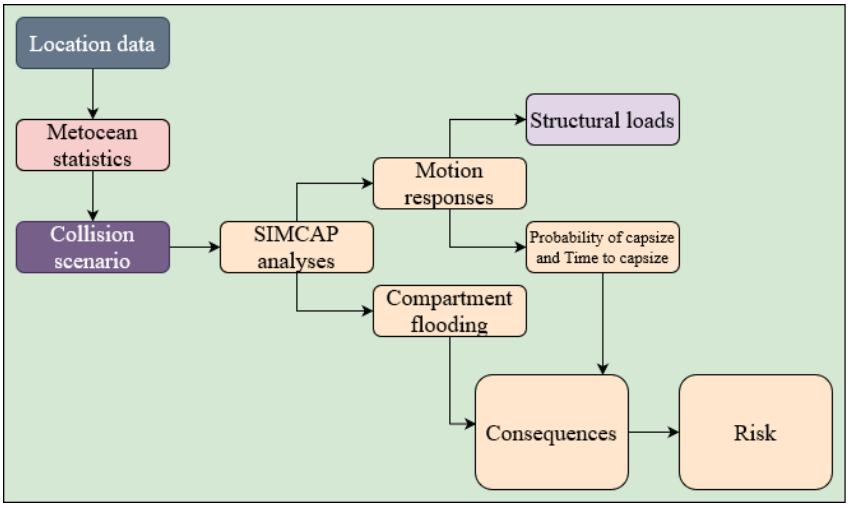

Figure 2.9 Risk assessment of ship stability.

2.4.1 Main dimensions of the model

The main dimensions of the damaged RoPax ship that is considered in this thesis, which is similar to the ship in the study done by Schreuder (2014) are given in Table 2.4.

Table 2.4 Main dimensions of the RoPax ship (Schreuder, 2014).

Parameter	Unit	Value
Length, Lpp	[m]	137.4
Breadth, moulded	[m]	24.2
Draft, aft	[m]	5.61
Draft, forward	[m]	5.17
Displacement	[m^3]	12,046
Vertical centre of gravity, VCG (above BL)	[m]	10.62
Metacentric height, GM	[m]	1.17
Radii of gyration in air, roll	[m]	8.954 (0.37*B)
Radii of gyration in air, pitch	[m]	37.1 (0.27*Lpp)

The dimensions of the tanker that is used in this thesis are similar to the tanker used for the development of the methodology for simulations of structural integrity done by Kuznecovs et al. (2021a) as shown in Table 2.5.

Table 2.5 Main dimensions of the tanker (Kuznecovs et al., 2021a).

Parameter	Unit	Value
Length overall, LOA	[m]	139.9
Length, Lpp	[m]	134.0
Breadth, B	[m]	21.5
Draft, T	[m]	7.4
Longitudinal centre of gravity, LCG	[m]	69.3
Centre of gravity, KG	[m]	5.0
Deadweight, DWT	[tonnes]	11,500
Total displacement	[tonnes]	16,200

2.4.2 SIMCAP analysis

The SIMCAP code is a numerical tool that was developed in an attempt to create a methodology for simulating damaged and intact ships in waves by Schreuder (2014). This tool was developed to study the motion responses of damaged ships in waves or the flooding of a ship that was damaged in a ship-ship collision as described in Section 2.2 and the time to capsize. As mentioned in Section 1.3 the damaged ship has no forward speed at the time of the collision.

This tool is also capable of assessing the different stages of compartment flooding realistically. This approach can in turn produce situations where the heel angles have exceeded 20°, which is the final angle of equilibrium (Schreuder, 2014). This also allows the assessment of progressive flooding through the damage openings and the different doors in the ship. The SIMCAP code uses a non-linear time-domain strip theory approach to accomplish these tasks (Schreuder, 2014).

For the stability analysis, the compartment is assumed to have no fluid inside it. After the collision, the only flow of fluid that takes place is the flow of seawater into the compartment. This is analysed through the SIMCAP code which gives the time for the compartment flooding and determines the stability of the ship.

The data obtained is then used to perform the analysis of the motion responses and compartment flooding using the SIMCAP code developed by Schreuder (2014). This code uses significant wave heights and wave encounter direction as the input. The different significant wave heights determine the sea states and the wave encounter frequency with the following equation (Schreuder, 2014),

$$T_p = 4\sqrt{H_s} \tag{2.1}$$

From Equation 2.1, the significant wave heights that were given to the tool as input which is then used to calculate the peak wave period. Here, the constant '4' is obtained from the simplification of other constant values which include g (acceleration due to gravity) and ρ_w.

The simulation is carried out for 750-time steps. These time steps are of two seconds each, with a total of 1500 seconds. In cases where the ship capsizes, the simulation is stopped after the ship achieved a roll angle of 180°, as seen in Figure 2.11. In cases where the ship does not capsize, the simulation was stopped prematurely as continuing the simulation would serve no purpose given that there would be no change in the weather conditions.

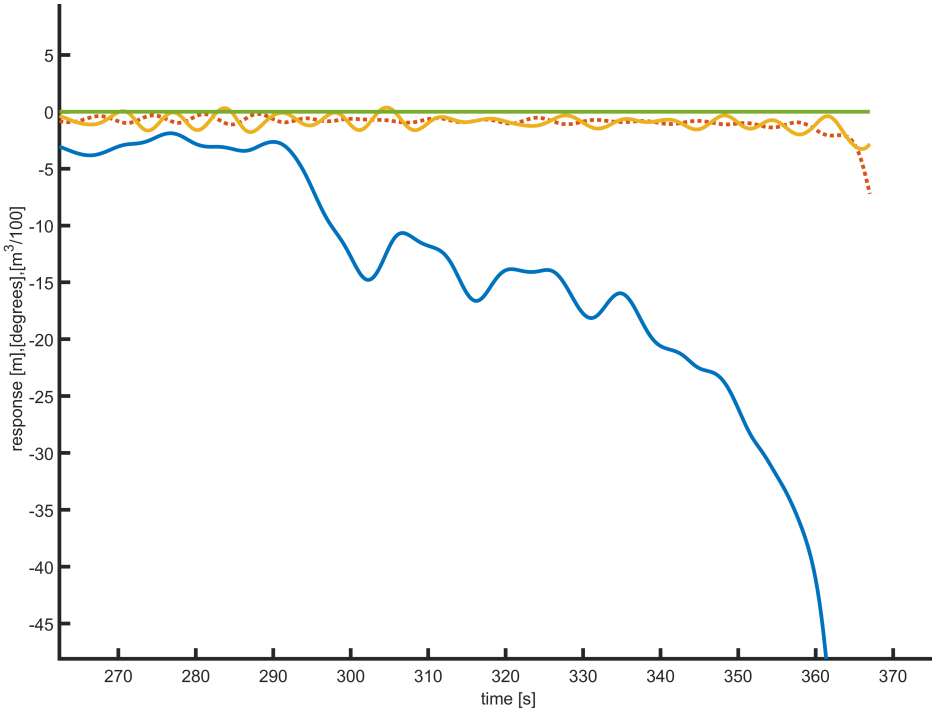

Figure 2.10 A section of the motion responses of the RoPax ship for a significant wave height of 3m and wave heading angle of 180°.

As given in Table 2.6, the significant wave heights obtained for both locations lie within a range of 6 m ranging from 0 m to a maximum of 6 m (refer to Section 3.1.1). Since the significant wave heights occur from different directions throughout the year, changing seasonally, the wave heading angles used for the simulations were in the range of 0° to 315°. In this thesis, waves with 0° heading angles are following waves and waves with 180° heading angles are head waves, which makes waves with heading angles of 90° and 270°, beam waves.

Table 2.6 Input weather data for SIMCAP simulations of the RoPax ship and tanker.

Time steps	750	1500 seconds						
Significant wave heights (m)	0	1	2	3	4	5	6	
Wave heading angles (deg)	0	45	90	135	180	225	270	315

The SIMCAP code generates two plots, a plot of the motion responses and another plot showing the compartment flooding. Figure 2.11 shows the plot of the motion responses for a wave height of 3 meters and a wave encounter direction of 180°. The contents of this plot are discussed in Chapter 3. Another plot that the SIMCAP code produces is the flooding in the damaged compartment and an example of it is shown in Figure 2.12.

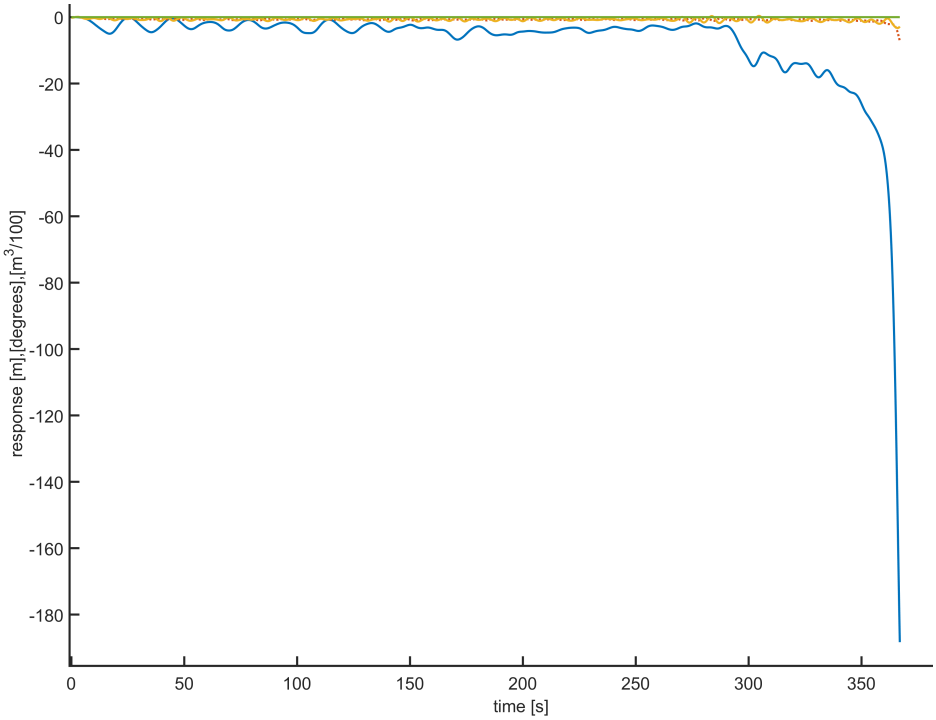

Figure 2.11 Full motion responses of the RoPax ship for a significant wave height of 3m and wave heading angle of 180°.

Figure 2.12 shows the compartment flooding of the RoPax ship for a significant wave height of 3m and a wave heading angle of 180°. As mentioned in Section 2.2, the four spaces damaged in the collision are the car deck, the main engine room (MER), and two spaces aft of the MER, represented by the red, black, blue, and green lines respectively. The car deck takes on the most amount of sea water as the volume of the car deck higher than the three other spaces considered.

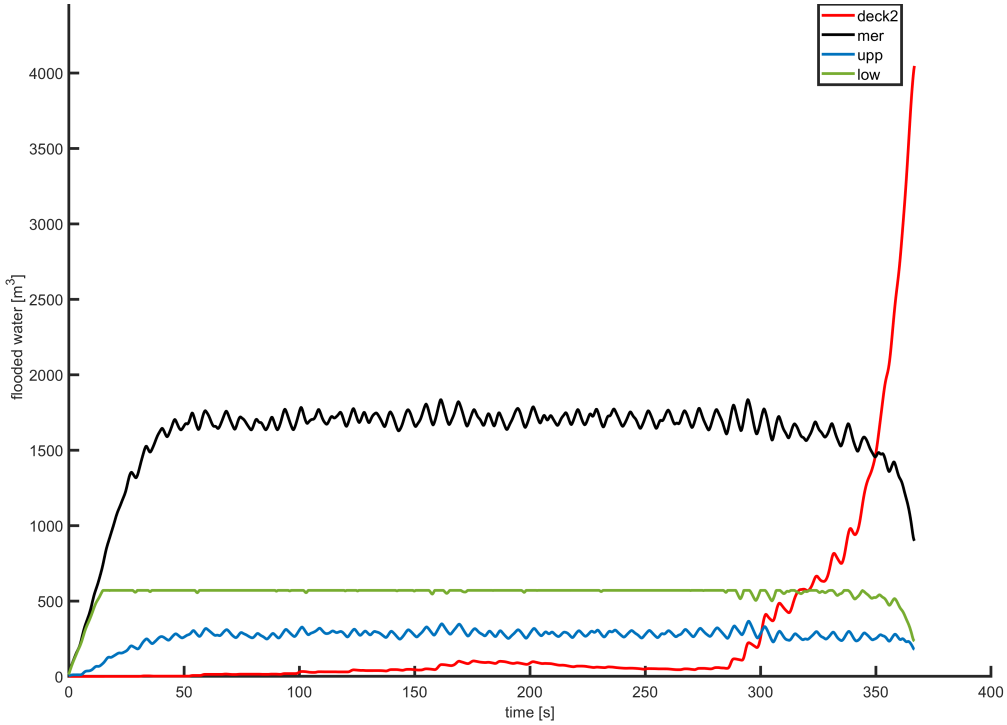

Figure 2.12 Compartment flooding of the RoPax ship for a significant wave height of 3m and wave heading angle of 180°.

2.4.3 Survival probability

IMO has guidelines specifically for the maximum time for evacuation for the RoPax ferries on fire incidents. The maximum time for evacuation refers to safely evacuating the crew and the passengers. It is mentioned in the document MSC.1/Circ.1238 (IMO, 2007) that the upper limit for the time for evacuation in RoPax ferries is 60 min. The time required for the evacuation could be estimated using the basic hand calculation or using some advanced techniques which saves time. The basic hand calculation manually computes the time required for each person to reach the rescue point and uses the hydraulic network principle for the formulation (IMO, 2007). And the advanced techniques use software to compute the evacuation time by using regression analysis formulae (IMO, 2007). From this information, the survival probability of crew & passengers could be estimated as,

$$P_{Survival} = \frac{T_{Actual}}{T_{Max}} \tag{2.2}$$

where, T_{Actual} - Actual time available for evacuation
T_{Max} – Maximum time for evacuation suggested by IMO

In case of collision, RoPax vessel has a higher tendency to capsize due to compartment flooding, unlike fire incidents. Extensive research from Vanem & Skjong (2004) on survival probability considering the probability of capsizing suggests that the maximum time for the evacuation during the collision and grounding scenarios in RoPax ferries must be between 10-15 min. To have a conservative approach on the assessment the least value of 10 min is considered as the maximum time for evacuation. Here the actual time available for evacuation can be regarded as the time needed for the vessel to capsize. Hence, the survival probability in this thesis is estimated as,

$$P_{Survival} = \frac{T_{Capsize}}{T_{Max,modified}} \tag{2.3}$$

where, $T_{Capsize}$ – Time for capsizing
$T_{Max,modified}$ – Modified maximum evacuation time; Vanem & Skjong (2004).

To check the sensitivity of the risk on the choice of a maximum time from the range suggested by Vanem & Skjong (2004), a sensitivity analysis is conducted.

2.4.4 Damage stability risk

The term risk here is evaluated by adopting the definition mentioned in the Formal Safety Assessment guidelines by IMO (2018). Thus, the risk is formulated as the product of the probability and the corresponding consequences of the hazard. The hazard considered due to the damage stability here is the capsizing of the vessel. The consequences are hence the loss of human lives onboard the vessel.

The action of capsizing of the vessel depends on the significant wave height and similarly, the consequence considered on the hazard depends on the inability to evacuate people from the damaged vessel. Thus, the probability of hazard in the damage stability risk will be the joint probability of occurrence of significant wave height and human fatalities. In this thesis, the probability of human fatalities is estimated with the help of survival probability (refer to Section 2.4.3). The quantification of the

consequences of human fatalities is adopted from IMO (2018). The following Equations 2.4 and 2.5 describe the methodology incorporated, where F denotes the fatality:

$$R_{Damage\ stability} = P(Hs\ \cap F) \times Consequences \quad (2.4)$$

$$R_{Damage\ stability} = P(Hs) \times \big(1 - P(Survival)\big) \times Consequences \quad (2.5)$$

2.5 Structural integrity simulation and ULS risk

To analyse the structural integrity of any vessel in the middle of an ocean, the primary concern should be to transform the non-linear wave loads into structural loads that can be simulated in a real-time situation. There are several methods suggested in the classification societies to transform the external loads. DNV GL AS (2018) in its description of wave loads suggested two methods to transform the external loads: Load transfer by pressure mapping; Load transfer by force mapping.

Tuitman et al. (2013) also found the structural response due to wave loads inspiring from the methods suggested by DNV GL AS (2018). The works of Xie et al. (2020) and Zhu et al. (2020) on mapping the seakeeping results on the structural deformation are also influenced by the methods suggested by DNV GL AS (2018). Zhang & Pedersen (2017) highlighted using a progressive collapse approach for estimating structural integrity. Researcher Yamada (2014) approximated the collision event to be an energy absorption incident for evaluating the structural integrity of the structure.

In this thesis, the structural integrity simulation is done using three steps: simulating the ultimate bending moments of the vessel, generating the structural loading history from the motion responses, and assessing the safety level of the vessel (Kuznecovs et al., 2021a). A brief overview of the module is displayed in Figure 2.13Figure 2.13. The motion responses indicated in Figure 2.10 are directly obtained from the results of the SIMCAP simulation on the stability and seakeeping analyses (Kuznecovs et al., 2021a). This data is regarded as the primary input for the structural integrity simulation.

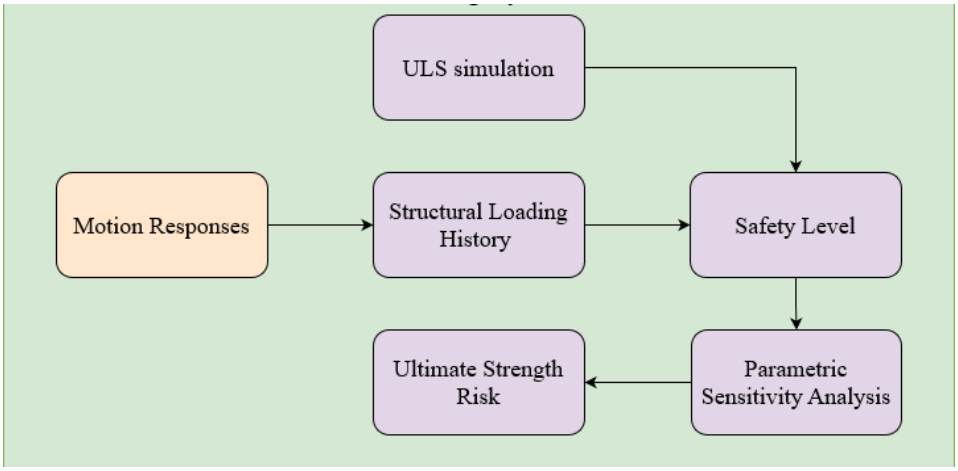

Figure 2.13 Structural integrity simulation methodology.

2.5.1 ULS simulation

For the ULS simulation, Yamada (2014) proposed an approach of using residual strength index (RSI) that indicates the amount of decrease in the ultimate strength of the vessel after damage. As an extension to this research Kuznecovs (2020) has done

quite an extensive investigation on the available methods for computing the ultimate bending moment. Kuznecovs (2020) stressed establishing proper damage opening characteristics in a finite element collision model else the ULS might have an overestimated value of up to 40%.

As a result of the research on ultimate and residual strength assessment of ship structure, Kuznecovs (2020) developed a tool URSA that is being used in this thesis to estimate the ultimate bending moments in the biaxial loading using the progressive collapse approach. Here the material used in the vessel structure is assumed to be elastic-perfectly plastic. The overview of the sub-module is displayed in Figure 2.14Figure 2.14.

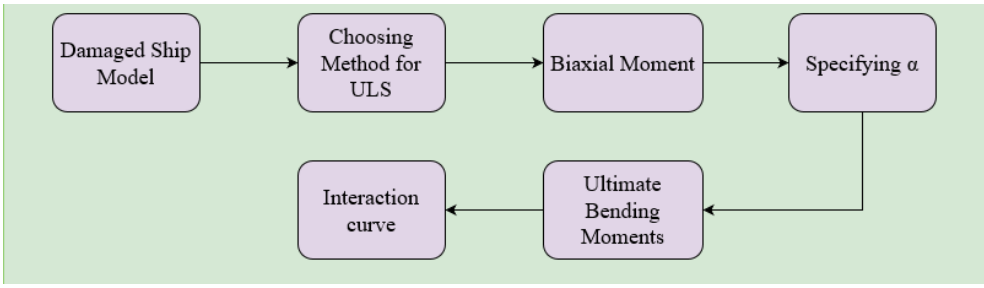

Figure 2.14 Overview of URSA.

The results from tool URSA (Kuznecovs, 2020) are used to understand the ultimate strength of the vessel section in biaxial bending loads (moments). It is named interaction curves, an example for the interaction curves is displayed in Figure 2.15Figure 2.15, where M_V is the pure vertical bending moment, M_H is the pure horizontal bending moment. This data is considered as one of the inputs for the safety assessment task while comparing the ultimate strength to the loading history. The tool URSA will not be used directly in this thesis rather considered as the backbone of this Section as all the inputs for developing the methodology is obtained from tool URSA. Thus, only the overview of tool URSA is presented here, the detailed description could be found in Kuznecovs (2020).

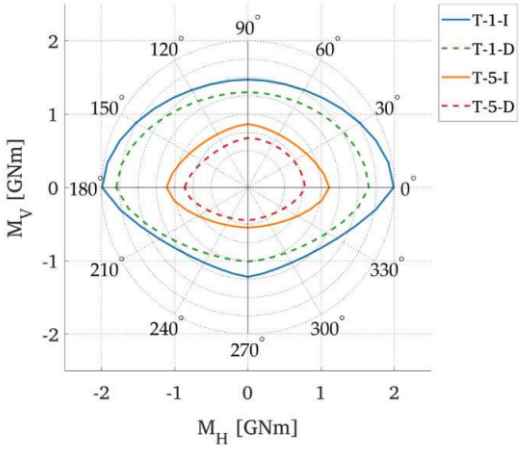

Figure 2.15 Ultimate biaxial moments interaction curve (Kuznecovs et al., 2021a).

2.5.2 Structural loading history

The structural loading history is computed by carrying out the seakeeping calculation on the obtained motion responses from the stability analyses as shown in Figure 2.10. The structural loading history by its name suggests computing the time history of the

wave loading. Again, the loading history is also obtained in terms of biaxial moments due to the change in the wave encountering angle.

This data is recorded for different vessels and damage scenarios described in Section 2.2 and used during the estimation of ultimate bending moments. The recorded data is then given as inputs for the safety assessment.

2.5.3 Safety assessment

The concept of structural adequacy (SA) has been used to evaluate the structural safety level of the vessel as suggested in the works of Kuznecovs et al. (2021a). Structural adequacy is defined as a ratio of the loading demand and the loading capacity of the structure. Here the loading capacity is a defined parameter based on the ultimate strength of the structure. If the capacity is defined as the ULS of the structure, then the structural adequacy of one represents the structure reaching its ultimate limit state (ULS).

Here Dang Van criterion on multiaxial high cycle fatigue is taken as an inspiration to assess the safety parameter η (structural adequacy) (Kuznecovs et al., 2021a). Structural adequacy is calculated for all the bending moment time series for all sections of the vessel. And both the capacity and demand interaction curves are plotted on one another. The demand here is the instantaneous total bending moment due to wave loads and capacity is the distance between the origin to the capacity curve closest to the demand (Kuznecovs et al., 2021a). Then the structural adequacy is calculated based on its definition, for the corresponding section of the vessel. The maximum obtainable value at each section is compared with all the sections and a maximum value among them is considered as the final structural adequacy value for the whole vessel as shown by Kuznecovs et al. (2021a).

The structural adequacy values are also computed for different wave encountering directions and the significant wave heights and illustrated using a polar plot; see Figure 2.16. Here the red dot indicates the vessel is damaged on the port side and different colours on the plot define the structural adequacy measure of the vessel for that combination of wave encounter angle and significant wave height.

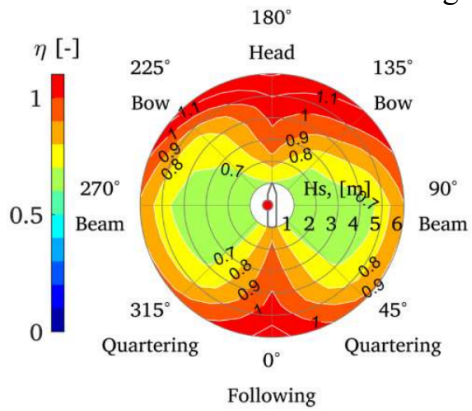

Figure 2.16 An example of structural adequacy polar plot.

2.5.4 Parametric sensitivity analysis

To assess the sensitivity of the safety level obtained in Section 2.5.3, an engineering approach of parametric sensitivity analysis is being done. This analysis will be done by introducing a partial safety index to both the inputs (capacity & demand) of structural adequacy for determining the safety level. This partial safety index accounts for the

uncertainties associated with the computation of both capacity and demand. The goal here is to achieve partial safety indexes below which the result does not or negligibly have any influence from the input variables.

2.5.5 Relative wave encountering angle

It is understood from the safety level assessment made in Section 2.5.3 that, SA plot does not depend on the ship heading direction instead it depends on the wave encountering direction along with the significant wave height. Thus, the quadrants of the SA plot are kept unchanged and defined for the ship axis (ship reference) pointing the bow towards 180º as shown in Figure 2.16. For this reason, the heading direction of the ship is always defined with the earth reference axis as in the compass.

The maximum likely wave encountering direction is extracted from the weather rose plot (refer to Section 2.3.2) which again is defined in the earth reference. Hence, there would be no difference in the wave encountering direction if the ship is pointing its bow towards the north since the 180º of both the references (earth & ship) coincide, as shown in Figure 2.17(a).

While considering other heading directions for the ship as shown in Figure 2.17(b), it is well inferred that for the assessment of safety level in the SA plot, the wave encountering direction must be a relative measurement.

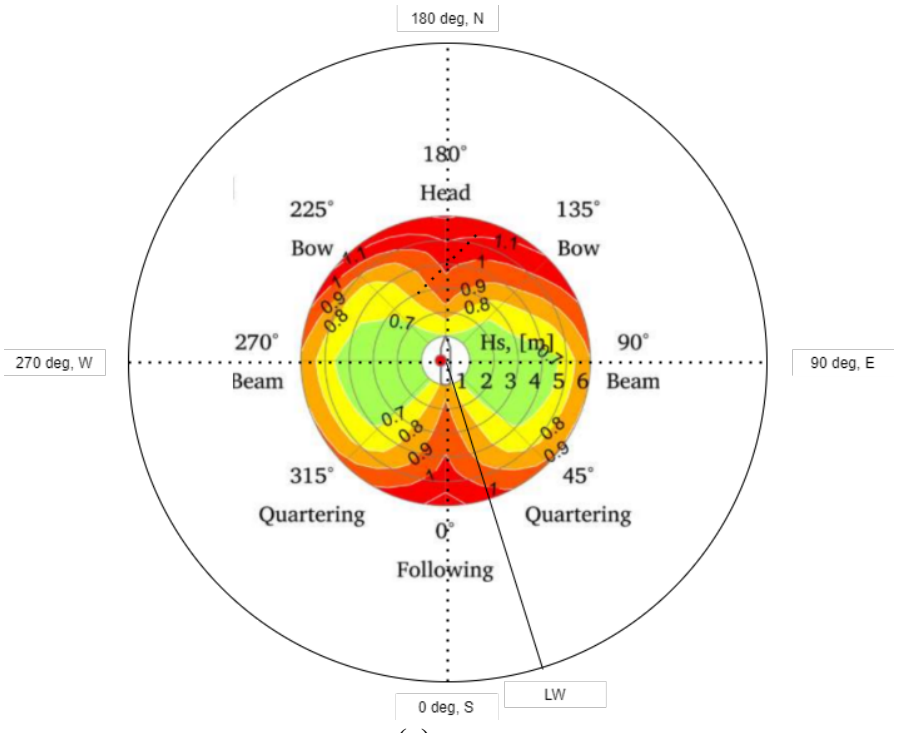

(a)

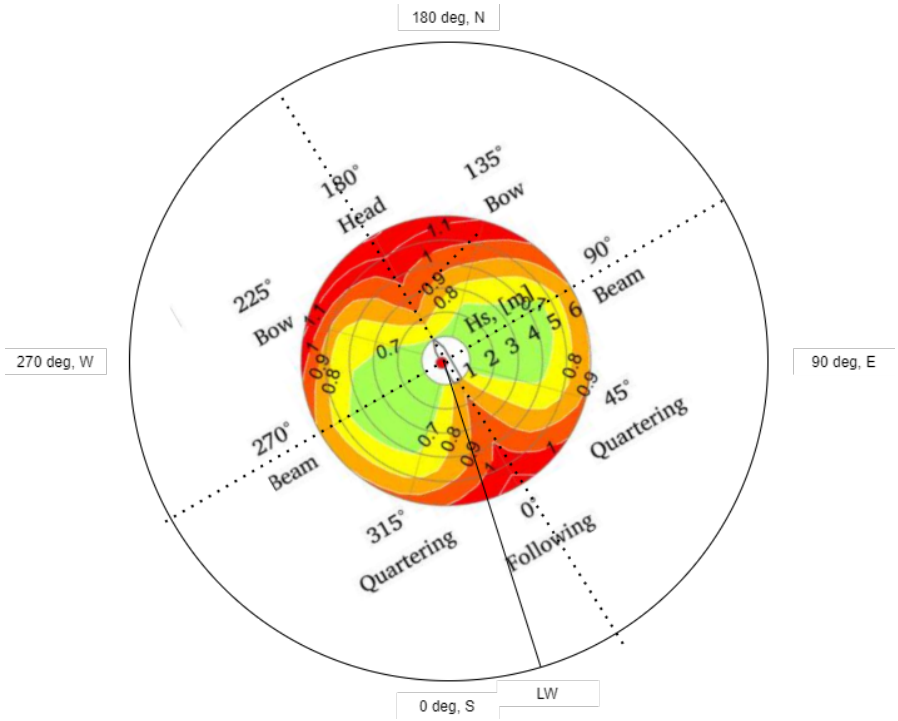

(b)

Figure 2.17 (a): Coinciding earth reference and ship reference axes, (b): Relative wave encountering angle for different heading direction.

The relative wave encountering angle is computed as described in the following steps:

$$Diff = 180 - \theta \tag{2.6}$$

$$\varphi_r = Diff + LW \tag{2.7}$$

If $\varphi_r < 0$

$$\varphi_r = \varphi_r + 360 \tag{2.8}$$

If $\varphi_r \geq 360$

$$\varphi_r = \varphi_r - 360 \tag{2.9}$$

where, θ - heading direction

φ_r - relative wave encountering angle

LW - maximum likely occurring wave direction

2.5.6 Probability of exceedance of ULS

The φ_r obtained from Section 2.5.5 is used for computing the structural adequacy values. The existing structural adequacy table has only the values corresponding to wave directions defined as the multiples of 45º. Thus, the values corresponding to the relative wave encountering angle other than multiples of 45º are obtained via the linear interpolation technique.

As seen in the structural adequacy polar plot in Figure 2.16, the concentric circles correspond to the increasing magnitude of the significant wave height. Here the probability of occurrence of danger SA could be assessed using the probability of occurrence of significant wave heights. This probability of occurrence of significant wave heights is already obtained from the weather rose plots (refer to Section 2.3.2). Hence, an inspection algorithm is set up to estimate the probability of danger SA or exceedance of ULS (P_{ULS}) and is computed as described below in Equation 2.10.

$$P_{ULS} = \sum P(Significant\ \ wave\ heigths|SA \geq 1) \quad (2.10)$$

2.5.7 ULS consequence and risk

In this thesis, the consequences to a damaged tanker after the exceedance of ULS are defined by establishing two options based on the information on ship-ship collision legal actions for the insurance claims (Williams, 2013). The two options are *Vessel abandoned* and *Vessel repaired*. Based on the real-time situation, these options could be chosen to predict the quantified consequence. The operations and activities happening exclusively in the above-defined options are described below.

If the vessel is abandoned, then it is considered that the total cargo present in the structure will be lost. Along with the cargo, the ship owners lose the present worth of the vessel (Williams, 2013). The crew members must be rescued before or after abandoning the vessel, and if any crew members are dead or injured must be compensated (IMO, 2018). Thus, the consequence of this option is the summation of all the activities and operations explained in this paragraph.

If the vessel is chosen to repair, it is considered that the cargo is fully recovered in the salvage operation. The activities after towing will be the repairs in the dockyard. So, the dockyard operation cost, the damaged equipment cost for replacement, lost revenue of the vessel on the days of repair along with compensating for the deaths and injuries of the crew members will be the consequences the shipowners need to bear.

To account for the market fluctuations on the oil price and vessel freight charges in the consequence quantification, a miscellaneous factor is defined to have a reasonable result. The cost of a crew death and injury is taken from IMO (2018), the details of the same are displayed in Table 2.7.

Table 2.7 Details of crew fatality and injury taken from IMO (2018).

Cost of fatality	4.61 mUS$
Cost of an injury	0.13 mUS$

Here the cost of an injury is evaluated as Quality Adjusted Life Years (QALY) and cost of fatality as Gross Cost of Averting a Fatality (GCAF). The values displayed in Table 2.7 corresponds to a relation: one prevented fatality equals 35 QALY. The detailed procedure for consequence quantification is documented and presented in Appendix 2. The ULS risk is computed using the guidance from IMO (2018), which is expressed as shown in Equation 2.11.

$$R_{ULS} = P_{ULS} \times Consequence_{ULS} \quad (2.11)$$

2.5.8 ULS risk mitigation action

Understanding the structural adequacy polar plots described in Figure 2.17, the main parameter that influences the ULS exceedance probability is φ_r. Thus, by changing the φ_r for the damaged vessel, the ULS exceedance probability can also be changed because of the variation of the structural adequacy values based on the φ_r as seen in Figure 2.17. Here since the damaged vessel is assumed to be of no forward speed, changing the φ_r refers to a smart manoeuvring of ship to a different heading direction.

As described above, the same methodology is repeated to give the ranking for the safe heading direction after collision. This is an iteration process where the P_{ULS} is checked

with all the standard wave encountering direction (multiples of 45° shown in Figure 2.16) and the minimum among them is saved as the Least P_{ULS}.

$$\theta_{safe} = \theta_{init} - (\varphi_{Least\ P_{ULS}} - \varphi_r) \quad (2.12)$$

where, $\varphi_{Least\ P_{ULS}}$ - wave encountering angle with least P_{ULS}
θ_{init} – initial heading direction
θ_{safe} – safe heading direction

To know how safe the proposed heading direction is for risk mitigation, a term safety measure is introduced in terms of percentage to express the level of safety with the proposed heading direction. Here a safety value of 100% refers to the probability of exceedance of ULS in the proposed heading direction as 0%.

$$Safety\ measure = 100 - P_{ULS} \quad (2.13)$$

2.6 Environmental impacts and risk

The environmental impacts and risks are studied using three major steps: estimation of the cargo outflow (oil discharge), simulation of the oil drift on the specified location, and finally the consequence analysis due to the oil leakage. A brief overview of the module is illustrated in Figure 2.18.

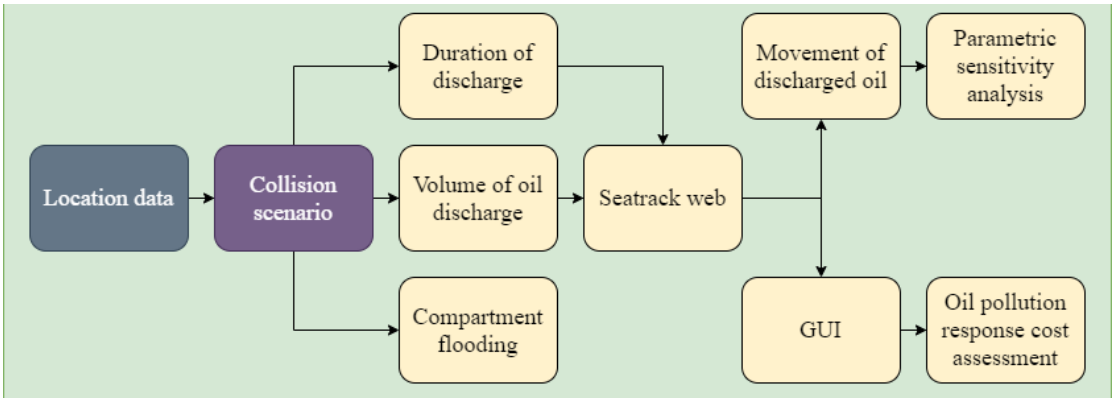

Figure 2.18: Overview of the environmental impacts and risk.

2.6.1 Simulation for oil drift

To quantify the consequences of the environmental impacts it is necessary to understand the drift of the oil once discharged into the seawater. Based on the density, viscosity, weather, sea currents, etc. the discharged amount of oil expresses its unique drift (Liungman & Mattsson, 2011).

Here the scope of the simulation is to understand the drifting pattern of discharged oil, the duration it takes to reach the shoreline, and the volume of discharged oil that stays on the water surface. To analyse these many parameters Seatrack Web (2021), a web application to simulate oil drift from points sources which was developed by SMHI (2021) will be used. This tool is well-known for meteorological simulations and is also used for the environmental rescue service by the Swedish coast guards (Olofsson & Eliasson, 2020).

The input parameters needed for the Seatrack Web continuous oil spill (SMHI, 2018) are listed below:

1. Discharge date and time
2. Discharge outlet depth
3. Discharge location (latitude & longitude)
4. The duration for the simulation
5. The type of oil being discharged
6. The volume and duration of the discharge

A simulation model will be generated for the given inputs and as a result, an animation of the oil drift and a numerical pattern of drift along with the corresponding numerical data points is obtained. An example of the results is displayed in Figure 2.19.

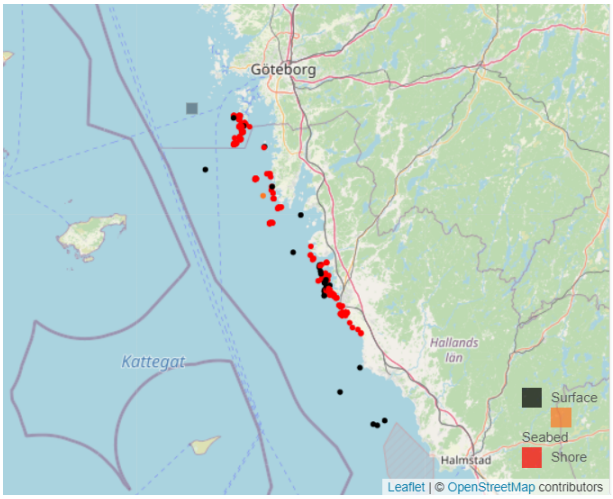

Figure 2.19 Example screenshot of Seatrack Web simulation animation result (Seatrack Web, 2021).

2.6.2 Parameters for oil drift simulation

For the oil drift simulation, the worst-case scenario for the environment according to this thesis was taken into consideration, that being the collision of tankers. As there could be scenarios where tankers collide, the possibility of cargo oil being spilt must be considered. Among the input parameters described in Section 2.6.1, only the location, the date of observation, the type of oil, and the amount of oil discharge are considered in this thesis for a parametric sensitivity analysis.

Although Seatrack Web (2021) does not take into account the source of the discharge, it should be noted that the oil drift simulations are done for discharges from tankers only and not from collisions between RoPax ships. Therefore, at this stage, it is necessary to specify the oil type that is discharged into the seawater due to the collision damage. The oils that are discharged can be largely categorized into three different categories based on their viscosity as done in the Seatrack Web (2021) application as this is the easiest way to differentiate between the oils and they are as follows:

1. Light oils (0-100 cSt)
2. Medium oils (100-1000 cSt)
3. Heavy oils (>1000 cSt)

where cSt is centistokes which is equivalent to millimeters^2/second [mm^2/s]. This is mainly done to simplify the simulations and narrow down the most impactful oil types among the three as there are too many types of oils that must be accounted for

otherwise. The discharge of these oils is then calculated with the assumption that the water does not enter the compartment that is damaged simultaneously. This is again done to simplify calculations as calculating both, the inflow of water and outflow of oil to and from the damaged compartment is beyond the scope of this thesis.

The size of the damage opening and the rough edges of the hole on the ship are two parameters that determine the rate of flow of oil from the ship, assuming the properties of the oil being discharged are known. The rate of discharge of the oil flow can then be calculated assuming that the damage opening is circular using Equation 2.14. This assumption is done to reduce the complexity of calculating the discharge through an irregular damage opening which would be a study on its own. It should be noted that this equation is simplified to narrow the scope of this thesis and needs to be improved in the future. The mass flow rate of the oil can be calculated with the following equation:

$$M = \rho \times A \times V \times C_d \tag{2.14}$$

where, ρ = Density of the fluid
A = Area of the hole
V = Velocity of discharge
C_d = Coefficient of discharge at the damage opening

The above equation is then used to calculate the mass flow rate of the oil being discharged. However, this equation does not consider the different motions of the ship which will change the rate of discharge of the oil. As a result, for simulating the oil drift from the oil discharged from the tanker, the volume of oil spilt is taken in percentages of the total volume of the damaged compartment (refer to Section 2.2). Specifically, three different volumes of 134 tonnes, 670 tonnes, and 1340 tonnes, which correspond to 10%, 50%, and 100% of the compartment capacity respectively.

Along with this, the days on which the simulations must be done are also changed. Due to the limited availability of data on Seatrack Web (2021), the simulations were distributed over three weeks for a parametric sensitivity analysis. Taking all these parameters into account, the two locations (North and South, from Section 2.1), three days of simulations, three different viscosities, and three different discharge volumes, which in total would be $2 \times 3 \times 3 \times 3 = 54$ simulations as visualised in Figure 2.20.

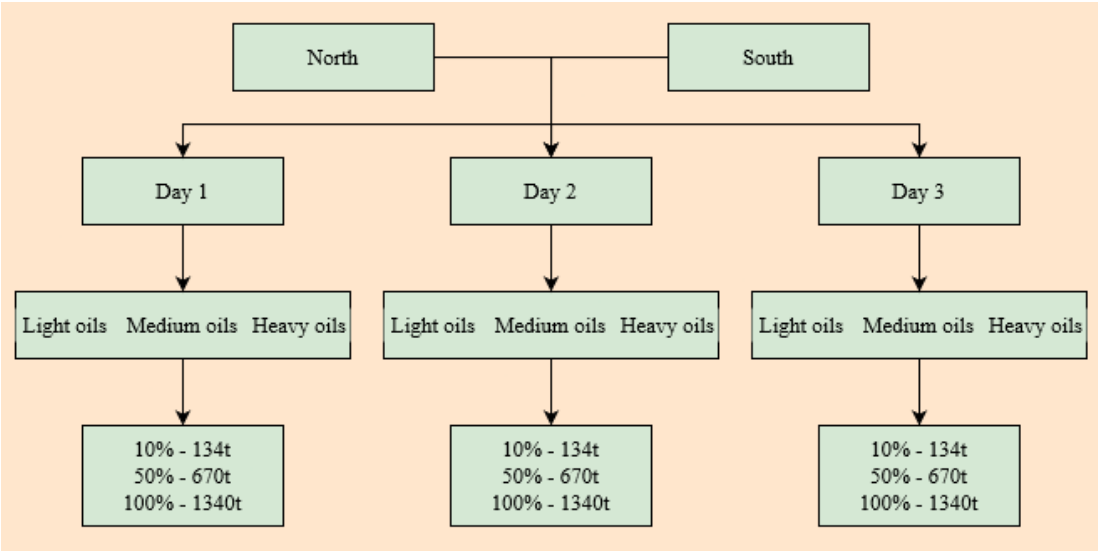

Figure 2.20: All possible combinations of the oil flow simulations.

2.6.3 Oil pollution response cost assessment

The results obtained from the Seatrack Web (2021) simulation such as the duration for the discharged oil to reach the shoreline, amount of oil on the seawater surface are used to understand a hypothetical coast guard operation after discharge. The 18 different hypothetical cases of oil discharge (3 volumes × 3 viscosities × 2 locations) as described in Section 2.6.2, had been discussed with the Swedish coast guard to obtain an approximate detail of their actions to prevent the impacts to the marine environment.

As per the suggestions from Swedish coast guard officials, the details of each operation such as the human resources, ships, boats, surveillance aircraft, environment protection equipment, etc. used for different hours with different numbers are estimated. The estimated data is compared with the monetary value guidelines (Wikingsson, 2020) of the Swedish coast guard to quantify the results of their operation.

3 Results and discussion

This Chapter presents the results obtained for the methodology presented in Chapter 2. The reasoning behind the obtained results and the assumptions that influence these results are also discussed in this Chapter. Section 3.1 displays the metocean conditions for different seasons followed by the seakeeping and stability analysis results in Section 3.2. Section 3.3 reflects the outcomes from the structural integrity simulation and describes the example scenarios to understand the feasibility of the developed tool. Finally, Section 3.4 displays the oil drift simulation results and discusses the importance of considering the environmental impact risks in the present world.

3.1 Metocean condition and statistics

To understand the metocean condition of the locations described in Section 2.1, the metocean statistics available from the past five years are extracted from CMEMS (2021) database. The extracted data is presented as the rose plots along with specifying the maximum likely occurring wave direction on the location. At last, to describe the variation of metocean conditions of the locations in detail, the difference in the probability of significant wave heights is presented.

3.1.1 Rose plots

The extracted metocean statistics from CMEMS (2021) are processed according to the methodology described in Section 2.3.1. The extracted data is based on the four different seasons from 2016 to 2020, and the illustration of the results is also done separately for 4 different seasons as shown in Figure 3.1 and Figure 3.2. Here the seasons are defined with 3 months of an interval as described in Table 3.1 and the LW in the rose plots refers to the maximum likely occurring wave direction.

Table 3.1 Definition of the seasons.

Season name	Spring	Summer	Autumn	Winter
Months covered	Mar-May	Jun-Aug	Sept-Nov	Dec-Feb

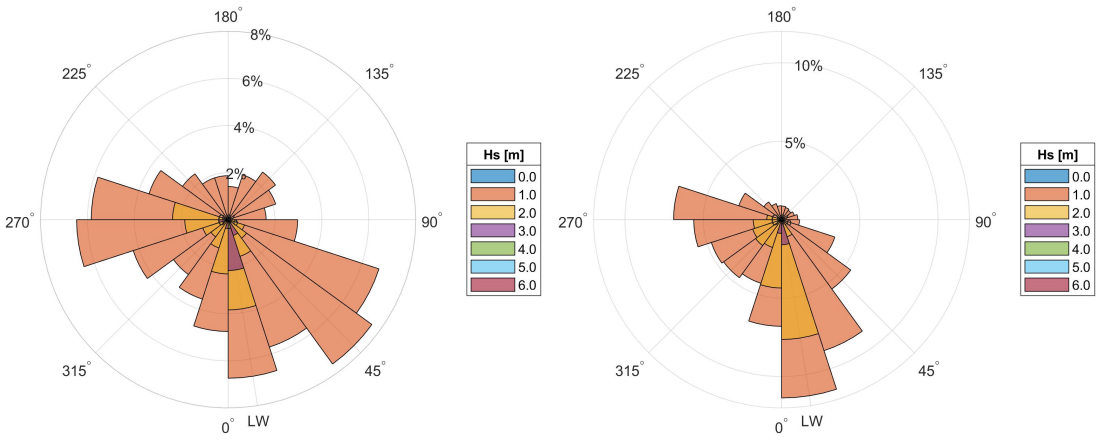

(a) (b)

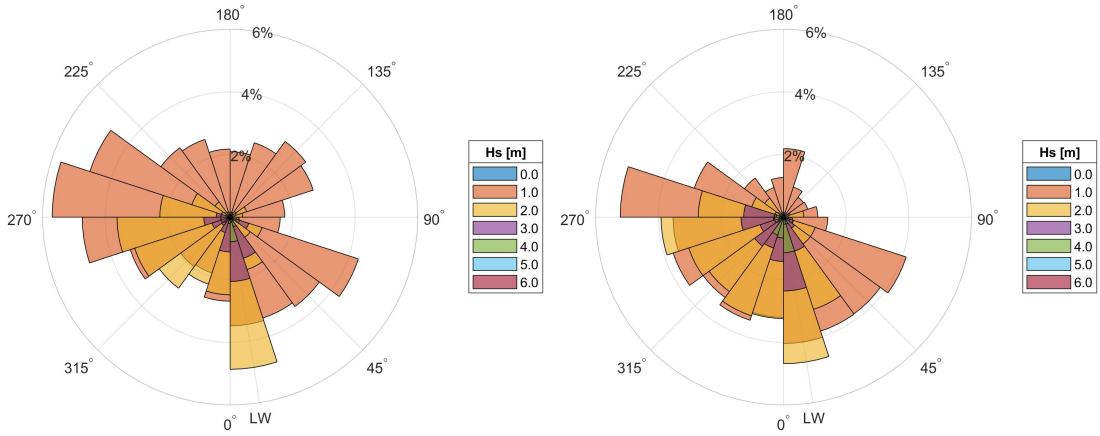

(c) (d)

Figure 3.1 Weather rose plot results for the location north. (a): Spring, (b): Summer, (c): Autumn, (d): Winter.

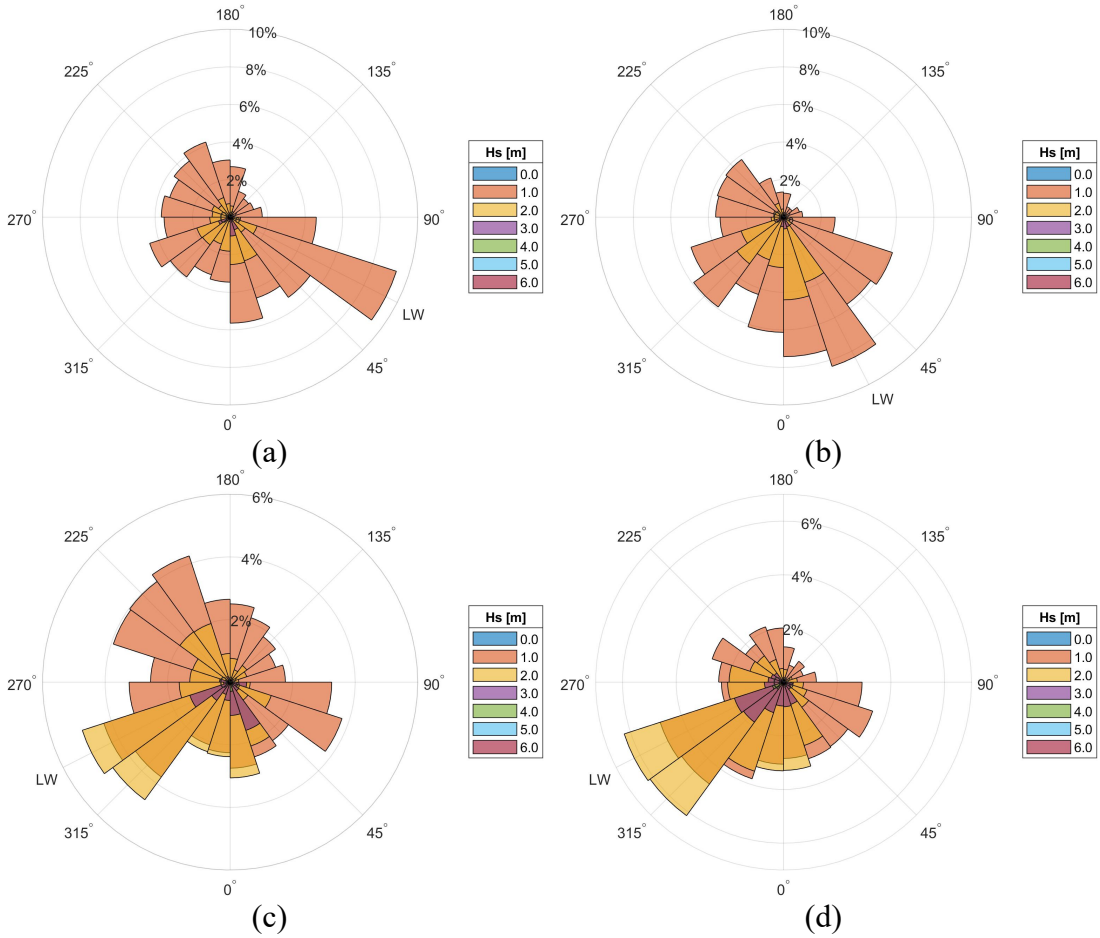

(a) (b)

(c) (d)

Figure 3.2 Weather rose plot results for the location south. (a): Spring, (b): Summer, (c): Autumn, (d): Winter.

3.1.2 Maximum likely occurring wave direction

The maximum likely occurring wave direction is assessed using the methodology explained in Section 2.3.1. The details of the result are displayed in Table 3.2. Except for the seasons, Autumn and Winter in location South, the maximum likely wave direction on the west coast of Sweden are always from the southeast direction.

Table 3.2 Results of the maximum likely occurring wave direction.

Location	Spring	Summer	Autumn	Winter
North	9°	9°	9°	9°
South	63°	27°	297°	297°

3.1.3 Probability of significant wave height

The probability of encountered significant wave heights is computed as described in Section 2.3.1. The rose plots displayed in Figure 3.1 and Figure 3.2, showed that the occurrence of significant wave heights above 3 m are negligibly insignificant. Hence, the significant wave heights between 3 to 6 m are clubbed together while displaying the results in this Section.

Table 3.3 Probability of occurrence (%) of significant wave height in the location north.

Seasons	0-1m	1-2m	2-3m	3-6m	>6m
Spring	72	21	6	1	0
Summer	68	27	5	0.5	0
Autumn	48	37	12	3	0
Winter	47	34	13	6	0.03

Table 3.4 Probability of occurrence (%) of significant wave height in the location south.

Seasons	0-1m	1-2m	2-3m	3-6m	>6m
Spring	73	22	5	0.2	0
Summer	71	25	3	0	0
Autumn	50	40	9	1	0
Winter	42	43	13	2	0

The difference between the metocean statistics of the two locations is well illustrated using a bar chart; see Figure 3.3. The results in Figure 3.3 express the sensitivity of the probability of occurrence of the significant wave heights in terms of the percentage change. Therefore, the negative result in the percentage change exhibits that the probability of occurrence of significant wave height has decreased by changing the location from North to South and thereby confirming the dominance of location North in the higher sea states.

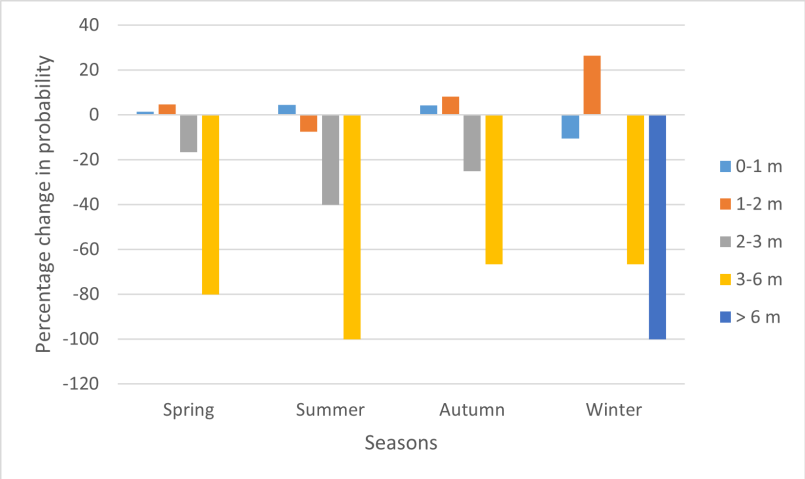

Figure 3.3 Sensitivity of the metocean statistics results on different seasons.

It can be inferred from Figure 3.3 that metocean condition for the location North dominates with higher sea states for all the seasons and for the lower sea states with significant wave heights between 0-2 m, location South has the dominance. And it can also be seen that Winter has harsh weather and Spring has mild weather for the past five years. The higher sea states dominate in the Winter and diminish when it reaches Spring. The season Summer and Autumn has almost similar metocean conditions.

3.2 Seakeeping and stability analyses

The seakeeping analyses are carried out on both the RoPax ship and the tanker. The need for a seakeeping analysis for RoPax ships is due to their vulnerability towards stability when damaged. Thus, the probability of capsizing, and survival probability of crew & passengers, and their consequences concerning risk are estimated for the RoPax ferry. At last, to strengthen the assumptions made concerning the stability among all the ship types, a motion response comparison is done between the tanker model assumed for the structural integrity simulation and the RoPax ferry model assumed for seakeeping and stability analyses.

3.2.1 Probability of capsizing

The SIMCAP code analyses of the RoPax ship were carried out as mentioned in Section 2.4.2 with the collision scenario and damage opening mentioned in Section 2.2. The probability of capsizing for a given wave direction and varying significant wave heights are shown in Table 3.5.

Table 3.5 Cases of ship capsize (X: capsize) for varying wave heights and wave heading angles.

Significant Wave height (m)	0	1	2	3	4	5	6
0°	-	-	-	X	X	X	X
45°	-	-	-	-	X	X	X
90°	-	-	-	X	X	X	X
135°	-	-	-	X	X	X	X
180°	-	-	-	X	X	X	X
225°	-	-	-	X	X	X	X
270°	-	-	X	X	X	X	X
315°	-	-	-	X	X	X	X

From Table 3.5, it is seen that the ship capsizes for wave heights over 2m and with the 270° direction for 2m wave height. In each scenario, the ship either capsizes or does not capsize and cases, where the ship does capsize, are represented by **X**. This is shown in Table 3.5, where the ship capsizing is depicted. It can be inferred that the worst-case scenario is when the wave direction is 270° for almost all the significant wave heights. A possible reason for this could be the occurrence of significant wave heights 1 m and 2 m from the respective direction, i.e., 270°, as seen in Figure 3.1 and Figure 3.2.

3.2.2 Time to capsize

The SIMCAP code analyses also determine the time to capsize for seven different significant wave heights (including calm sea, i.e., H_s = 0 m) for the RoPax ship as mentioned in Table 2.6 and are shown in Table 3.6.

Table 3.6 Time to capsize for the RoPax ferry (all times are in seconds).

Significant Wave height (m)	0	1	2	3	4	5	6
0°	0	0	0	210	160	160	210
45°	0	0	0	480	450	460	480
90°	0	0	0	360	390	390	360
135°	0	0	0	240	240	240	240
180°	0	0	0	200	200	150	200
225°	0	0	0	230	230	230	230
270°	0	0	300	230	230	200	240
315°	0	0	0	170	170	130	170

From Table 3.6, it can be seen that the average time to capsize for waves from 315° is the shortest, with an average capsize time of 160 seconds, and can be considered as the worst-case scenario for the damaged RoPax ship. The capsize times obtained are extremely short and hence reduces the survival probability. The highest average capsize time is obtained when the wave heading angle is at 45° with an average capsize time of 470 seconds which could be regarded as the safest heading direction for an efficient evacuation. A possible reason for this could be the location of the damage opening as seen in Figure 2.5 (b). The waves from the 45° direction reduces the heeling angle caused by the damage opening.

3.2.3 Damage stability GUI

Based on the methodologies described earlier in Section 2.4, all the simulation results are saved in an internal database. The survival probability estimation could be done based on the number of passengers and crew onboard the damaged vessel. Thus, the total number of passengers and crew is considered as the inputs for the consequence and damage stability risk. To make the risk analysis user-friendly, the whole methodology is replicated into a graphical user interface (GUI) as shown in Figure 3.4. Here the wave encounter angle is defined based on the ship reference i.e., by considering the bow pointing towards 180°.

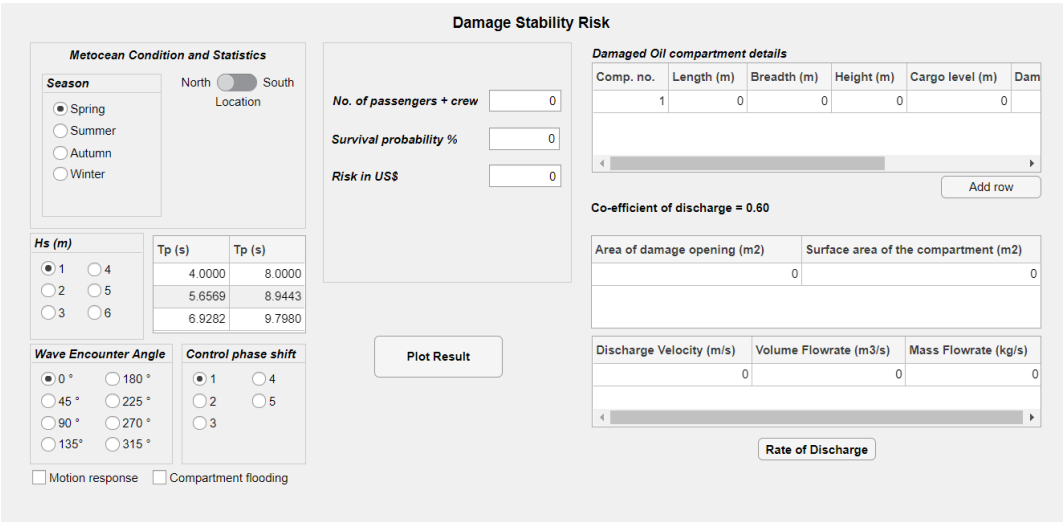

Figure 3.4 Damage stability GUI.

3.2.4 Sensitivity analyses

Sensitivity analyses are done on the results of:

1. Damage stability risk corresponding to the two defined locations.
2. Damage stability risk for using two extreme values (10 & 15 min) of the time range suggested by Vanem & Skjong (2004).

All the obtained risk in this Section corresponds to the worst-case scenario of vessel heading direction: 270°, as described in Section 3.2.1. For the first sensitivity analysis the results are expressed in terms of percentage change of risk from changing the location North to South for different seasons by considering maximum time for evacuation as 10 min (refer to Section 2.4.3); see Figure 3.5.

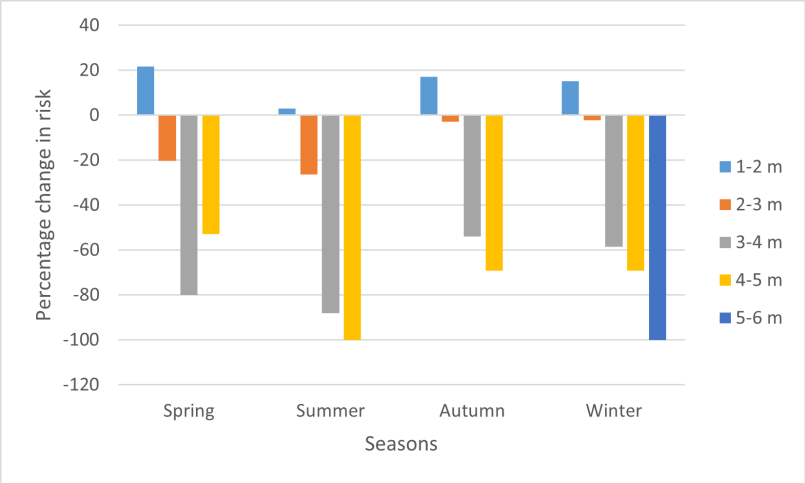

Figure 3.5 Sensitivity of the damage stability risk on the location.

As it is seen in Figure 3.5, for a significant wave height of more than 2 m, the damage stability risk decreases by changing the location from North to South (negative percentage change). This result is supported by the outcomes of Section 3.1.3, as it was seen that the location South dominates for the lower sea states (0-2 m), hence location North has the higher dominance on the damage stability risk for significant wave heights except 0-2 m. These results depict the significance of the metocean condition of the location on the damage stability risk. For the second sensitivity analysis, the results are expressed similarly as the percentage change of risk from considering maximum time for evacuation from 10 min to 15 min for location North (as it dominates for most of the sea states); see Figure 3.6.

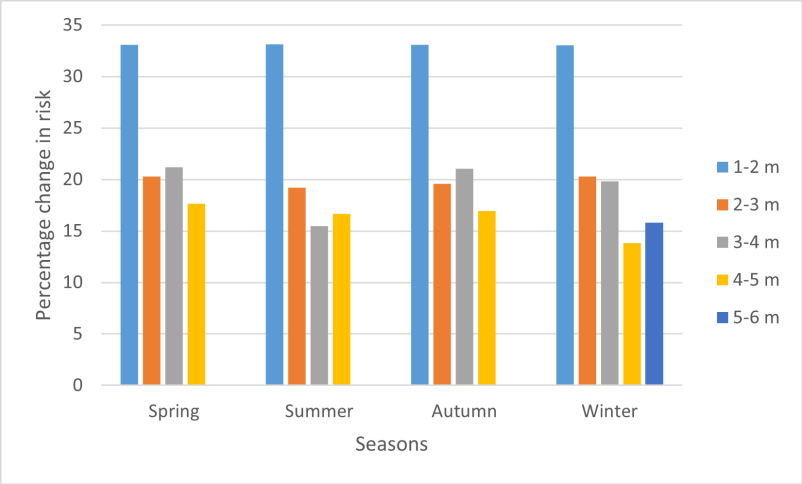

Figure 3.6 Sensitivity of the damage stability risk on the maximum time for evacuation.

It can be seen in Figure 3.5 and Figure 3.6 that Winter is the only season having a probability of occurrence of significant wave height 5-6 m, the risk for all the other seasons corresponding to 5-6 m significant wave heights are zero. Thus, only Winter has the damage stability risk for all the encountered significant wave heights. The percentage change of damage stability risk for choosing the maximum time for evacuation 10 to 15 min is presented in Figure 3.6. There is a clear increase in the risk for all the seasons, the maximum increase being 33% and the minimum being 14%. This adds up to an average of 23.5% increase for all the sea states for increasing the maximum time for evacuation by 5 min i.e., approx. 4.7% increase in risk for each minute increase in maximum time for evacuation. Here maximum time for evacuation is the time required to safely evacuate the whole crew and all passengers. Thus, more the maximum time for evacuation, less is the response to embarkation while the time for capsizing remains the same.

3.2.5 Motion responses of the tanker vessel

The simulations that were done on the RoPax ship were carried out for the tanker as well. From the SIMCAP simulations done on the tanker vessels, it is seen that the tanker does not capsize for any significant wave height from any direction. Although the tanker is extremely stable in all scenarios within the range of significant wave heights considered in this thesis even when damaged, the damage stability simulations were done to study the motion responses and use those results as the inputs to the URSA tool. There were a few outliers, however, that showed the tanker gaining significantly high roll angles through the course of the simulation as shown in Figure 3.7 (a) and (b). The cause for this is the free surface effect in the tanker as there are multiple liquid surfaces in a tanker in the compartments and various other tanks in the ship. As the motion responses of the tanker were simulated for study purposes, this thesis will not delve into a comparison.

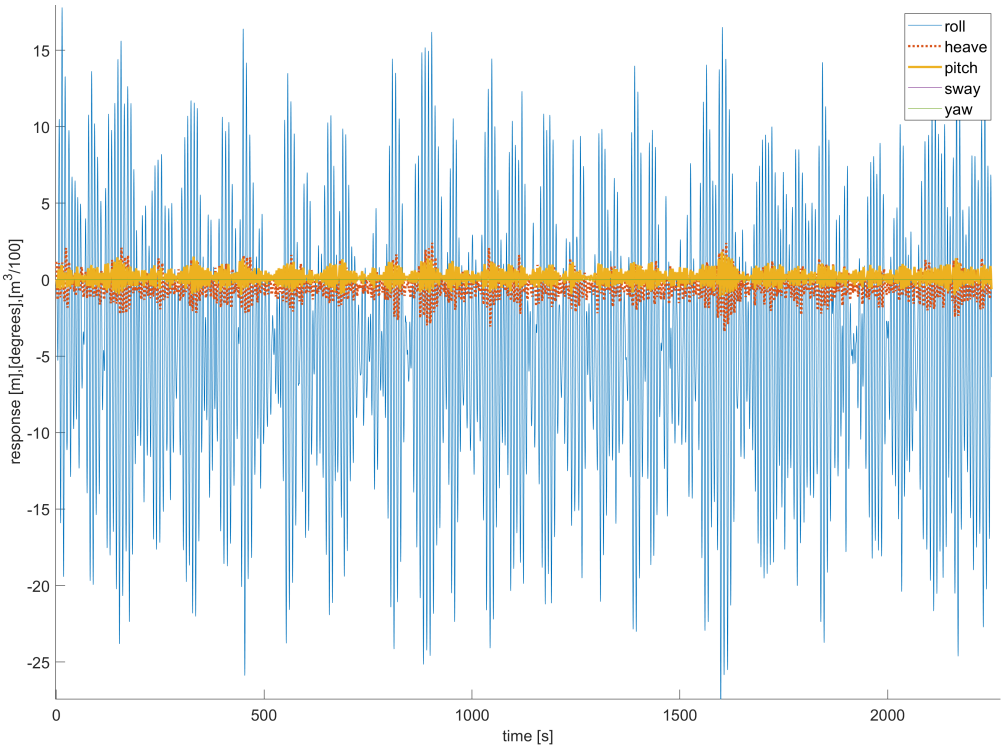

(a)

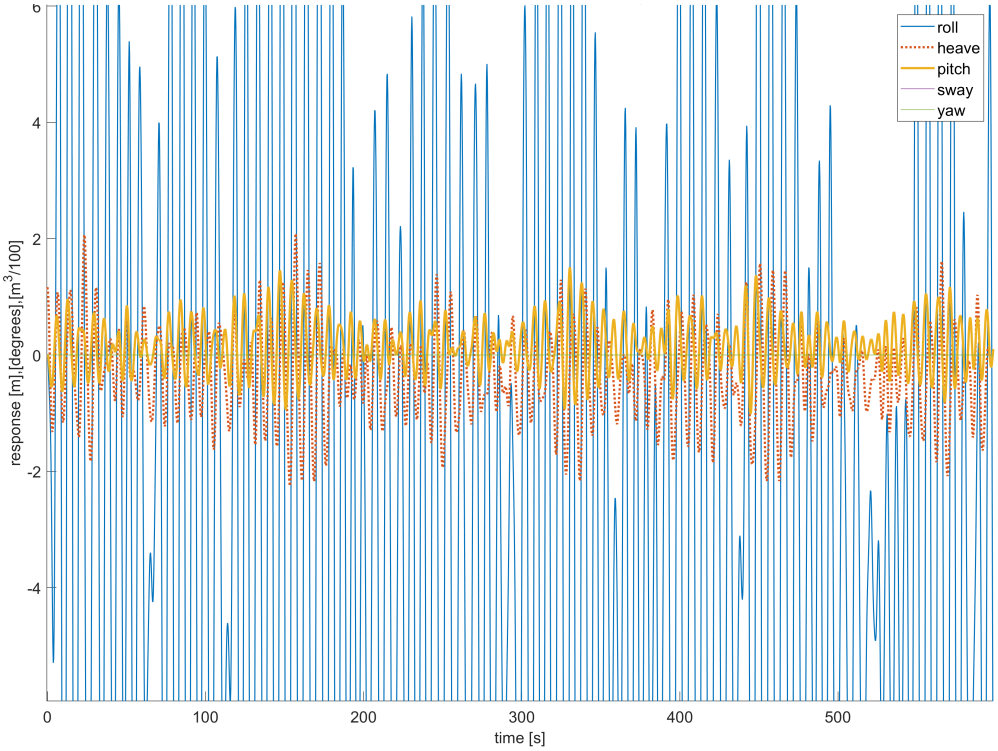

(b)

Figure 3.7 Motion responses of a tanker for a significant wave height of 4m and a wave heading angle of 90°, (a) the complete motion response and (b) zoomed-in section of the motion response.

3.3 Structural integrity simulation and ULS risk

In this thesis, to showcase the developed methodology, the structural integrity simulation is only done for the tanker ship model. Due to the absence of strength decks and the presence of hollow compartments unlike RoPax ships, the tanker vessel is considered as the vulnerable ship type for the structural integrity simulation when damaged. The ULS exceedance probability, its consequences, and risk are hence estimated only for the tanker ship models obtained from Kuznecovs et al. (2021a). The influence of the metocean condition of the location on the results is presented using sensitivity analyses. At last, to showcase the methodology developed for the ULS risk, the consequences are presented by defining an example scenario, and thereby the efficiency of risk mitigation action is presented.

3.3.1 Structural adequacy plot

The structural integrity simulation was done for two tanker ship models obtained from Kuznecovs et al. (2021) with the same dimensions and damage opening but with different corrosion levels as described in Section 2.2. The first vessel (T1V5) is as-built with no corrosion, the second vessel (T5V5) is a corroded vessel of approximately 25 years of age. In the present thesis, the structural loading history for the vessel is generated based on the obtained motion response histories after the seakeeping and stability analyses. Using the loading histories and the interaction curve parameters, the structural adequacy values are computed as explained in Section 2.5.3. The structural adequacy values η computed are illustrated using polar plots as shown in Figure 3.8.

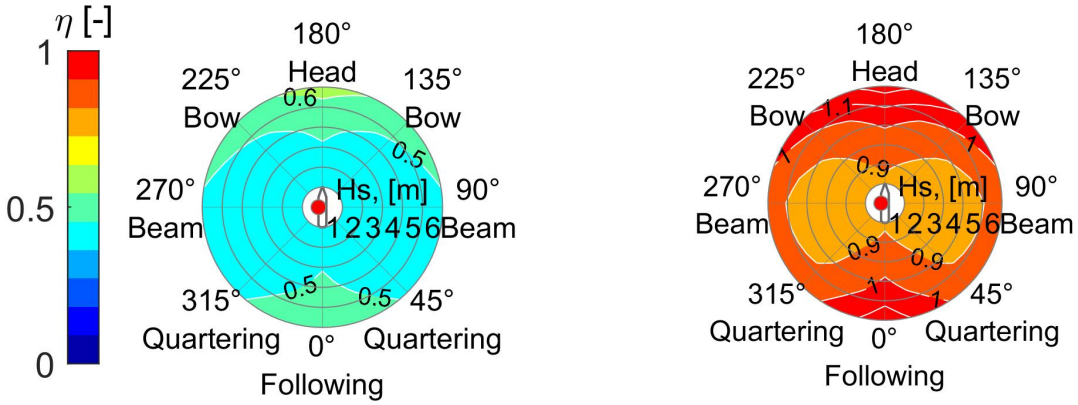

Figure 3.8 Structural adequacy plot obtained from the structural integrity simulation. Left: T1V5, Right: T5V5.

3.3.2 Parametric sensitivity analysis

Accounting for all the uncertainties due to tanker modelling, assessing environmental loads, material specification, geometrical definition, etc. the capacity measure in the structural adequacy is decreased, and the demand is increased. This leads to a conservative solution that is believed reliable due to the accountability of uncertainties. Therefore, as an initial estimation, capacity factors are chosen to be 0.95, 0.90, 0.85 and similarly, the demand factors are chosen to be 1.05, 1.10, 1.15.

To understand the impact of uncertainties, a sensitivity analysis is done on the ULS exceedance probability by changing the partial safety indexes considering the worst-case scenario (heading 180°, like wave 0°, winter season). The results of the sensitivity analysis are illustrated using a bar chart as displayed in Figure 3.9.

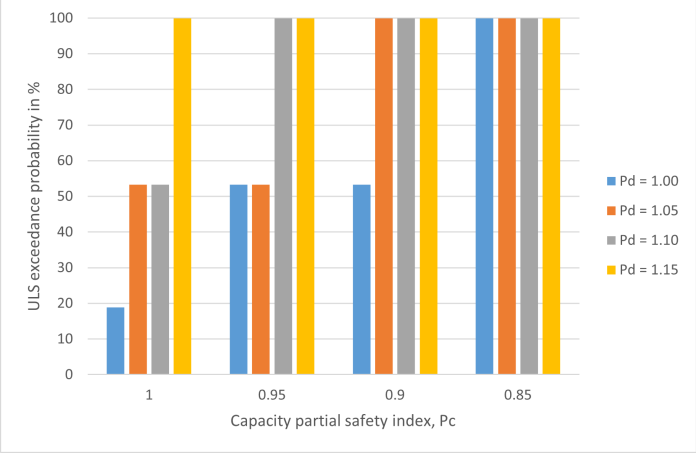

Figure 3.9 Parametric sensitivity results for the partial safety index.

Here a suitable combination of 5% increase and decrease in demand and capacity respectively is chosen that resulted in 53% ULS probability. It is assumed that the result is conservative and reliable but a detailed study on the indexes must be done to come up with the best suitable combination that is highly reasonable. As discussed in Section 2.5.3, the risk analysis of ULS exceedance could be quantified using structural adequacy. Thus, by introducing the partial safety indexes to both demand and capacity, the structural adequacy values hence obtained will be conservative. Now a structural adequacy value equal to or more than 1 could be considered dangerous and subjected to consequences.

3.3.3 ULS risk GUI

Based on the methodologies described in Sections 2.3 and 2.5, the metocean statistics for the past 5 years are classified for four different seasons, and two locations and made accessible for mapping the results while estimating ULS exceedance probability. To understand the changes in the ULS exceedance probability due to partial safety index, the respective structural adequacy plots must the visualized. Similarly, to understand the proposed risk mitigation action, a visualization of the result is much needed. Finally, to define the consequences based on the current market situation, separate input fields must be available for the user. Therefore, integrating all the requirements and easing the whole process of risk assessment, an automated tool is developed and replicated as GUI. This interface is specially developed for a user-friendly experience in risk assessment. A snapshot of the interface is displayed in Figure 3.10.

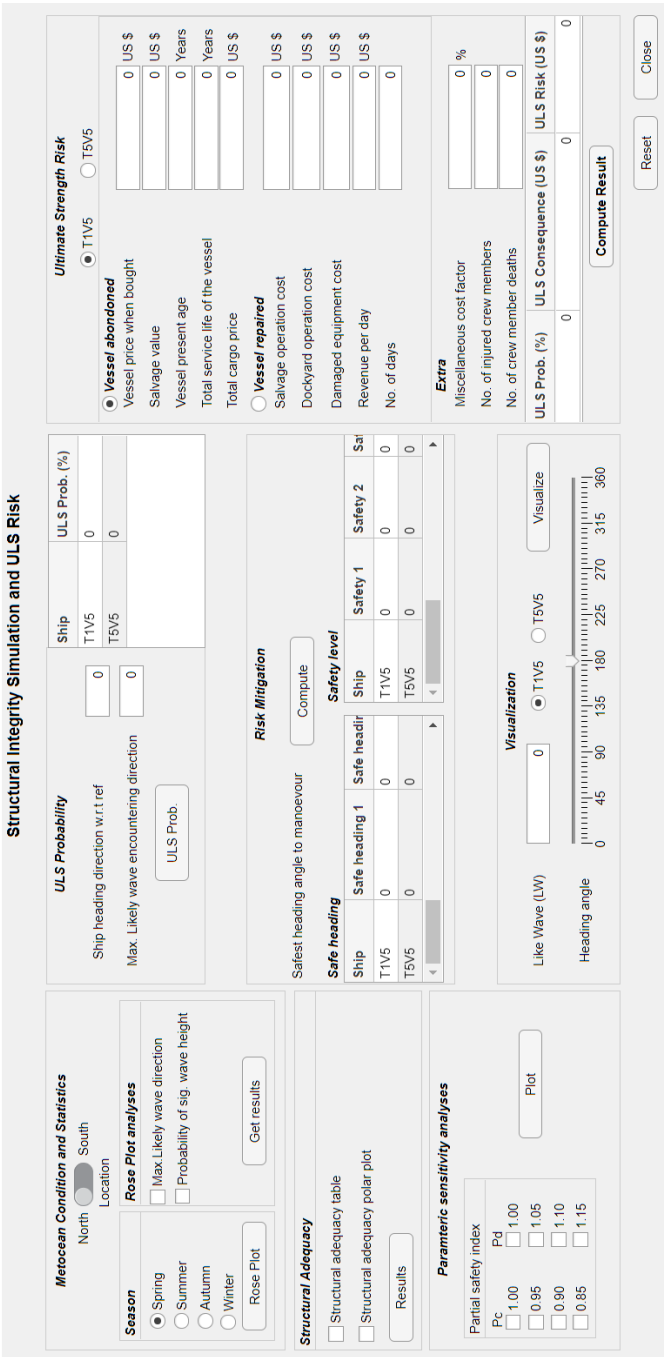

Figure 3.10 Structural integrity simulation and ULS risk analysis tool GUI.

3.3.4 Showcasing ULS risk and mitigation measures

To check the feasibility of the tool built for structural integrity, ULS risk, and the reliability of mitigation measures, an example scenario is showcased with a reasonable input for the ULS risk GUI, and the results for the same are obtained. The example problem was a collision-damaged tanker T5V5 (described in Section 3.3.1) facing its bow to the heading direction 188° in the location North in October. The details of the vessel and the post-collision operation are shown in Table 3.7.

Table 3.7 Post-collision consequence quantification inputs.

Consequences	Quantity	Reference
Vessel price when bought	20 mUS $	(Compass Maritime, 2021)
Vessel age	25 years	(Kuznecovs & Ringsberg, 2021)
Salvage value	6 mUS $	(Compass Maritime, 2021)
Total cargo price	5 mUS $	(Oil Price, 2021)
Dockyard operation cost	600,000 US $	(Pardo, 2013)
Damaged equipment cost	400,000 US$	(Pardo, 2013)
Freight revenue	15,000 US $/day	(Shipfinance, 2021)
Salvage operation cost	500,000 US $	(Chiu et al., 2017)
No. of crew members injured	3	(EMSA, 2020)
No. of crew members dead	2	(EMSA, 2020)
No. of days for the vessel repair	20	(Pardo, 2013)
Miscellaneous factor	7%	(Shipfinance, 2021; Oil Price, 2021)

3.3.4.1 ULS probability

Based on the defined inputs from Table 3.7, the maximum likely occurring wave direction is obtained as 9° from the GUI. The heading direction of 188° and the maximum likely occurring wave direction of 9° yields the ULS probability as shown in Table 3.8.

Table 3.8 ULS probability result for the example scenario.

Ship	ULS probability (%)
T5V5	52.13

3.3.4.2 ULS consequence and risk

Like the computation of ULS probability based on the inputs specified in the example scenario, the ULS consequence and risk are also computed. Here the risk is calculated for both the available options of the ULS consequences for a constructive comparison. To display the results, a snapshot of the Ultimate strength risk part of the GUI is directly displayed in Figure 3.11.

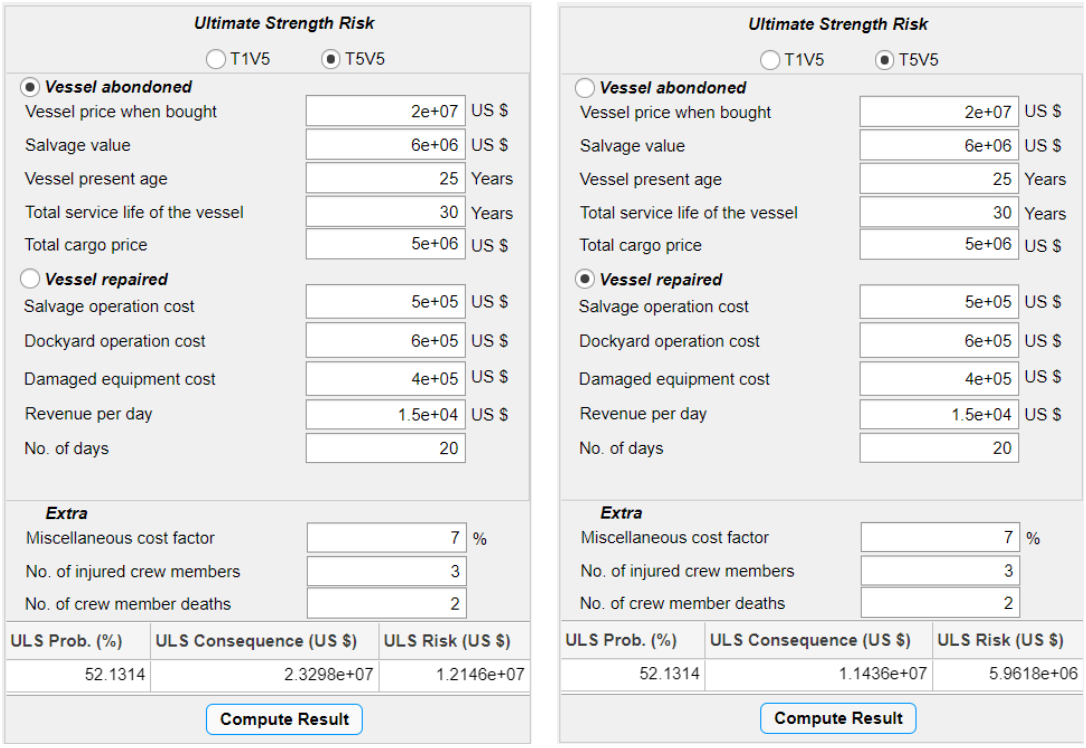

(a) (b)

Figure 3.11 ULS consequence and risk results. (a): Vessel abandoned, (b): Vessel repair.

3.3.4.3 Risk mitigation actions

Based on the ULS probability obtained in Section 3.3.4.1, the safest heading direction the tanker could be manoeuvred to change the relative wave encountering angle (see Figure 3.12) and reduce the ULS exceedance probability is presented in Table 3.9. Here only the smart manoeuvre is considered for risk mitigation as described in Section 2.5.8.

Table 3.9 Safe heading ranking result to reduce ULS probability.

Ship	Rank 1	Rank 2	Rank 3	Rank 4	Rank 5	Rank 6	Rank 7	Rank 8
T5V5	144°	99°	279°	234°	54°	324°	189°	9°

The proposed options (ranks) to manoeuvre the ship to change the relative wave encountering the angle is based on the decreasing order of its corresponding safety level. Thus, the safety level associated with each option is displayed in Table 3.10 respectively.

Table 3.10 Safety level of corresponding safe heading rank.

Ship	Level 1	Level 2	Level 3	Level 4	Level 5	Level 6	Level 7	Level 8
T5V5	97.10	97.10	97.10	97.10	84.77	84.77	47.87	47.87

3.3.4.4 Visualization of safe heading

Since there is no 100% safe level of heading direction for manoeuvring for the vessel T5V5 as suggested in Table 3.10, the first four proposed heading direction options of being 97.10% safe are adopted to manoeuvre the vessel and are presented in Figure 3.12. Here the LW refers to the maximum likely occurring wave direction corresponding to the specified location and season.

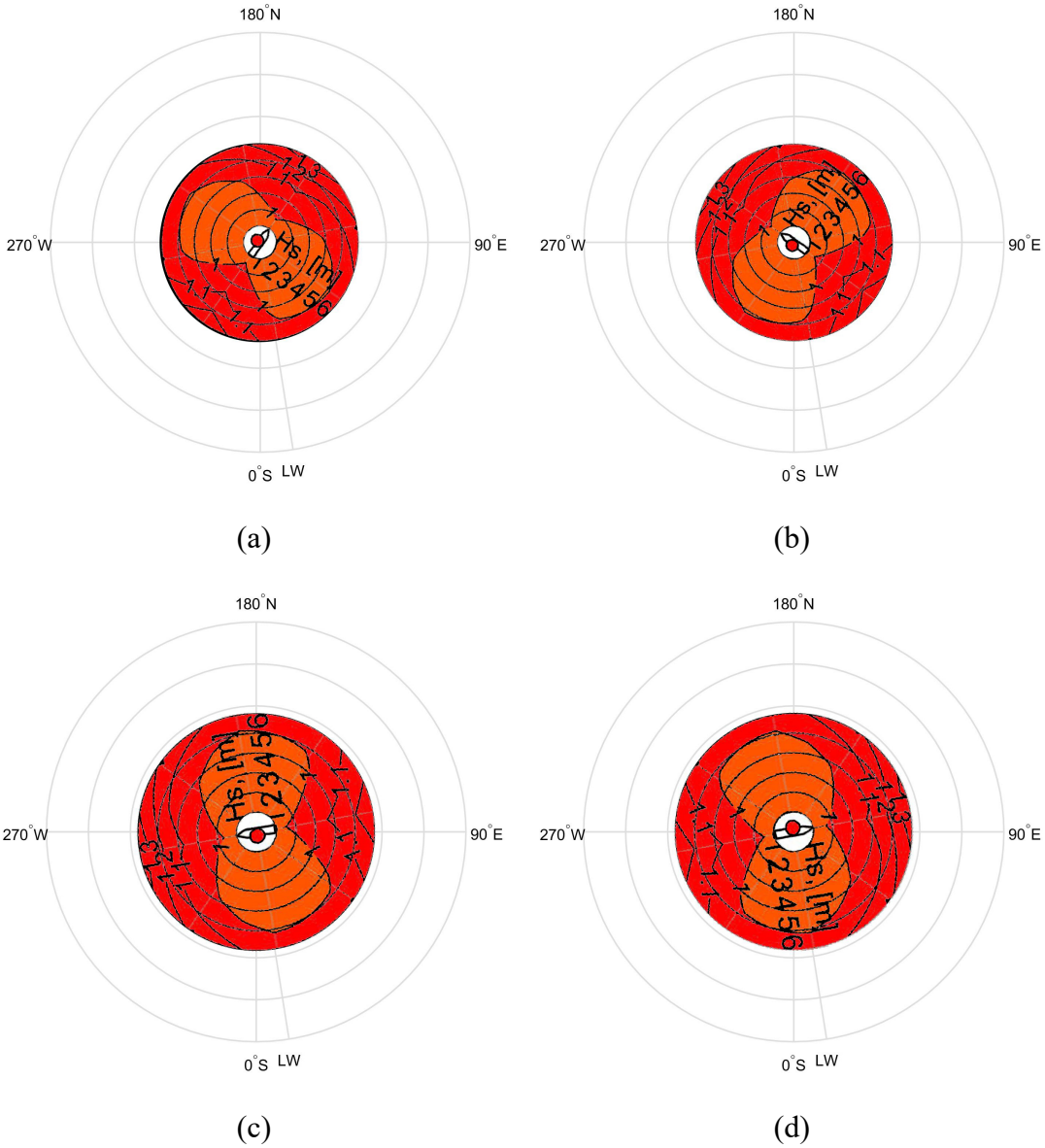

Figure 3.12 Visualization results of safe heading. (a): 144°, (b): 234°, (c): 279°, (d): 99°.

3.3.4.5 Risk mitigation

Changing the heading direction of the vessel from 188° to 97.1% safe heading directions 144° or 99° or 279° or 234° would decrease the ULS exceedance probability. This will in turn decrease the ULS exceedance risk. An analysis has been carried to study the difference between the ULS exceedance risk when the mitigation measure of manoeuvring the vessel to the safest heading direction is made. The results of the analysis are displayed in Table 3.11 and Figure 3.13.

Table 3.11 Change in the ULS exceedance probability after risk mitigation measure.

Ship	ULS prob. Before	ULS prob. After	Percentage change
T5V5	52.13	2.90	94.43 (decrease)

The change in the ULS exceedance probability as seen in Table 3.11 is reflected in the estimation of ULS exceedance risk. The results of the ULS exceedance risk after incorporating the risk mitigation measure are displayed in Figure 3.13.

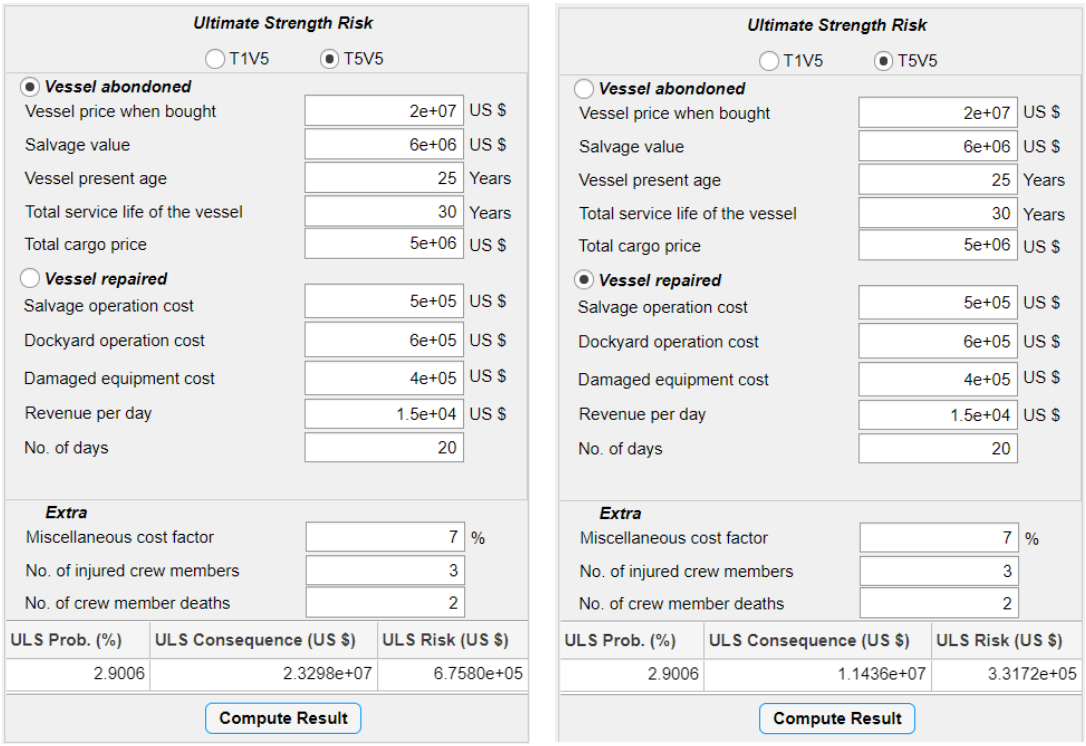

(a) (b)

Figure 3.13 Results of ULS exceedance risk after incorporating the risk mitigation measures. (a): Vessel abandoned, (b): Vessel repaired.

3.3.5 Sensitivity analyses

To check the sensitivity of the ULS exceedance risk on the location and metocean conditions, a series of sensitivity analyses are done on the showcasing example problem defined in Section 3.3.4 for different seasons. It was observed that the metocean condition of the two locations has a significant influence on the ULS exceedance risk with a maximum of 1657% and a minimum of 7% difference in Winter and Summer respectively. The results of the analysis are presented in Figure 3.14.

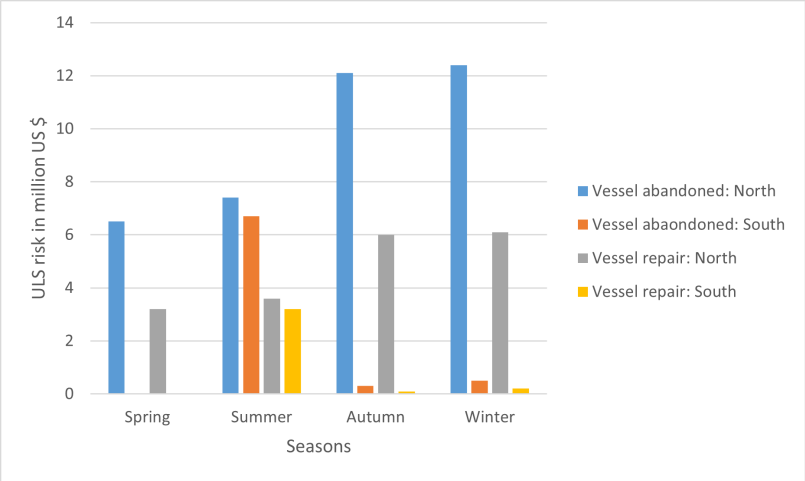

Figure 3.14 Sensitivity analyses of the ULS risk on different locations.

3.4 Environmental impacts and risk

As discussed in Section 2.6.2 on oil drift simulation, the 18 simulations were carried out and tested for three different days for the sensitivity analysis. The results of the sensitivity analysis, the results of using inputs from the Swedish coast guards, and some insights on the natural resource damage and shoreline clean-up assessments were presented and discussed in this Section.

3.4.1 Parametric sensitivity analyses

The parametric sensitivity analyses of the oil flow simulations are done to visualize the variation of the parameters, mentioned in Section 2.6.2, and how they behave in different scenarios. The data is measured in time steps, where each time step is 15 minutes for a total number of 577 time steps and a total of 144 hours of simulation time, and each data is plotted against the corresponding data from day 2 and day 3. As the access to the metocean statistics on Seatrack Web (2021) is limited to two weeks (the week before and the week after) on a commercial license, three days with a week's gap between them were chosen for this sensitivity analysis. The days chosen are given in Table 3.12.

Table 3.12 Days chosen for the parametric sensitivity analysis.

Day 1	26th April 2021
Day 2	3rd May 2021
Day 3	10th May 2021

The first sensitivity analysis was done on the viscosity of heavy oils and its variation with time on the days chosen and is shown in Figure 3.15. Heavy oils were chosen for this analysis as both, the light oils and medium oils behave similarly to heavy oils. The viscosity of oils starts at 4740 cSt, but the change in viscosity is quite significant, especially on Day 3. The behaviour of the oils in the North and the South are very similar.

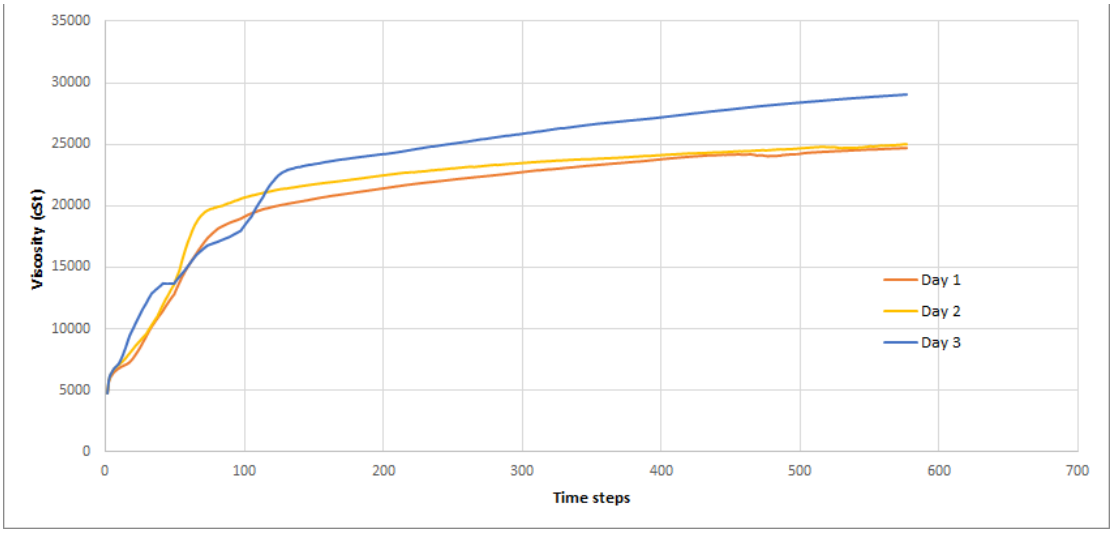

(a)

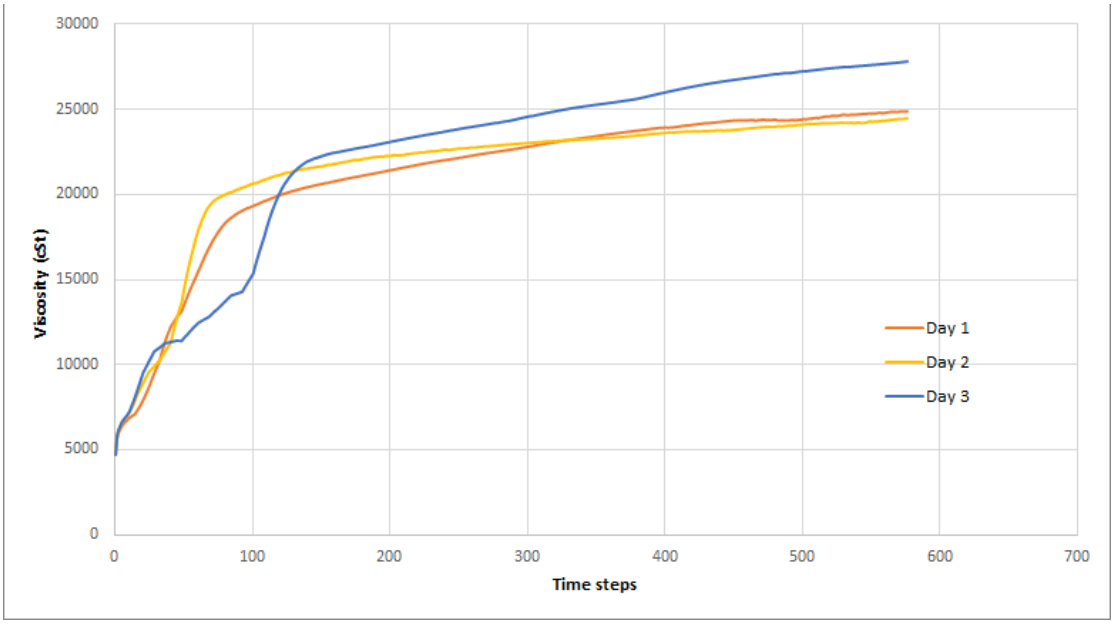

(b)

Figure 3.15 Variation of viscosity of heavy oils on different days. (a): Location North, (b): Location South.

The second sensitivity analysis was done on the volume of oils of the three viscosities on the surface of the sea on different days, as shown in Figure 3.16, Figure 3.17, and Figure 3.18. The changes in the volume of light oils on the surface is due to the dispersion of the oil. As the name suggests, light oils are very light and easy to get dispersed due to sea currents, tides, and other ships on the route. This causes a fluctuation in the volume of light oils present on the surface of the sea. Medium oils and heavy oils have a steadier behaviour in the North on all three days, but Day 3 in the South is quite peculiar. All the oil that was on the surface when the discharge of oil took place, gets deposited on the shorelines as the winds and the currents in both locations are towards the northeast.

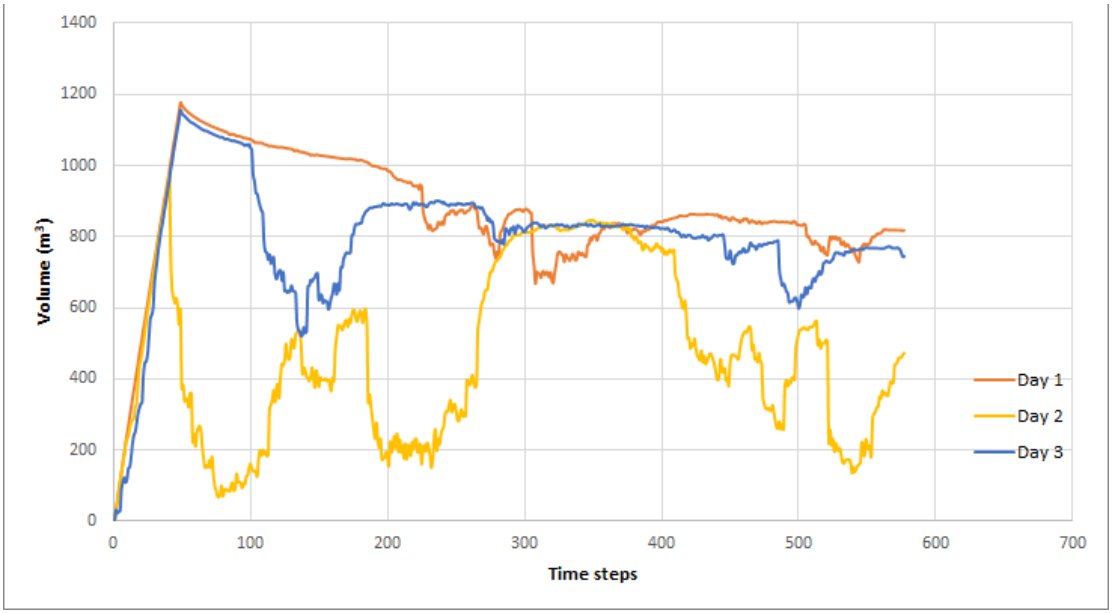

(a)

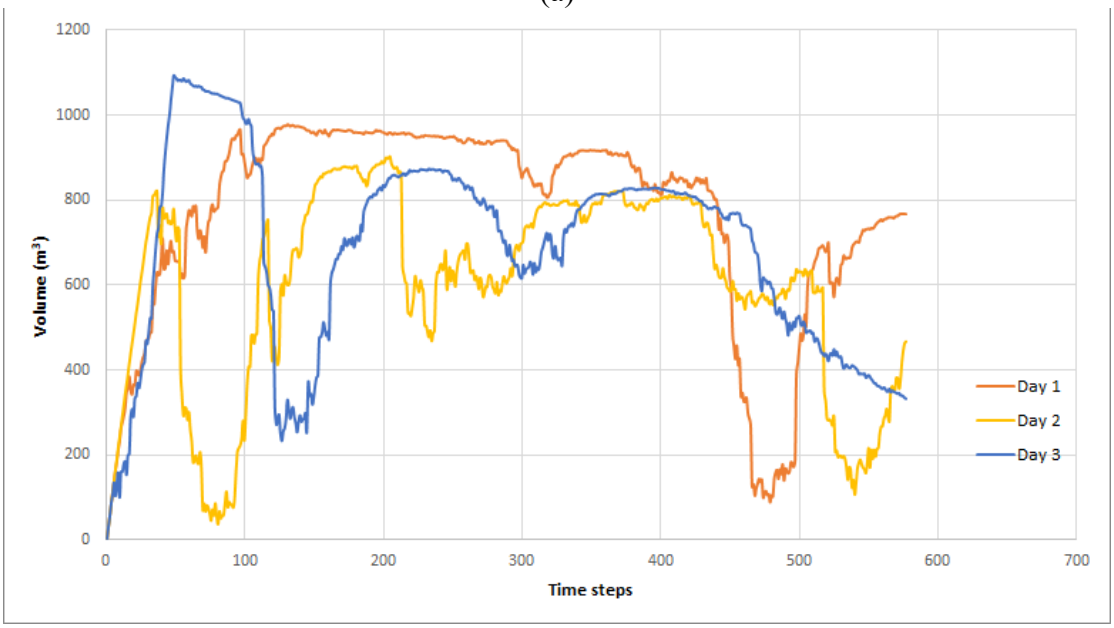

(b)

Figure 3.16 Light oils on the surface of the sea on different days. (a): Location North, (b): Location South.

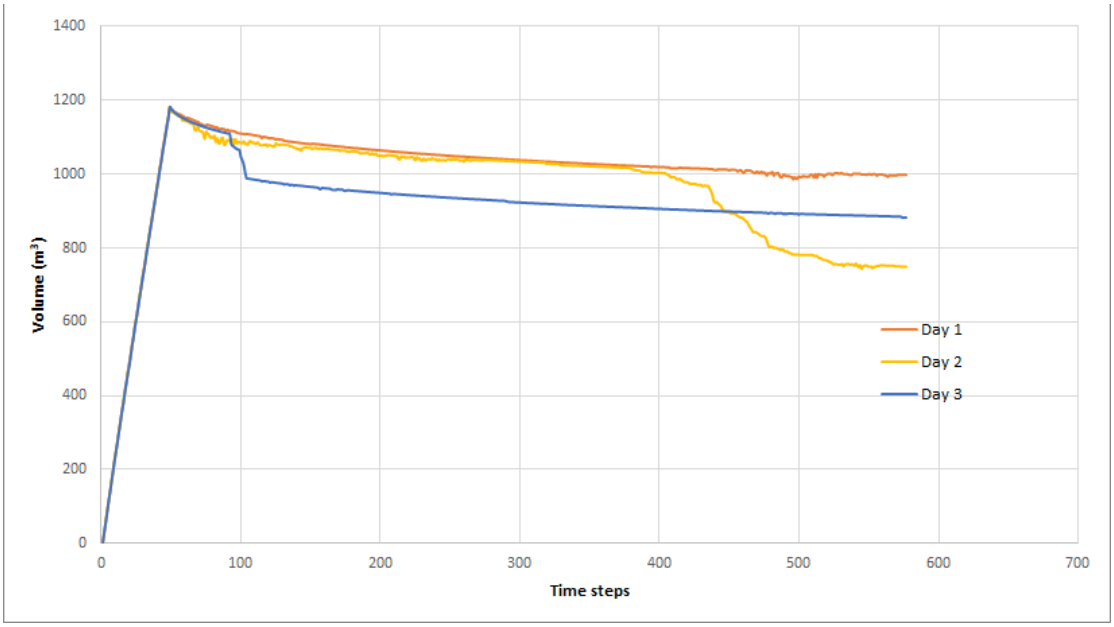

(a)

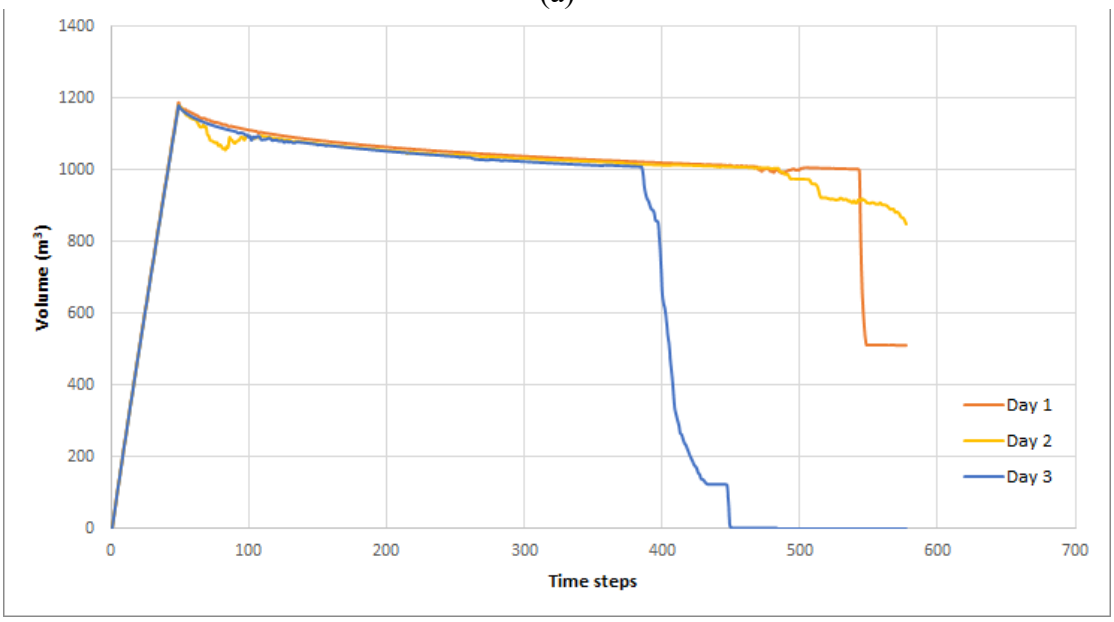

(b)

Figure 3.17 Medium oils on the surface of the sea on different days. (a): Location North, (b): Location South.

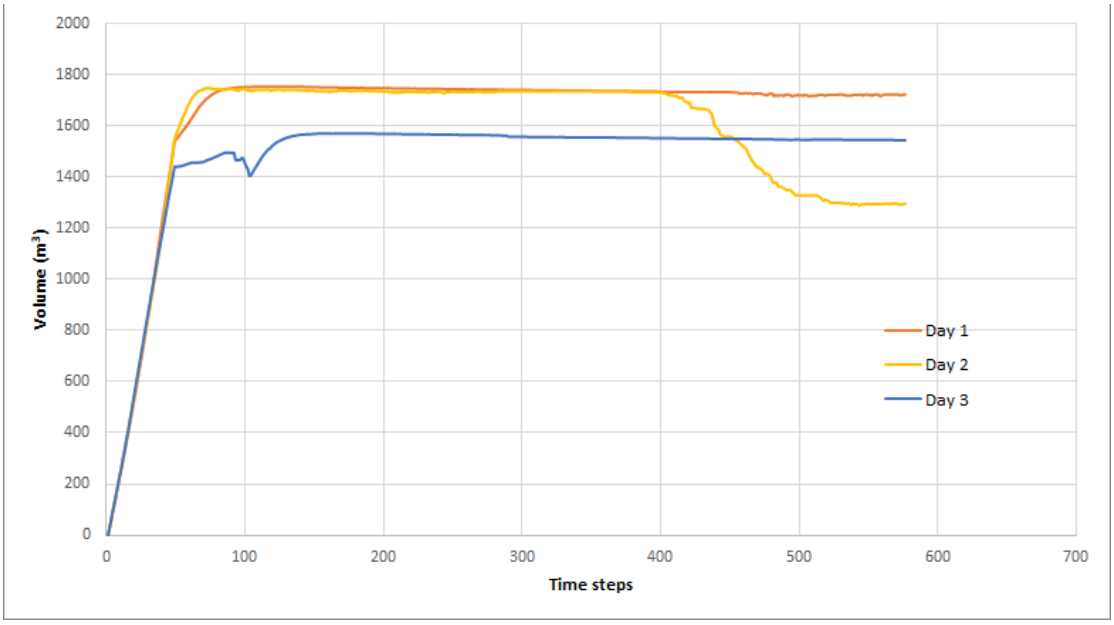

(a)

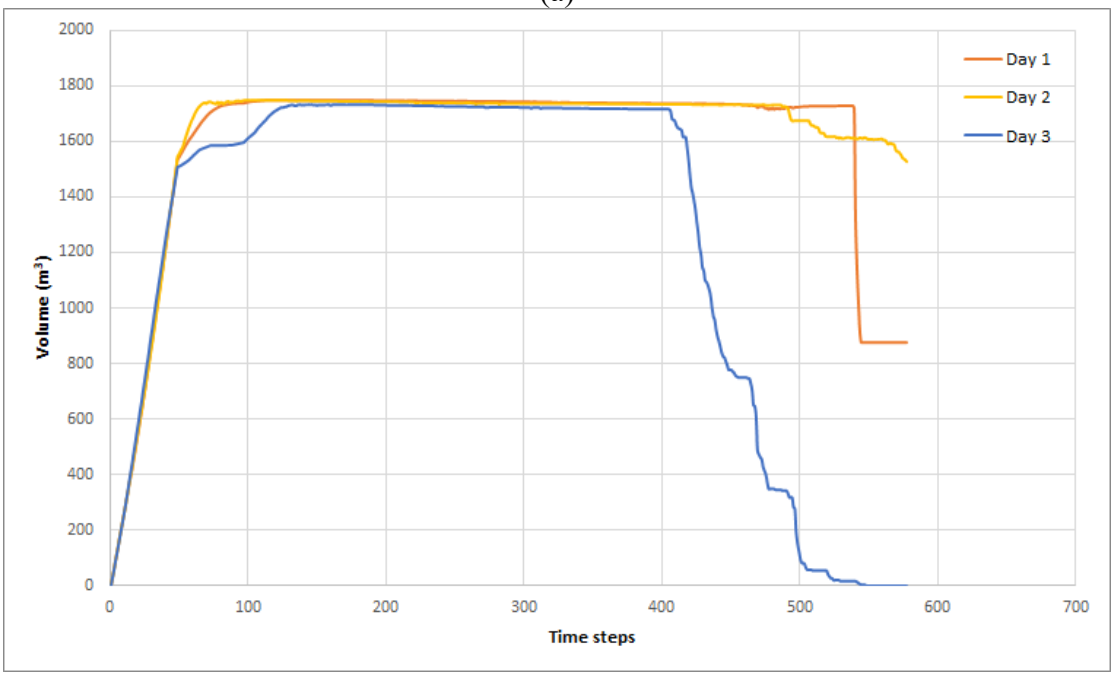

(b)

Figure 3.18 Heavy oils on the surface of the sea on different days. (a): Location North, (b): Location South.

The third sensitivity analysis was done on light oils that get deposited on the seabed as shown in Figure 3.19. As light oils disperse more, the chances of deposition on the seabed increases whereas, with medium and heavy oils, there is little to no deposition taking place as it does not disperse as easily. It is seen that Day 2 in the North has a significantly higher volume of oil being deposited on the seabed but is quite on the opposite side in the South and both, Day 1 and Day 3 have a higher volume of deposition in the South.

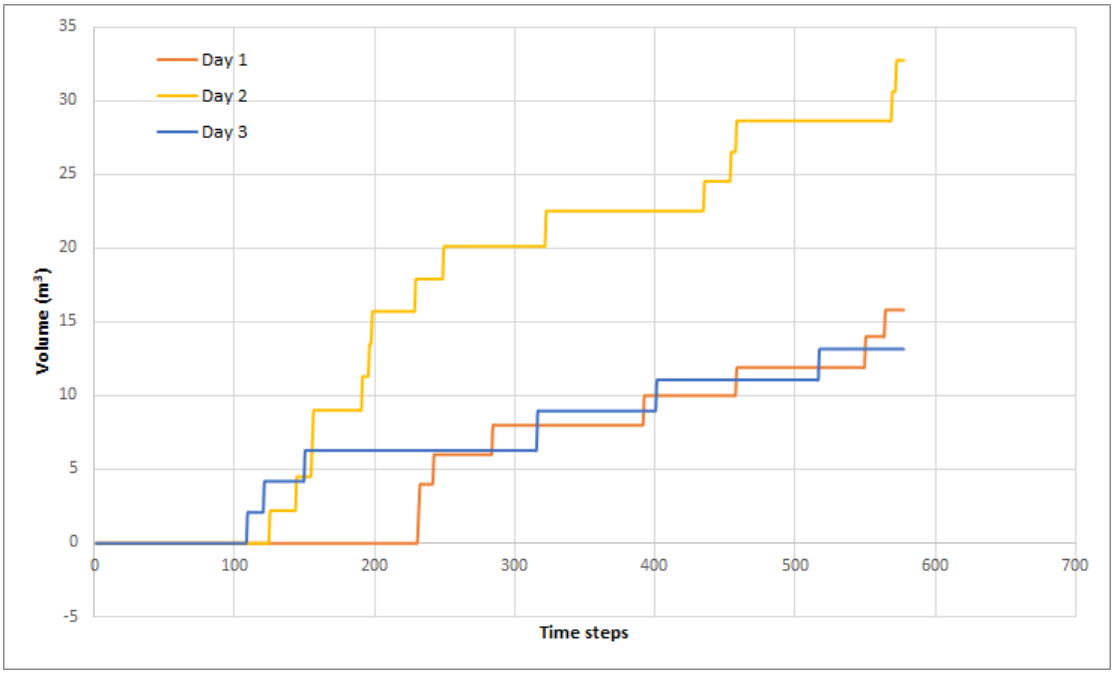

(a)

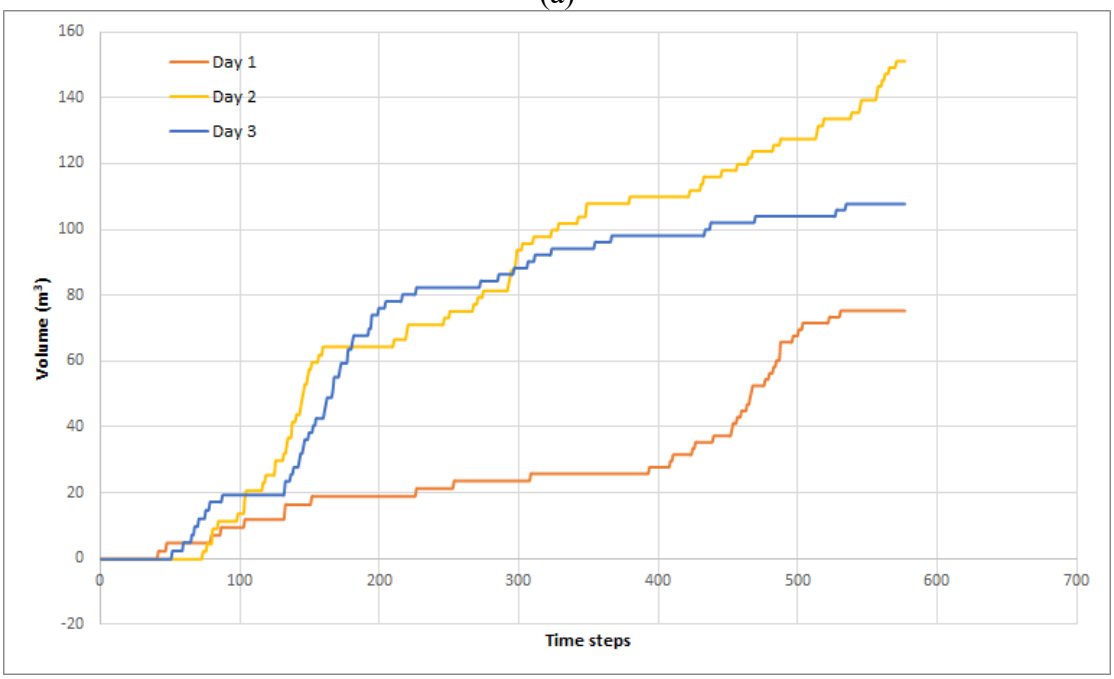

(b)

Figure 3.19 Deposition of light oil on the seabed. (a): Location North, (b): Location South.

The fourth sensitivity analysis was done on the deposition of oils on the shoreline for different viscosities on different days and is shown in Figure 3.20, Figure 3.21, and Figure 3.22. In Figure 3.20, there is some deposition of light oils on Day 1 and Day 3 on the shoreline, and a considerable volume of light oils on Day 3 is deposited on the shoreline in the North, whereas in the South, there is little to no deposition of light oils on Day 1 and Day 2 on the shoreline but there is a significant amount of light oils being deposited on the shoreline on Day 3.

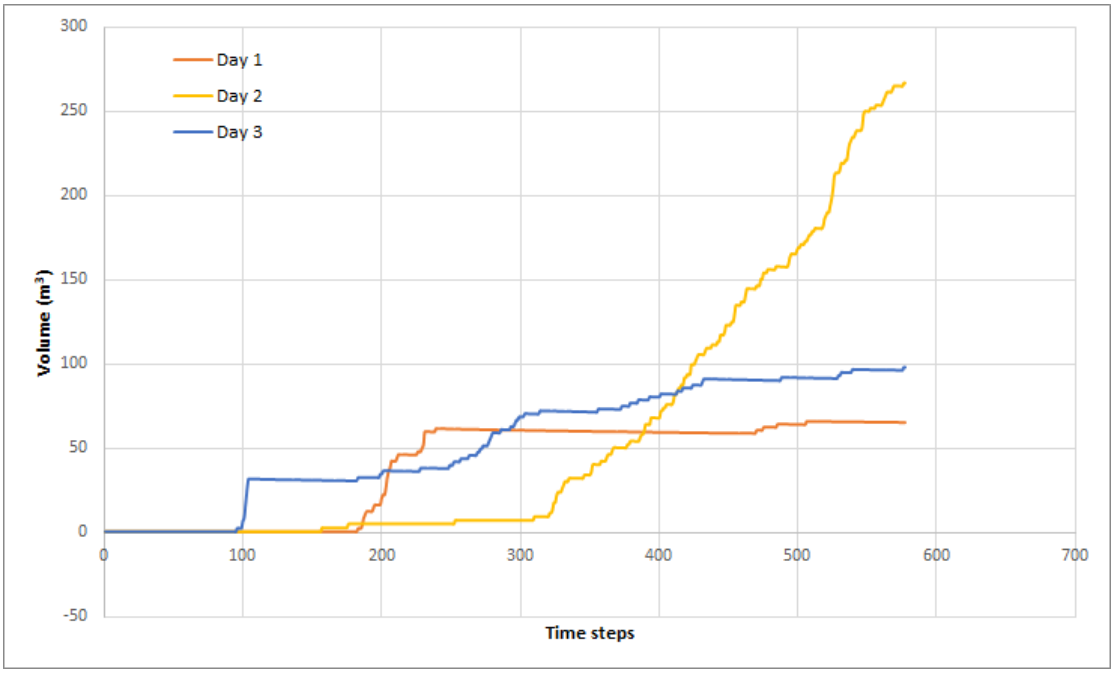

(a)

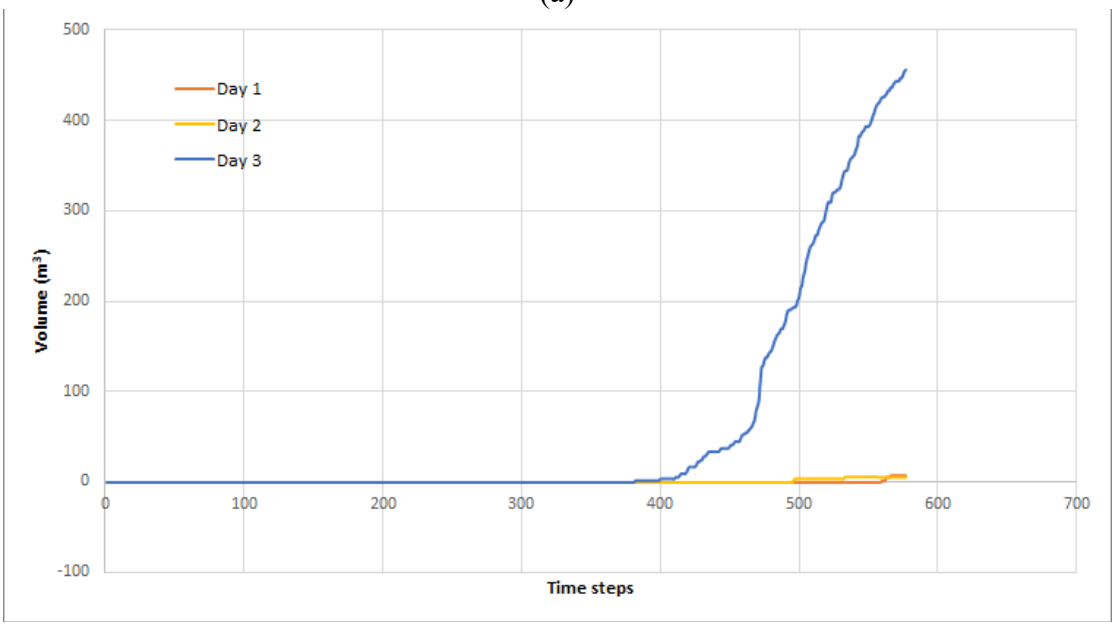

(b)

Figure 3.20 Deposition of light oil on the shoreline. (a): Location North, (b): Location South.

In Figure 3.21, the volume of medium oils deposited on the shoreline in the North on Day 3 is extremely high while the deposition on Day 2 is almost half of that on Day 3, and Day 1 is nearly a fifth of the volume deposited on Day 3. In the South, the volume of medium oils deposited on the shoreline is considerably less than the volume deposited on the shoreline in the North. Day 1 has almost no deposition, Day 2 has the highest volume deposition and Day 3 is mostly constant after the first 100 time steps.

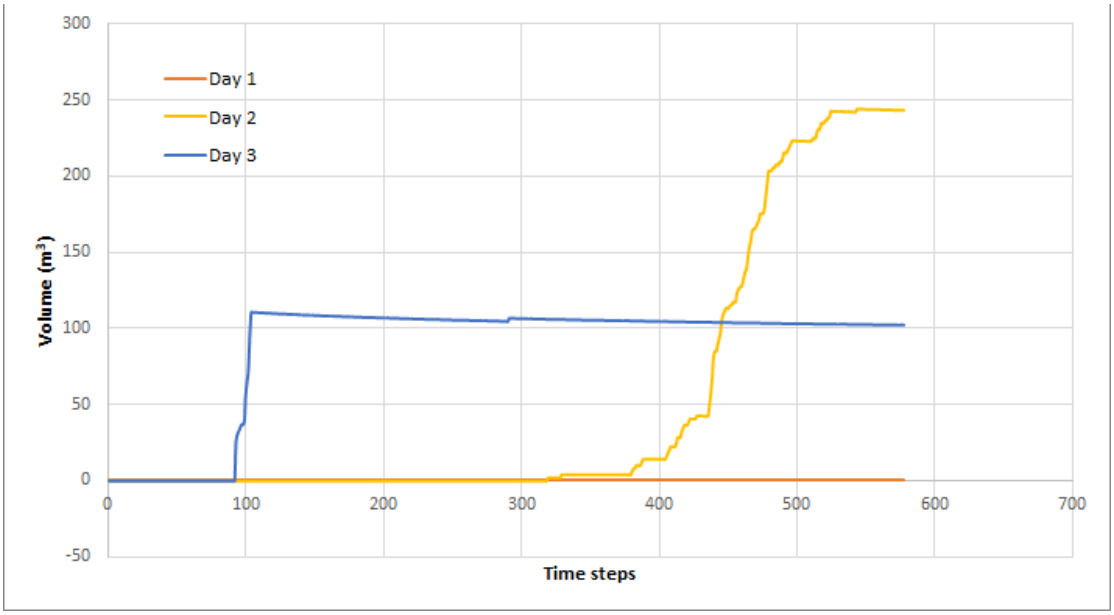

(a)

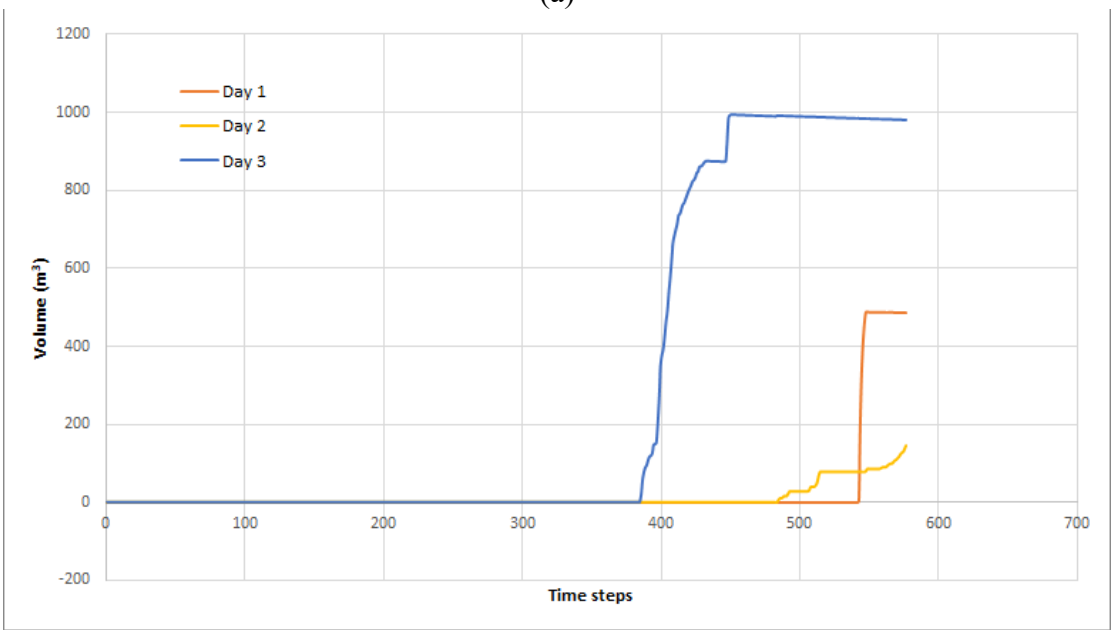

(b)

Figure 3.21 Deposition of medium oil on the shoreline. (a): Location North, (b): Location South.

In Figure 3.22, in the North, Day 1 has the highest volume of heavy oils being deposited on the shoreline, Day 2 has nearly a third of the volume deposited on Day 1 and there is no oil deposited on the shoreline on Day 3. In the South, Day 3 is almost all of the oil being deposited on the shoreline with the deposits on Day 2 being slightly less than half of that of Day 3. Day 1 has significantly lower deposition in the South as well.

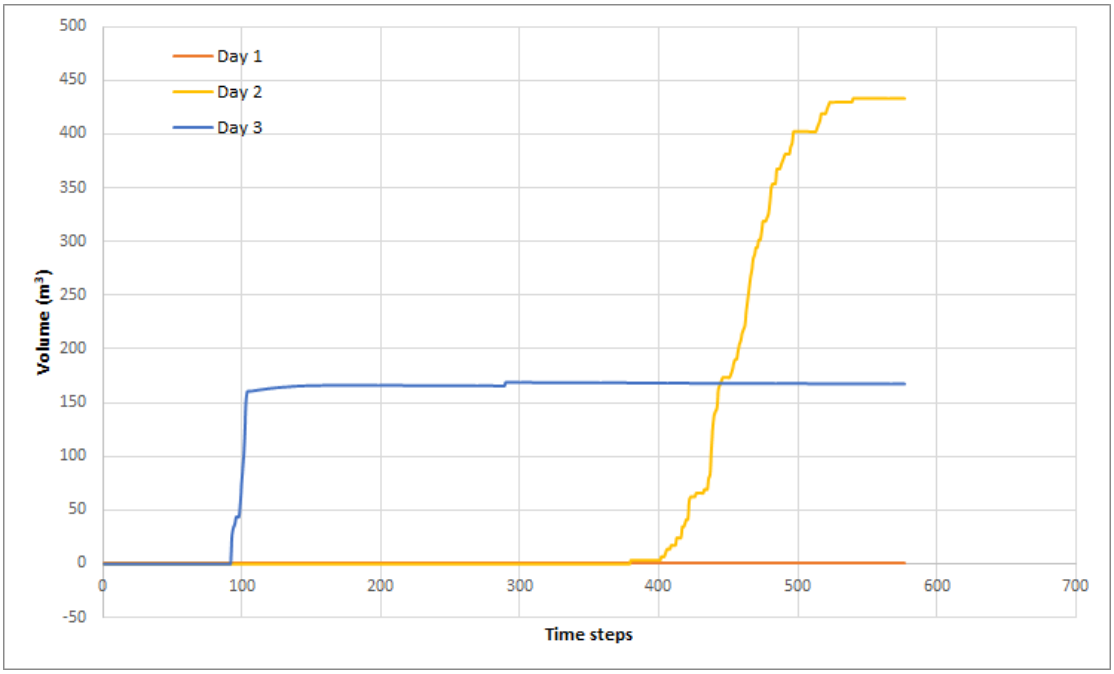

(a)

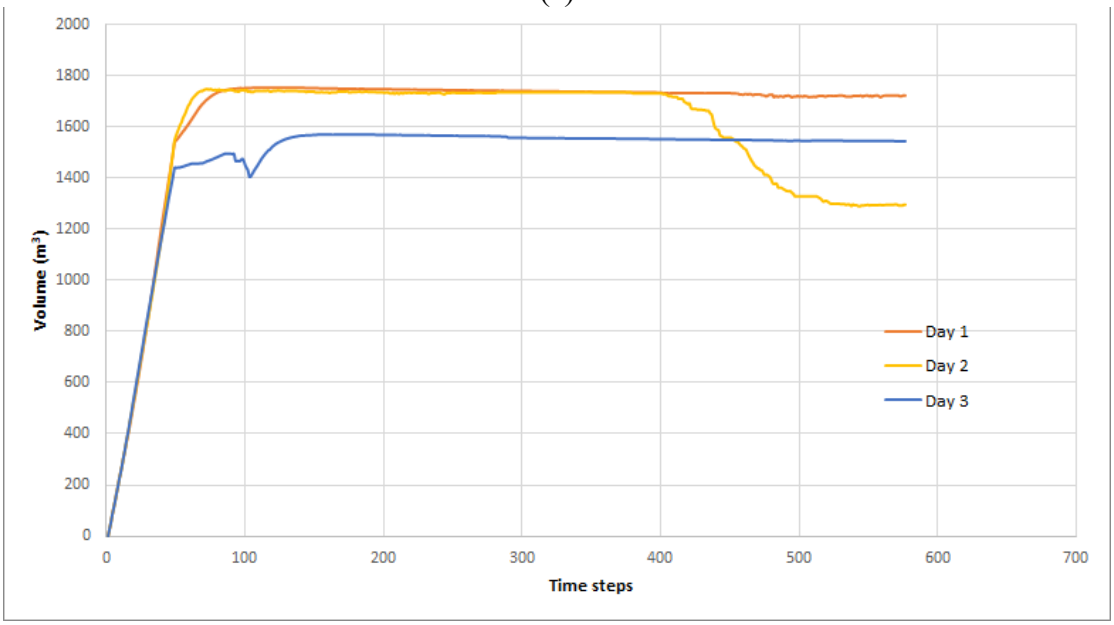

(b)

Figure 3.22 Deposition of heavy oil on the shoreline. (a): Location North, (b): Location South.

From the parametric sensitivity analyses done on the oil drift simulation, it is seen that location plays an important role in the behaviour and movement of oil on the surface of the water. These movements of the oils rely heavily on the metocean conditions at the chosen locations. The locations, although quite close to each other being only 54 NM away from each other showed very different metocean conditions and oil movement. From the parametric sensitivity analyses done, it can be seen that the South location has a higher risk of having oils deposited on the shoreline due to the existence of the Danish coastline and the Swedish coastline close to the southern location chosen than the northern location.

3.4.2 Environmental impact consequence GUI

The monetary value list obtained from the Swedish coast guards is studied and understood. This helped to understand the various equipment available in the coast guard reservoir, the resources it needs for the operation, and a brief idea on how effectively it could be used. Since the details available on the monetary values of the equipment, resources and operation are found in Wikingsson (2020), an automated tool is built such that it could be used to estimate the price for the oil spill consequences if only the clean-up and rescue operation is concerned. To have a user-friendly experience and to ease the process of understanding oil pollution response operation, a GUI is developed; see Figure 3.23.

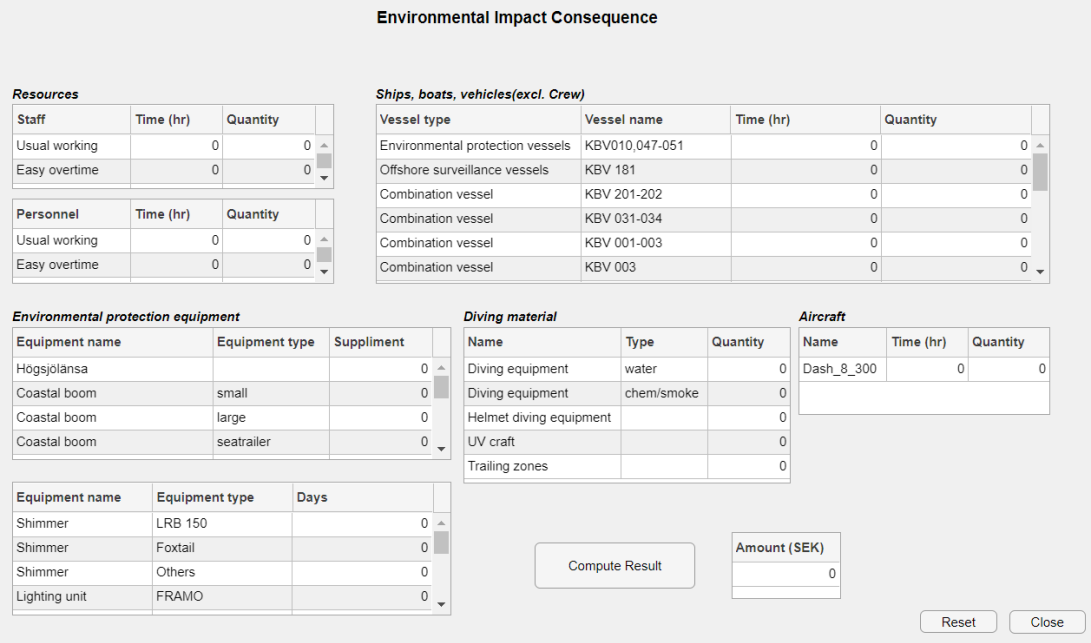

Figure 3.23 GUI for the oil spill clean-up operation.

3.4.3 Oil pollution response cost assessment

As discussed earlier in Section 2.6.3, the oil pollution response cost assessment is done by a thorough investigation on the technical specification of vessels available at Swedish coast guard stations (Kustbevakningen, 2017). A brief description of the specifications is given below:

- The vessel KBV 001-003 series has an oil intake of 400 m3/hr for 10000 cSt and 100 m3/hr for 1 million cSt.
- The vessel KBV 031-034 series has an oil intake of 150 m3/hr for 10000 cSt.
- For any accident with more than 100 m3 of spillage, two smaller vessels (031-034 series) and one larger vessel (001-003 series) will be deployed.
- The capacity of oil that could be stored in the larger vessel is 1050 m3 and 255 m3 in the smaller vessel.
- The operation from the Swedish coast guards starts with inserting booms to close the damage opening and thereby decreasing the discharge rate.
- Hence diving equipment is generally used while inserting booms.
- The Dash 8-300 aircraft is used for patrolling the site throughout the operation.

Based on the specification and the details of the vessel obtained from the coast guard (Kustbevakningen, 2017), the cost assessment is done. For a quick response operation,

it is assumed that the coast guards start their operation from their nearest station to the location. Hence it is believed that all the required vessels and equipment are available in their nearest station. Thus, the station Gothenburg is considered as the Swedish coast guard station for the accident in location North, and similarly station Falkenberg for location South.

The assessment is done for the worst cases in the set of 18 simulations (refer to Section 2.6.2). The worst case is considered as maximum volume (100% compartment i.e.,1340 tonnes) of discharge for three different viscosities and two different locations. Totally six cases were assessed for the consequence quantification. The consequences quantified for the six cases are given in Table 3.13 and the detailed assessment spreadsheet is displayed in Appendix 3.

Table 3.13 Oil pollution response consequence.

Oil	North	South
Heavy >1000 cst	191000 US $	194000 US $
Medium >100 & <1000 cst	195000 US $	198000 US $
Light <100 cst	215000 US $	219000 US $

The cost displayed in Table 3.13 for the oil pollution response is inclusive of all the operating, fuel, and clean-up costs. Here the cost for the oil pollution response is found to be higher for lighter oils, this is because of its larger volume due to lighter density or coast guard vessels' inefficiency towards light oil recovery. The cost for location South is obtained to be equally more for all the viscosities of oil, this is because of the logistic time as the Swedish coast guard station is slightly far from the discharge location compared to location North. Here the average cost obtained for the oil pollution response is US $ 154/tonne which do not agree with the cost-effective analysis proposed by European Maritime Safety Agency (Floristean et al., 2017) i.e., € 223.8/tonne (US $ 273/tonne with €1 = US$ 1.22 conversion rate) for good weather conditions. The reason for this difference is the assumption made in this thesis that the response operation starts immediately after the accident report.

It was assumed that the consequence quantification was done on an ideal case by assuming a 100% recovery of spilt oil. Due to the inefficiency of oil clean-up because of the variation in the sea states (Floristean et al., 2017), a significant amount of oil has a chance of reaching the shoreline. A study on the cost-effectiveness and efficiency of EMSA's oil pollution response services (Floristean et al., 2017) concludes that the clean-up cost per tonne of oil spilt for the shoreline will be approx. 100 times more than cleaning-up cost per tonne of oil in the ocean. Due to the time constraints faced during this thesis, the shoreline clean-up is not touched upon, but rather believed that this criterion cannot be disregarded due to its significant consequence and a model must be developed in the future and integrated along.

3.4.4 Natural resource damage assessment

Natural resource damage assessment (NRDA) is usually done after the oil spillage clean-up. It is also considered one of the consequences of oil spillage. This assessment is done by forming a committee or a trustee that consists of natural scientists and experienced economists of the country (Meade, 2019). The assessment methods, techniques, and their goals, and motivation depend on the country in which it is being carried out. Hence two such examples are discussed below.

3.4.4.1 NRDA in the U.S

In the U.S, natural science and social science experts work together with close cooperation helping each other replicating their knowledge to understand the extent of loss of natural resources and specifying the type and amount of restoration required (Meade, 2019). A non-market evaluation is generally carried out to estimate the cost of impacts to the natural resources due to hazardous chemical leakage. Hence, there exist trustees such as NOAA in the U.S to act on behalf of the public to quantify the losses and to reimburse the public for their hassles (NOAA, 2021). NOAA established the Damage Assessment, Remediation and Restoration Program (DARRP) (DARRP, 2021) to carry out the three steps involved in an NRDA:

- Preliminary injury assessment
- Injury assessment and restoration planning
- Restoration implementation

To understand the extent of restoration planning and implementation charges and costs, two case studies on the biggest oil spillages in U.S waters are presented below.

***The Exxon Valdez incident (1989)*:**

The incident is considered as one of the largest environmental catastrophes in U.S history, with 11 million gallons of an oil spill (approx. 35,750 tonnes) to the ecologically sensitive locations (DARRP, 2020-b). More than 1300 miles of the shoreline were disturbed due to the spill and the impacts also targeted the fish and wildlife habitats (DARRP, 2020-b). For the restoration projects planned, the Exxon corporation had three distinct parts for the settlement (Exxon Valdez Oil Spill Trustee Council, 2009): ***Criminal plea agreement,*** $12 million was sanctioned to the North American Wetlands Conservation Fund, and $13 million to the National Victims of Crime Fund. ***Criminal Restitution,*** this settlement is basically for the injuries and impacts on the fish, wildlife, and the regions of the spill. $100 million was settled for this cause. ***Civil Settlement,*** Exxon corporation agreed to pay $900 million over 10 years. This settlement also agreed for a provision of a reopener window during which the government could make claims up to an additional $100 million for the next four years.

The government demanded an extra $92 million as a reopener window for the continued presence of oil in the habitats of Prince William Sound and Gulf of Alaska beaches (Exxon Valdez Oil Spill Trustee Council, 2009). Around $996 million was paid by the Exxon corporation as civil settlement, out of which Exxon corporation was reimbursed with $39.9 million for co-operating with the clean-up work that took place after the settlement (Exxon Valdez Oil Spill Trustee Council, 2009).

The Deepwater Horizon incident (2010):

This incident is considered as the biggest disastrous oil leakage happened in the U.S water to date, discharging 134 million gallons of oil (approx. 435,500 tonnes) due to an explosion that occurred on the Deepwater Horizon drilling platform in the Gulf of Mexico (DARRP, 2020-a). The owners of the oil rig agreed to the early restoration projects with an estimation of $1 billion.

As an early restoration planning, The Florida Coastal Access Project defined by the trustees involved the acquisition of four coastal project locations in the Florida Panhandle (ALABAMA et al., 2016). As the next stage of this project, the final design and construction of the parks and amenities are done in each of these four locations

(ALABAMA et al., 2016). The trustees estimated the project to cost $34 million, and they are also thinking of utilizing an amount of $11 million on the second phase of the project which in total would cost approx. $45.5 million (ALABAMA et al., 2016). As per the Trustee's final inclusive plan for the restoration, the oil rig company BP is agreed to pay up to $8.8 billion which is regarded as the biggest civil settlement in the U.S history (DARRP, 2020-a).

3.4.4.2 NRDA in Europe

In Europe, NRDA is carried out in a way unlike it is done in the U.S. The Baltic Sea Action Plan (HELCOM, 2007) highlights its goal "favourable conservation status of marine biodiversity". Elofsson (2008) in their research discussed the possible methods of estimating the costs for the environmental changes or damages. To meet the environmental targets defined by HELCOM, Elofsson (2008) believes the estimated cost must be a measure of the resources given up by the public due to its physical damage. Considering the cost parameter, Elofsson (2008) estimates for a possible reduction of 360 kton nitrogen per year in the HELCOM area that would approx. be equal to 1600 million Euros per year. Similarly for a reduction of phosphorous emissions by 18.5 kton would eventually cost 350 million Euros (Elofsson, 2008).

The Swedish Environmental Protection Agency in its guidance to valuing ecosystem services (Naturvårdsverket, 2018) describes the scope of its methods using monetary valuation study examples. Primarily the idea here is to showcase the effects of demand and supply of the natural resources influenced by the change in the supply of the ecosystem services (Naturvårdsverket, 2018). An example of evaluating the algal coverage along the west coast of Denmark is presented in Naturvårdsverket (2018) that showed if the number of plaice increases by one million, this yields an increase in profits on a total of DKK 456 million over 55 years. Hence it can be concluded that a direct cost evaluation of the impacts caused due to any accidents is not done so far in the history of Europe. But looking at the monetary values in the examples all over the world it seems to be necessary to account for restoration planning and implementation even in Europe at least soon.

4 Summary and conclusions

This thesis presented a methodology developed to assess risks associated with a collision-damaged ship structure. The developed methodology is based on the metocean conditions of the accident location. By defining a showcasing accident scenario on the RoPax ship, motion responses and compartment flooding was analysed, and the damage stability risk was presented. Similarly, for a tanker vessel the structural integrity simulation, post-collision structural safety was investigated, and risk mitigation action was proposed. The oil discharge from the damage and its drifting pattern was observed, and an oil pollution response cost assessment tool was developed and showcased by assuming a hypothetical scenario. Finally, the risk analysis tool was developed and replicated using separate GUIs.

Metocean conditions and statistics

The methods of mapping the metocean conditions on the wave loads are adopted from the literature studies and the difference in their influence on the wave loads are clearly shown for different seasons of the year. The difference in the sea wave characteristics between the two locations shown in the rose plots concludes the significance of adopting metocean conditions in the developed methodology. It was found that except for the season Autumn and Winter in the location South, most often the sea waves are from the southeast direction. Through a sensitivity analysis it was found that except for the lower sea states (0-2 m), location North dominates with a higher probability of harsh waves. Despite the locations being not far from each other (approx. 54 NM apart), the sensitivity analysis proved that the metocean condition of the location is highly sensitive and plays a very major role in the risk analysis.

Seakeeping and stability analyses

From the SIMCAP analysis done on the RoPax ship, it was seen that the RoPax ship capsizes for waves with a significant wave height of 3m and above. The worst-case scenario would be if the wave heading angle is between 270° and 315° and the safest being 0° through 45°. Through a sensitivity analysis, it was found that the metocean condition of the location has a significant influence on the damage stability risk with location North dominating for all the seasons and it was also concluded that the damage stability risk increases by approximately 4.7% for each minute increase in the maximum time for evacuation and the risk to capsize in the North are higher. Through the comparative analysis done on the tanker, it was concluded that tanker does not capsize for any heeling angle, and hence the assumption made on choosing the ship type for the showcasing holds tight.

Structural integrity simulation and ULS risk

The structural integrity simulation was carried out for two tanker ship models. For the defined damage profile, it was found that the as-built vessel does not have any chance of ULS exceedance, and the corroded vessel has a higher probability of ULS exceedance depending on the encountered wave direction and heights. The worst-case (ULS exceedance) for the corroded vessel after the damage is any following or head seas with significant wave heights more than 4 m. The mitigation action proposed using a showcasing scenario showed that a simple act of manoeuvring the vessel by 40° decreased the ULS risk by 94%. Through sensitivity analyses, the influence of the metocean condition between the locations was found to be significant with a difference of a maximum of 1657% in Winter and a minimum of 7% in Summer.

Environmental impacts and risk

Seatrack web tool was used for the sensitivity analysis of 18 scenarios. It was shown that for both locations the viscosity of the oil varies considerably during the simulation. It was concluded that light oils have the tendency to get dispersed on the surface of the sea more quickly compared to the other oils and are a great challenge for the clean-up operation. Considering the oil deposition on the seabed, again the light oils are found to be a considerable threat concerning the clean-up operation. From the results of oils getting deposited on the shoreline, it was concluded that in two out the three days, only the medium and heavy oil pose a significant risk of shoreline clean-up. From all the sensitivity analyses, it was found that the parameters considered on defining the 18 showcasing scenarios have a significant influence on the oil drift and hence strengthens the assumptions made.

From the economical evaluation of the oil pollution response, it was found that the lighter oil discharged would cost more than the heavier oils. A conclusion was drawn that this difference is because of the coast guard vessels' inefficiency towards the light oils or due to the increase in the volume of light oil due to its lower density. A disagreement was found between the cost quantification model developed in this thesis and the cost model proposed by EMSA. This concludes that the assumption made on the immediate response operation is not valid and must be changed. It was observed from the literature study that the cost for the oil clean-up on the shore will be 100 times more than the oil clean-up in the ocean and concluded that this criterion must not be neglected in the oil pollution response. With the case studies made on the NRDA carried out in Europe and the US, it was clearly shown that the assessment techniques vary for different region and has a drastic difference on treating the lost natural resource and valuing the lost habitats due to the pollution.

5 Future work

Metocean statistics

Extracting the metocean statistics based on four seasons of the year has limited the accuracy of the maximum likely occurring wave direction results. As the results tend to be in the southeast direction for most of the seasons, expanding the resolution further by extracting data based on the months will further enrich the accuracy of the results. It was seen that data extracted using the ML method with one standard deviation lost a considerable amount of data for computing the probability of occurrence of significant wave heights. Their results influenced damage stability and ULS exceedance risk. To eliminate this limitation, a sensitivity analysis on the consideration of data range must be done.

Seakeeping and stability analyses

Simultaneous flow of oil and water from the damaged compartment in the tanker must be studied as currently, only water flow out of the Tanker can be simulated in the SIMCAP code. The assumption of replacing the actual time for evacuation with time for capsizing has a significant influence on the accuracy of the result. The actual time for evacuation is divided into awareness time, travel time, embarkation time, and launching time (IMO, 2007). Considering the total time for capsizing as the actual time for evacuation makes the whole assessment an ideal case. Therefore, for more reliable results on the survival probability, a thorough analysis based on the methods for estimating actual time for evacuation recommended by IMO must be done. The SIMCAP analyses were done without considering the ship manoeuvring after a collision, and countermeasures against progressive flooding. A general outline for future work would be to suggest options to prevent capsize of the ship or delay the time to capsize.

Structural integrity simulation and ULS risk

The structural integrity simulation done in tool URSA accounts for only the progressive collapse methods (Kuznecovs, 2020). Developing the URSA tool to also account for the cyclic loading will further enhance the reliability of the developed methodology by considering the accumulated fatigue damage. The partial safety index assumed for the sensitivity analysis of structural adequacy measure was specifically to account for the various uncertainties associated with its estimation. The index values were chosen randomly with a + and - 5% from the reference; so, to increase the accuracy of the ULS exceedance probability a detailed analysis for estimating the partial safety index must be done. A comparison analysis must be done for the obtained ULS consequence to check the sensitivity of the developed methodology with the real case examples. The consequences in the developed methodology limits for structural adequacy values more than one. Hence, the methodology can be further improvised by integrating the intermediate structural adequacy values and their consequences.

Environmental impacts and risk

The assumption made on the immediate response operation from the coast guards for the oil clean-up resulted in the assessment as an ideal case. Considering the awareness time and the decision-making time before starting the oil pollution response operation, can yield results with better accuracy. The assessment made by Floristean et al., (2017) shows that the weather condition plays a very major role in the cost assessment. For the same oil clean-up with different weather conditions in Floristean et al., (2017), it was concluded that the efficiency of the clean-up operation decreases by 50% for not so

favourable weather conditions. This conclusion contradicts the assumption made on the efficiency (100%) of the clean-up operation by the coast guards. Hence, adopting at least 3 different sea state options in the oil pollution response cost assessment makes the result much more reliable and accurate. An extensive study must be done on the shoreline clean-up assessment and their models for quantification must be integrated in the future.

6 References

ALABAMA, State of Florida, State of Louisiana, State of Mississippi, State of Texas, NOAA, U.S Department of Interior, U.S Environment Protection Agency, & USDA. (2016). Deepwater Horizon Oil Spill Phase V Early Restoration Plan and Environmental Assessment. *Deepwater Horizon Oil Spill Natural Resource Damage Assessment.* Retrieved May 09, 2021, from https://repository.library.noaa.gov/view/noaa/17721.

Asariotis, R., Assaf, M., Benamara, H., Hoffmann, J., Premti, A., Rodríguez, L., Weller, M., Youssef, F., Bradford, G., Crowe, T., Davidson, N., Faghfouri, M., Garratt, M., Hutley, S., Konsta, K., De Langen, P., Lehmacher, W., Malby, S., Merk, O., … Visser, D. (2018). Review of Maritime Transport 2018.

Asariotis, W. J. R., Assaf, M., Ayala, G., Ayoub, A., Benamara, H., Chantrel, D., Hoffmann, J., Larouche-Maltais, A., Premti, A., Rodríguez, L., Sun, S., Youssef, F., Abbas, H., Bradford, G., Cariou, P., Crowe, T., Davidson, N., Manuel, J., Orejas, D., … Verhoeven, P. (2020). Review of Maritime Transport 2020.

Brown, A. J. (2002). Collision scenarios and probabilistic collision damage. *Marine Structures*, *15*, 335–364.

Chiu, C.-S., Liu, C.-P., Chang, K.-Y., Tseng, W.-J., & Chen, Y.-W. (2017). Cost of salvage - a comparative form approach. *Journal of Marine Science and Technology*, *25*(6), 742–751. https://doi.org/10.6119/JMST-017-1226-15.

CMEMS. (2021). Copernicus Marine Environment Monitoring Service. Retrieved February 10, 2021, from https://marine.copernicus.eu/.

Collision de navires en Corse : quels risques pour l'environnement ? (2018). https://www.europe1.fr/societe/collision-de-navires-en-corse-quels-risques-pour-lenvironnement-3774185.

Compass Maritime. (2021). Compass Maritime Weekly Market Report. Retrieved May 11, 2021, from https://compassmar.com/reports/Compass Maritime Weekly Market Report.pdf.

DARRP, N. (2021). Damage Assessment, Remediation, and Restoration Program. Retrieved May 10, 2021, from https://www.darrp.noaa.gov/.

DARRP, N. (2020). Deepwater Horizon | Oil Spills | Damage Assessment, Remediation, and Restoration Program. Retrieved May 9, 2021, from https://www.darrp.noaa.gov/oil-spills/deepwater-horizon.

DARRP, N. (2020). Exxon Valdez | Oil Spills | Damage Assessment, Remediation, and Restoration Program. Retrieved May 9, 2021, from https://darrp.noaa.gov/oil-spills/exxon-valdez.

DNV GL AS. (2018). Class Guideline: Wave loads. Retrieved February 05, 2021, from https://rules.dnvgl.com/docs/pdf/DNVGL/CG/2018-01/DNVGL-CG-0130.pdf.

Elofsson, K. (2008). The costs of environmental improvements in the Baltic Sea and Skagerrak A review of the literature. *Swedish Agency for Marine and Water Management.* ISBN: 978-91-620-5876-0.pdf.

EMSA. (2020). Annual Overview of Marine Casualties and Incidents 2020. *European Maritime Safety Agency.* ISSN: 1098-6596.

Exxon Valdez Oil Spill Trustee Council. (2009). Exxon Valdez Oil Spill Trustee Council 2009 Status Report. Retrieved May 09, 2021, from https://www.cerc.usgs.gov/orda_docs/DocHandler.ashx?task=get&ID=7.

Floristean, A., Porteron, S., Winberg, J., Amstrup, M. H., Le Den, X., Ostergaard, J., O'connell, K., & Kowal, E. (2017). Study on the cost effectiveness and efficiency of EMSA's oil pollution response services. *The European Maritime Safety Agency*. Contract number: EMSA/NEG/08/2016, Retrieved February 26, 2021, from https://ec.europa.eu/transport/sites/default/files/2018-cost-effectiveness-and-efficiency-of-emsa-oil-pollution-response-services.pdf.

GTA Forecasting. (2021). IHS Markit. Retrieved May 19, 2021, from https://ihsmarkit.com/products/gta-forecasting.html.

HELCOM. (2007). Action Plan – Full Text. *HELCOM Baltic Sea Action Plan*. Retrieved May 8, 2021, from https://helcom.fi/baltic-sea-action-plan/action-plan/.

HELCOM. (2021). Baltic Marine Environment Protection Commission. Retrieved March 15, 2021, from https://helcom.fi/.

IMO. (2007). Guidelines for evacuation analysis for new and existing passenger ships. *International Maritime Organization.* MSC.1/Circ.1238, Ref. T4/4.01.

IMO. (2008). Non-mandatory guidelines on security aspects of the operation of vessels which do not fall within the scope of SOLAS chapter xi-2 and the ISPS code. *International Maritime Organization.* MSC.1/Circ.1238, Ref. T2-MSS/2.11.1.

IMO. (2018). Revised Guidelines for FSA for use in the IMO rule-making process. *International Maritime Organization, 44 (2)*. MSC-MEPC.2/Circ.12/Rev.2.

Kustbevakningen. (2017). Fartygskatalog - Kustbevakningen. Retrieved May 20, 2021, from https://kustbevakningen.se/materiel-- teknik/fartyg/fartygskatalog/ kombinationsfartyg/.

Kuznecovs, A, & Ringsberg, J. W. (2021). A 3D ultimate limit state surface for intact and collision-damaged ship hulls. *Marine Structures*.

Kuznecovs, A. (2020). Ultimate and Residual Strength Assessment of Ship Structures *Chalmers University of Technology*. https://research.chalmers.se/publication/516227/file/516227_Fulltext.pdf.

Kuznecovs, A., Schreuder, M., & Ringsberg, J. W. (2021). Methodology for the simulation of a ship's damage stability and ultimate strength conditions following a collision. *Marine Structures*, *79*, 103027. https://doi.org/10.1016/j.marstruc.2021.103027

Lavidas, G., & Polinder, H. (2019). North sea wave database (NSWD) and the need for reliable resource data: A 38 year database for metocean and wave energy assessments. *Atmosphere*, *10*(9), 1–27. https://doi.org/10.3390/atmos10090551

Liungman, O., & Mattsson, J. (2011). Scientic Documentation of Seatrack Web; physical processes, algorithms and references. *Swedish Meteorological and Hydrological Institute (SMHI).* Retrieved May 20, 2021, from https://stw.smhi.se/doc/1.15600!Seatrack%20Web%20Scientific%20Documentation.pdf

Love, A. (2020). Preventing ship collisions. *Ship Technology*. Retrieved May 19, 2021, from https://www.ship-technology.com/features/ship-collisions/.

MarineTraffic. (2021). Global Ship Tracking Intelligence | AIS Marine traffic. Retrieved February 2, 2021, from https://www.marinetraffic.com/en/ais/home/centerx:-11.6/centery:40.2/zoom:2.

Meade, Q. (2019). The True Cost of an Oil Spill: Q&A with a NOAA Economist. *Office of Response and Restoration.* Retrieved April 17, 2021, from https://response.restoration.noaa.gov/true-cost-oil-spill-qa-noaa-economist-0

Naturvårdsverket. (2018). Guide to valuing ecosystem services. *Swedish Environmental Protection Agency.* ISSN: 0282-7298.

NOAA. (2021). What is a Natural Resource Damage Assessment? *National Ocean Service*. Retrieved May 9, 2021, from https://oceanservice.noaa.gov/facts/nrda.html.

Oberg, E., Jones, F. D., Horton, H. L., Ryffel, H. H., McCauley, C. J., & Brengelman, L. (2020). Machinery's Handbook 31st Edition. In *Machinery's Handbook (31st Edition)*. Industrial Press. https://app.knovel.com/hotlink/toc/id:kpMHE00033/machinerys-handbook-31st/machinerys-handbook-31st.

OECD. (2021). Ocean shipping and shipbuilding. Retrieved May 19, 2021, from https://www.oecd.org/ocean/topics/ocean-shipping/.

Oil Price. (2021). WTI Crude Oil Price Charts. Retrieved May 20, 2021, from https://oilprice.com/oil-price-charts/45.

Olofsson, J., & Eliasson, P. (2020). Program for environmental rescue service at sea. Retrieved May 20, 2021, from https://www.kustbevakningen.se/globalassets/documents/hallbar-havsmiljo/program-for-miljoraddningstjanst-til-sjoss.pdf.

Pardo, A. T. (2013). An introductory view of salvage claims. *Technical University of Catalonia.* Retrieved May 12, 2021, from http://www.dolphin-maritime.com/public/an%20introductory%20view%20of%20salvage%20claims.pdf.

Petroleum, Q. (2021). Conversion Factors. *Qatar Petroleum*. Retrieved May 25, 2021, from https://qp.com.qa/ar/Pages/ConversionFactor.aspx.

Ringsberg, J. W., Li, Z., Johnson, E., Kuznecovs, A., & Shafieisabet, R. (2018). Reduction in ultimate strength capacity of corroded ships involved in collision accidents. *Ships and Offshore Structures*, *13*, 155–166. https://doi.org/10.1080/17445302.2018.1429158.

Safety4sea. (2020-a). Marine Safety Investigation Report. *Transport Malta.* Retrieved May 22, 2021, from https://safety4sea.com/wp-content/uploads/2020/04/Transport-Malta-Safety-investigation-into-the-collision-between-the-Maltese-registered-LNG-carrier-ASEEM-and-the-Hong-Kong-registered-VLCC-SHINYO-OCEAN-2020_03.pdf.

Safety4sea. (2020-b). Transport Malta Investigation. Retrieved February 3, 2021, from https://safety4sea.com/transport-malta-investigation-collision-of-lng-carrier-and-vlcc-attributed-to-vhf-communication/.

Schreuder, M. (2014). Development, Implementation, Validation and Applications of a Method for Simulation of Damaged and Intact Ships in Waves. *Chalmers University of Technology.* ISBN: 978-91-7385-972-1. https://research.chalmers.se/publication/193130/file/193130_Fulltext.pdf.

Schreuder, M., Hogström, P., Ringsberg, J. W., Johnson, E., & Janson, C. E. (2011). A method for assessment of the survival time of a ship damaged by collision. *Transactions - Society of Naval Architects and Marine Engineers*, *119*(2), 603–619.

Seatrack Web. (2021). Swedish Meteorological and Hydrological Institute (SMHI). Retrieved April 17, 2021, from https://stw.smhi.se/

SHARC. (2021). SHARC - Structural and Hydro mechanical Assessment of Risk in Collision and grounding. *Chalmers University of Technology.* https://research.chalmers.se/en/project/9203.

Shipfinance. (2021). Shipping-market-review-may-2021. Retrieved May 11, 2021, from https://www.shipfinance.dk/media/2098/shipping-market-review-may-2021.pdf.

Shipping fact (2021). International Chamber of Shipping. Retrieved May 19, 2021, from https://www.ics-shipping.org/shipping-fact/shipping-and-world-trade-driving-prosperity.

SMHI. (2018.-a). SeaTrack Web Documentation. Retrieved May 20, 2021, from https://stw.smhi.se/player/help/classic/?domain=helcom#background

SMHI. (2021.-b). Swedish Meteorological and Hydrological Institute. Retrieved April 17, 2021, from https://www.smhi.se/q/Lindholmen/Göteborg/3331628

Spanos, D., & Papanikolaou, A. (2011). Numerical simulations for charaterizing Time to Capsize. *E.U. Research Project*, *D4.3*(FP7-RTD-218532).

Splash247. (2019). UAE authorities dish out fines to owners involved in dangerous tanker prang. Retrieved May 26, 2021, from https://splash247.com/uae-authorities-dish-out-fines-to-owners-involved-in-dangerous-tanker-prang/

Transportstyrelsen. (2011). Published accident investigation reports. Retrieved May 12, 2021, from https://www.transportstyrelsen.se/en/shipping/Accidents--near-misses/Accident-Investigation-Reports1/Published-accident-investigation-reports/.

Tuitman, J. T., Bosman, T. N., & Harmsen, E. (2013). Local structural response to seakeeping and slamming loads. *Marine Structures*, *33*, 214–237. https://doi.org/10.1016/j.marstruc.2013.06.002

Vanem, E., & Skjong, R. (2004). Collision and grounding of passenger ships - risk assessment and emergency evacuations. *Proceedings of the 3rd International Conference on Collision and Grounding of Ships, 2004*, *2002*, 195–202.

Wikingsson, A. W. (2020). Riktlinjer om uppdragsverksamhet och avgifter samt ersättning för miljöräddningstjänst. *Kustbevakningen.*

Williams, R. (2013). Gard Guidance on Maritime Claims and Insurance. *Gard AS.* ISBN: 978-82-90344-33-2.

Xie, H., Liu, F., Tang, H., & Liu, X. (2020). Numerical study on the dynamic response of a truncated ship-hull structure under asymmetrical slamming. *Marine Structures*, *72*, 102767. https://doi.org/10.1016/j.marstruc.2020.102767

Yamada, Y. (2014). Numerical study on the residual ultimate strength of hull girder of a bulk carrier after ship-ship collision. *Proceedings of the International Conference on Offshore Mechanics and Arctic Engineering - OMAE*, *4A*. https://doi.org/10.1115/OMAE2014-23811

Zhang, S., & Pedersen, P. T. (2017). A method for ship collision damage and energy absorption analysis and its validation. *Ships and Offshore Structures*, *12*, S11–S20. https://doi.org/10.1080/17445302.2016.1254584

Zhu, Z., Ren, H., Li, C., & Zhou, X. (2020). Ultimate Limit State Function and Its Fitting Method of Damaged Ship under Combined Loads. *Journal of Marine Science and Engineering*, *8*(2), 117. https://doi.org/10.3390/jmse8020117

7 Appendices

7.1 Appendix 1: Seakeeping and stability analyses

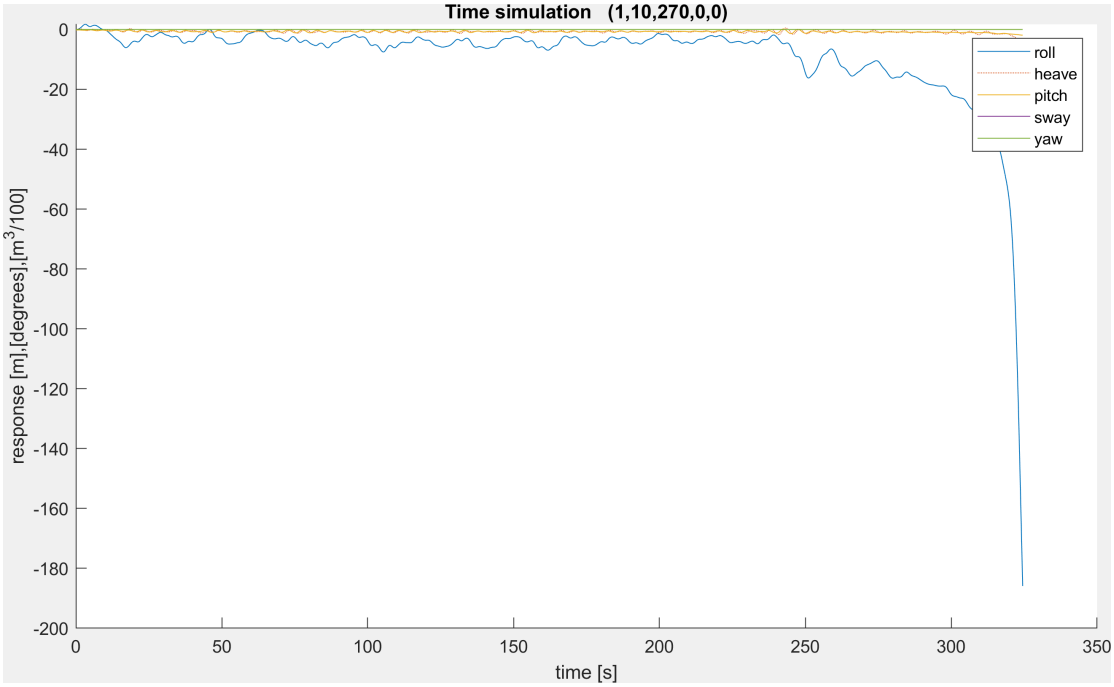

(a)

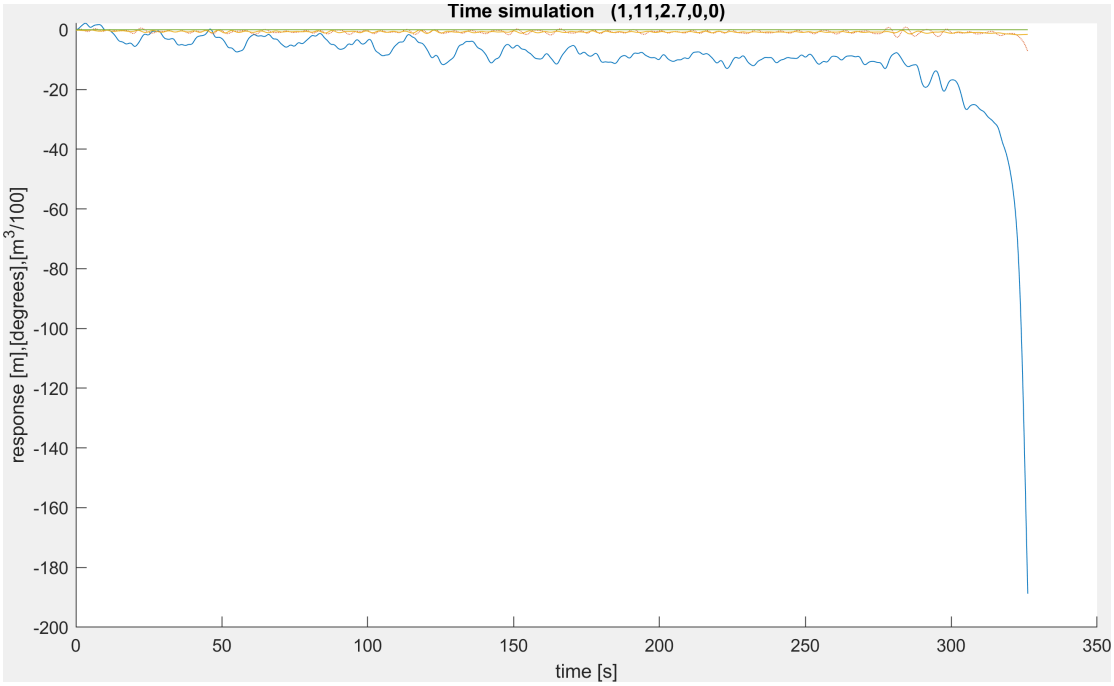

(b)

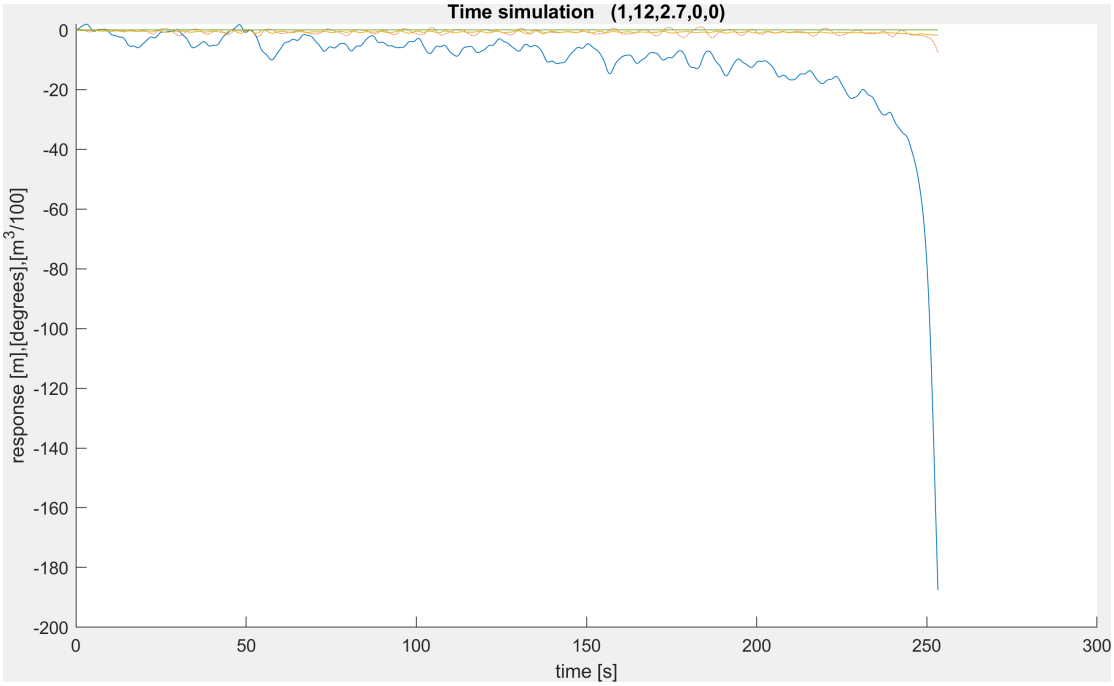
Time simulation (1,12,2.7,0,0)
response [m],[degrees],[m3/100]
time [s]
0
-20
-40
-60
-80
-100
-120
-140
-160
-180
-200
0
50
100
150
200
250
300

(c)

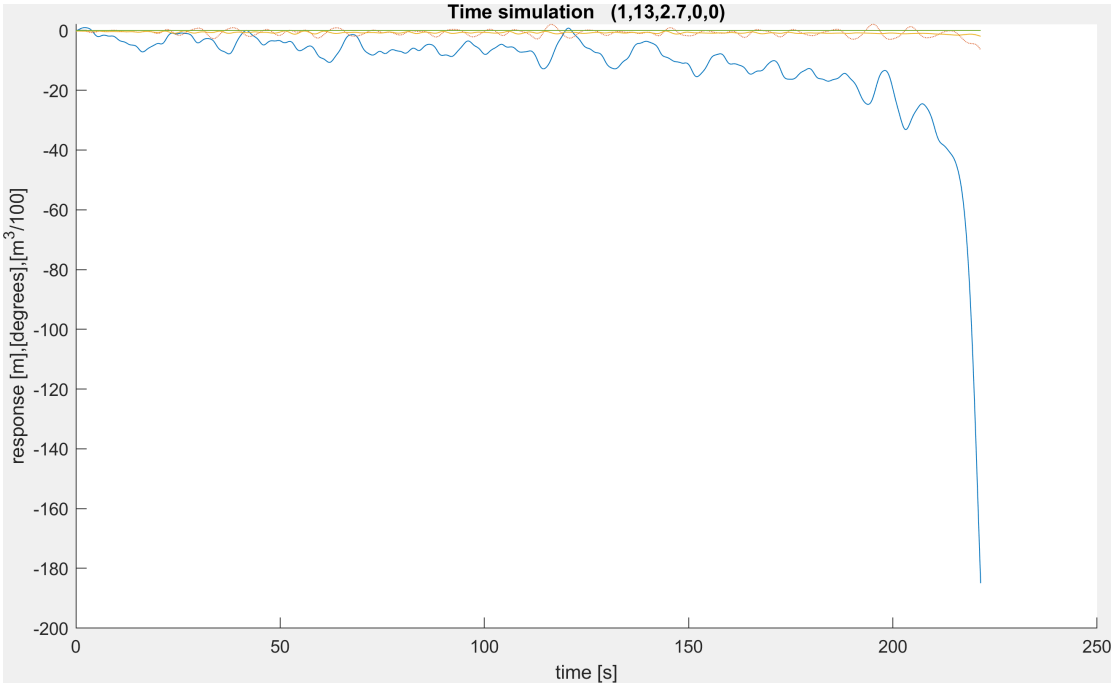
Time simulation (1,13,2.7,0,0)
response [m],[degrees],[m3/100]
time [s]
0
-20
-40
-60
-80
-100
-120
-140
-160
-180
-200
0
50
100
150
200
250

(d)

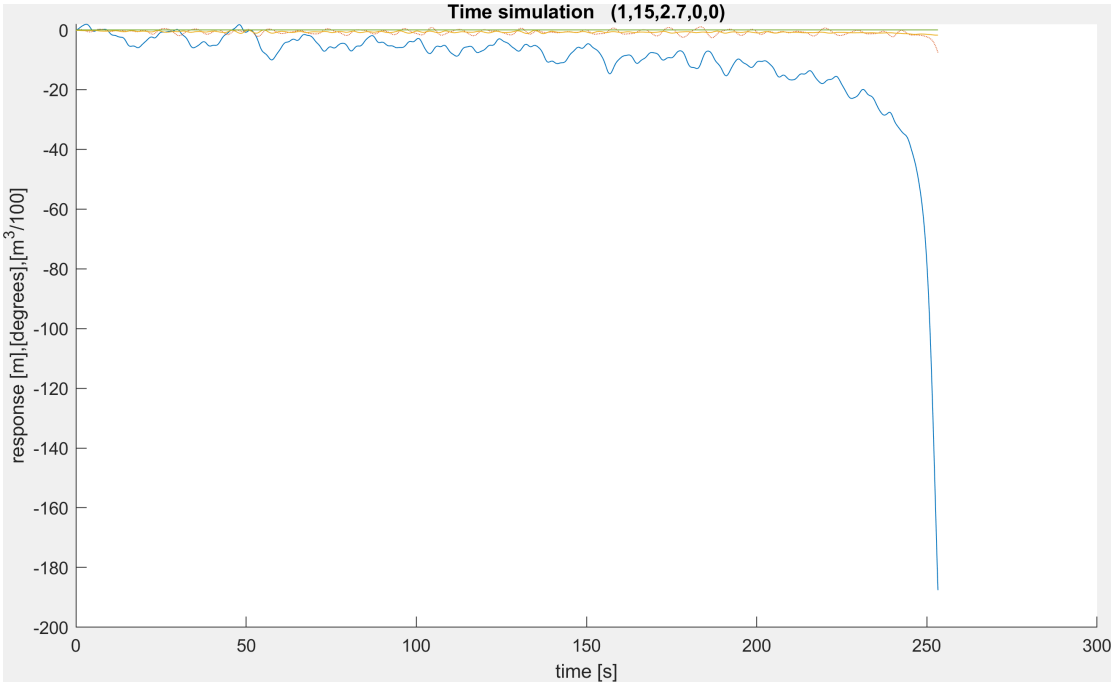

(e)

Figure 7.1 Motion responses of the RoPax ship for the worst wave heading angle i.e., 270° for (a) H_s=2m, (b) H_s=3m, (c) H_s=4m, (d) H_s=4m, (e) H_s=5m, (f) H_s=6m.

7.2 Appendix 2: Structural integrity simulation and ULS risk

A 2.1 Procedure behind the ULS exceedance consequence quantification

- Price A of the vessel after x years (vessel age) with n years of service life and S as the scrappage value is obtained as (Oberg et al., 2020):

$$A = \frac{(P - S) \times (n - x)}{n} + S \tag{7.1}$$

where P is the price of the vessel when bought.

- The present price of WTI crude oil per barrel is obtained from Oil Price (2021). And the total price of the lost cargo (oil) is computed as:

$$P_{1\ tonne} = 7.33 \times P_{1\ barrel} \tag{7.2}$$

$$P_{cargo} = P_{1\ tonne} \times V_{compartment} \times N_{compartment} \tag{7.3}$$

where, $P_{1\ tonne}$ – Price for 1 tonne of oil
$P_{1\ barrel}$ – Price for 1 barrel of oil [1 tonne = 7.33 US barrel (Petroleum, 2021)]
P_{cargo} – Total price of the lost cargo
$V_{compartment}$ – Volume of 1 compartment.
$N_{compartment}$ – Total number of compartments

- Price of lost revenue P_R is estimated as:

$$P_R = Revenue\ per\ day \times N_{repair} \tag{7.4}$$

where N_{repair} – Number of days for repair

- The inflation rate I due to market risk is estimated as:

$$\mathrm{I} = 1 + \left(\frac{misc}{100}\right) \tag{7.5}$$

where *misc* – Miscellaneous factor

- Consequences on crew deaths and injury is estimated as:

$$P_{death} = 4.61e6 \times N_{death} \tag{7.6}$$

$$P_{injury} = 0.13e6 \times N_{injury} \tag{7.7}$$

where, N_{death} – Number of people dead

N_{injury} – Number of people injured

- The consequences due to ULS exceedance is computed as:

1. Vessel abandoned consequence

$$P_{abandon} = A + (P_{cargo} \times I) + P_{death} + P_{injury} \tag{7.7}$$

2. Vessel repaired

$$P_{repair} = P_{salvage} + P_{dockyard} + P_{equip} + (P_R \times I) + P_{death} + P_{injury} \tag{7.8}$$

where, $P_{salvage}$ – Salvage operation claims incl. vessel towing fare.

$P_{dockyard}$ – Hull damage repair cost from the dockyard

P_{equip} – Damaged equipment cost for replacement

7.3 Appendix 3: Environmental impacts and risk

Table 7.1 Oil clean-up operation assessment for 100% discharge, heavy oil, location north.

Item/Resource	Time(hr)	Quantity	Suppliment	Capacity (m3/hr)	Total discharge (mt)	Total volume (m3)	Req. time (hr)	Logistic time (hr)
KBV 001-003	5.7	1		400	871	879.71	2.2	3.46
KBV 031-034	5.0	2		150	234.5	236.845	1.6	3.46
Högsjölänsa			1					
Diving equip water		2						
Diving equip helmet		2						
Dash 8 300 aircraft	24	1						
Staff	5.7	45						
Personnel	5.7	50						

Table 7.2Oil clean-up operation assessment for 100% discharge, medium oil, location north.

Item/Resource	Time(hr)	Quantity	Suppliment	Capacity (m3/hr)	Total discharge(mt)	Total volume (m3)	Req. time (hr)	Logistic time (hr)
KBV 001-003	6.0	1		400	911.2	1002.32	2.5	3.46
KBV 031-034	5.0	2		150	214.4	235.84	1.6	3.46
Högsjölänsa			1					
Diving equip water		2						
Diving equip helmet		2						
Dash 8 300 aircraft	24	1						
Staff	6.0	45						
Personnel	6.0	50						

Table 7.3 Oil clean-up operation assessment for 100% discharge, light oil, location north.

Item/Resource	Time(hr)	Quantity	Suppliment	Capacity (m3/hr)	Total discharge(mt)	Total volume (m3)	Req. time (hr)	Logistic time (hr)
KBV 001-003	5.6	1		400	737	862.29	2.2	3.46
KBV 031-034	5.0	3		150	201	235.17	1.6	3.46
Högsjölänsa			1					
Diving equip water		2						
Diving equip helmet		2						
Dash 8 300 aircraft	24	1						
Staff	5.6	60						
Personnel	5.6	65						

Table 7.4 Oil clean-up operation assessment for 100% discharge, heavy oil, location south.

Item/Resource	Time(hr)	Quantity	Suppliment	Capacity (m3/hr)	Total discharge(mt)	Total volume (m3)	Req. time (hr)	Logistic time (hr)
KBV 001-003	5.9	1		400	871	879.71	2.2	3.66
KBV 031-034	5.2	2		150	234.5	236.845	1.6	3.66
Högsjölänsa			1					
Diving equip water		2						
Diving equip helmet		2						
Dash 8 300 aircraft	24	1						
Staff	5.9	45						
Personnel	5.9	50						

Table 7.5 Oil clean-up operation assessment for 100% discharge, medium oil, location south.

Item/Resource	Time(hr)	Quantity	Suppliment	Capacity (m3/hr)	Total discharge(mt)	Total volume (m3)	Req. time (hr)	Logistic time (hr)
KBV 001-003	6.2	1		400	911.2	1002.32	2.5	3.66
KBV 031-034	5.2	2		150	214.4	235.84	1.6	3.66
Högsjölänsa			1					
Diving equip water		2						
Diving equip helmet		2						
Dash 8 300 aircraft	24	1						
Staff	6.2	45						
Personnel	6.2	50						

Table 7.6 Oil clean-up operation assessment for 100% discharge, light oil, location south.

Item/Resource	Time(hr)	Quantity	Suppliment	Capacity (m3/hr)	Total discharge(mt)	Total volume (m3)	Req. time (hr)	Logistic time (hr)
KBV 001-003	5.8	1		400	737	862.29	2.2	3.66
KBV 031-034	5.2	3		150	201	235.17	1.6	3.66
Högsjölänsa			1					
Diving equip water		2						
Diving equip helmet		2						
Dash 8 300 aircraft	24	1						
Staff	5.8	60						
Personnel	5.8	65						

DEPARTMENT OF MECHANICS AND
MARITIME SCIENCES
CHALMERS UNIVERSITY OF TECHNOLOGY
Gothenburg, Sweden 2021
www.chalmers.se

CHALMERS
UNIVERSITY OF TECHNOLOGY